CHAPTER 3

RESULTS AND DISCUSSION

3.1 Electrochemical behavior of ketone compounds

3.1.1 Electrochemical behavior of Cyclohexanone compound

3.1.1.1 Cyclic voltammetry of blank solution at glassy carbon electrode

Cyclic voltammograms of all blank solutions were recorded in the potential window of 1.000 V to -3.000 V vs Ag/AgCl. No significant peak was obtained, indicating that there was no significant impurities as show in Figure 11.

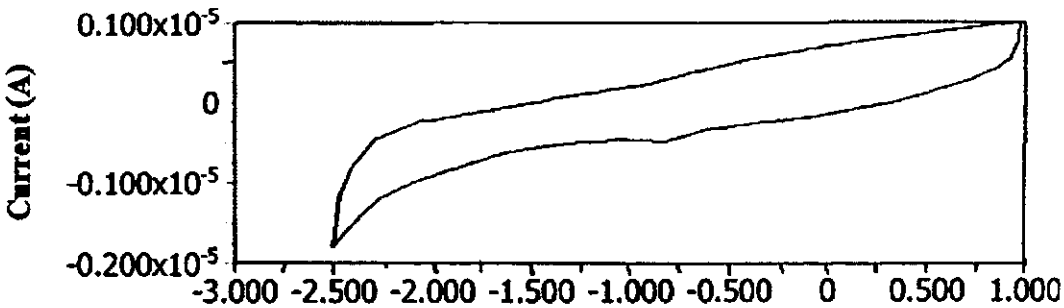

Figure 11 Cyclic voltammograms of blank solution at glassy carbon electrode in 50 ml CH_3CN which 0.1 M TBAP as a supporting electrolyte with scan rate of 100 mV/s.

3.1.1.2 Redox behavior of Cyclohexanone compound

Cyclic voltammogram which in the potential window of 0.000 V to -2.500 V vs Ag/AgCl which there is no peak, indicating that there was no redox reaction in this compound as shown in Figure 12.

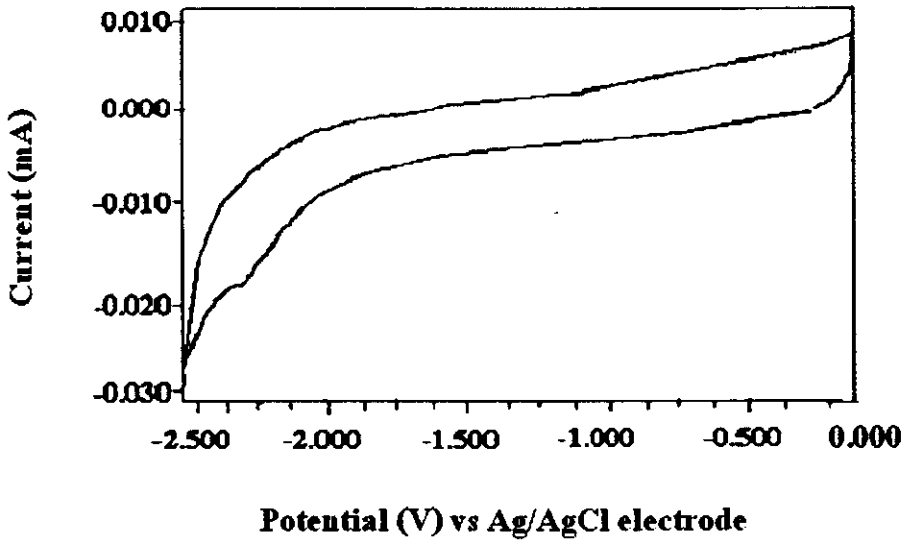

Figure 12 Cyclic voltammogram of 1.0 x 10^{-3} M Cyclohexanone at GCE in CH_3CN 50 ml which TBAP (0.1 M) as supporting electrolyst, scan rate of 100 mV/s and resting potential is -0.0011 V.

Discussion

Cyclohexanone does not exhibit any significant peak, indicating that there are no redox reaction at glassy carbon electrode. Cyclohexanone radical product is not facilitated to occur by the absence of resonance effect to stabilize it.

3.1.2 Electrochemical behavior of Benzophenone compound

3.1.2.1 Cyclic voltammetry of blank

Cyclic voltammogram (CV) of blank solution was recorded in the potential window of -1.250 to -3.000 V vs Ag/AgCl. Indicating that there was no significant impurities.

3.1.2.2 Redox behavior of Benzophenone compound

When Benzophenone is put in CH_3CN, it exhibits one redox couple as shown in Figure 13.

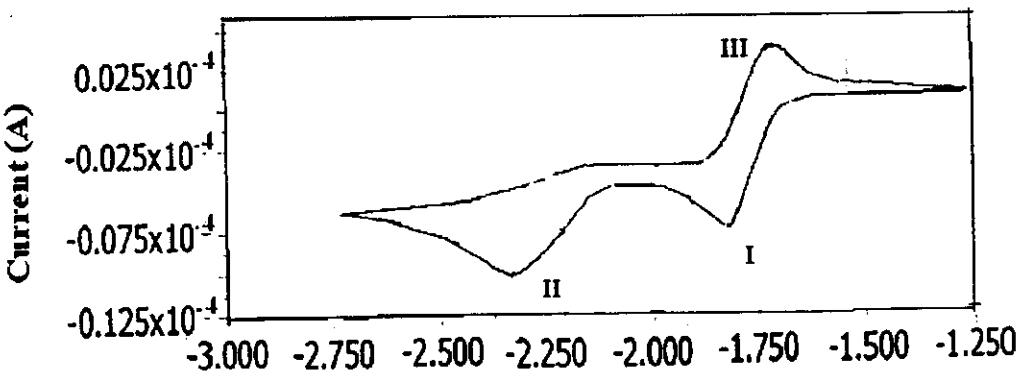

Figure 13 Cyclic voltammogram of 1.0 x 10^{-3} M Benzophenone at GCE in 50 ml CH_3CN, 0.1 M Tetrabutylammonium hexafluorophosphate with the scan rate of 100 mV/s within the potential window is -1.250 to -3.000 V and resting potential is -1.350 V.

Discussion

Benzophenone exhibits two steps of reduction as shown in Figure 13. The first redox couple occurs at Epc_1 = -1.835 V, Epa_1 = -1.723 V and $\dot{E}$ = -1.779 V vs Ag/AgCl. This behavior is similar to enones as in previous of enones studies (Abdirisak *et al.*, 2002).

The reduction of Benzophenone to its ketyl anion radical in anhydrous acetonitrile is electrochemically reversible and chemically reversible (Ipa_1/Ipc_1 = 1.05).

The $\triangle Ep_1$ (112 mV) is somewhat higher than the theoretical value ($\triangle Ep_1$ = 59 mV), reflecting that the electron transfer is quite slow at this scan rate (100 mV/s). Slow electron transfer causes the peak separation to increase. The differences of the anodic and cathodic peak potentials (ΔEp_1) increased with increase of the scan rate from 0.1 to 0.6 V/s also indicated non Nernstian behaviour (>59 mV) (Moharram and Ghoneim, 2004).

Both reduction and oxidation are purely diffusion controlled due to graph exhibits a linear relationship between peak currents and square root of scan rate as shown in Figure 14. Detailed studies reveal that its electron transfer follows: Randles-sevcik equation. $Ip = (2.69 \times 10^5)n^{3/2}AD^{1/2}v^{1/2}C^*$ where n is the number of electron on molecule, [Ip is the maximum current in A, A is the electrode area in cm^2, D is the diffusion coefficient in cm^2s^{-1}, C is the concentration in mol/cm^3 and υ is the scan rate in V/s] (Esma *et al.*, 2004).

Table 15 The relationship of square root of scan rate with current peaks of Benzophenone

Scan rate (mV/s)	Square root of scan rate $(mV/s)^{1/2}$	Ipc_1 (A)	Ipc_2 (A)	Ipa_1 (A)
100	10.00	5.949×10^{-6}	9.620×10^{-6}	6.246×10^{-6}
200	14.14	8.531×10^{-6}	2.970×10^{-5}	8.960×10^{-6}
300	17.32	1.016×10^{-5}	4.064×10^{-5}	1.067×10^{-5}
400	20.00	1.120×10^{-5}	4.902×10^{-5}	1.176×10^{-5}
500	22.36	1.259×10^{-5}	5.851×10^{-5}	1.322×10^{-5}
600	24.49	1.403×10^{-5}	6.750×10^{-5}	1.473×10^{-5}

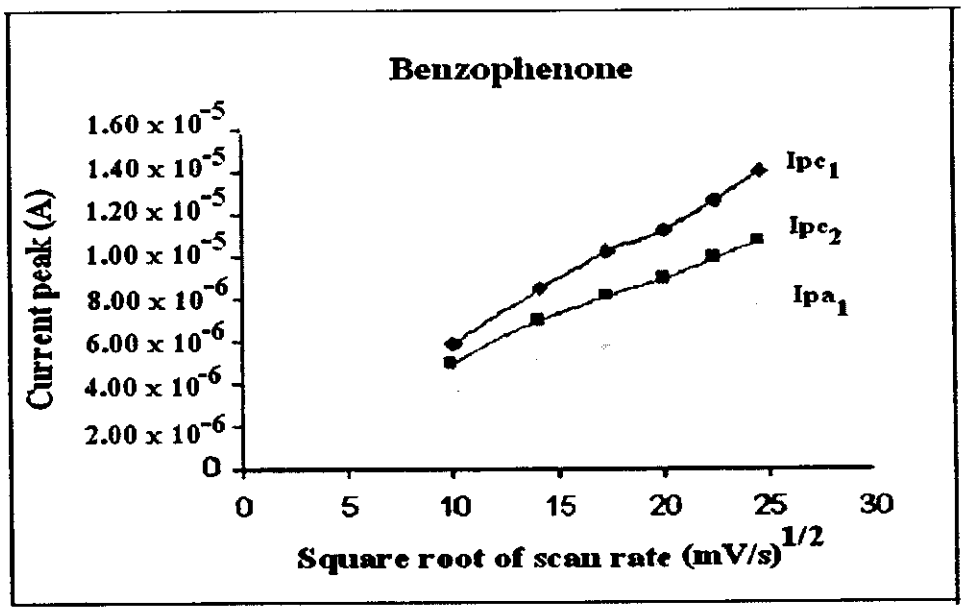

Figure 14 Linear plot showing the dependence of Benzophenone (1 mM) reduction and oxidation current peak (Ipc_1, Ipc_2 and Ipa_1) with various square root of scan rate for glassy carbon electrode

There is one independence reduction peak which occurs at Epc_2 = -2.294 V. This peak is electrochemically irreversible and is no oxidation couple. The second oxidation peak can not appear due to Benzophenone has no second carbonyl group in the structure in the same way as quinones.

The reaction of Benzophenone is shown in Scheme 1. The reaction sequence shown in Eqs. (1)-(3) takes place.

The first electron uptake yields a stable ketyl radical anion, which is further reduced at more negative potentials (1). The ketyl radical anion can be reduced to form dianion in the second reduction step (2). The dianion of benzophenone is a strong base and is therefore rapidly protonated by any proton donor HA present in the solution (3) (Abdirisak *et al.*, 2002).

The second oxidation can not appear due to Benzophenone has no second carbonyl group in the structure.

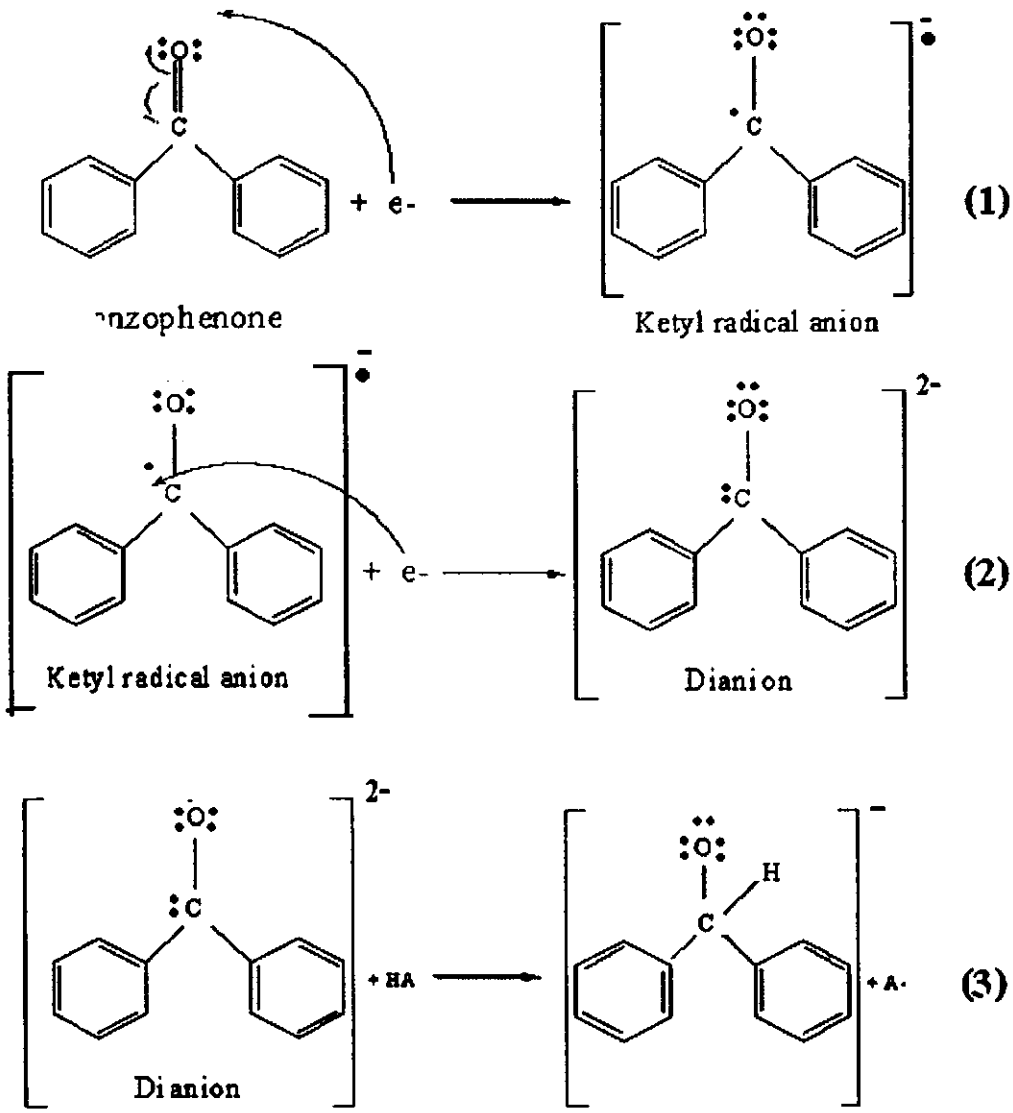

Scheme 1 The mechanism of Benzophenone which occur two reduction and one oxidation reaction (Abdirisak *et al.*, 2002).

3.1.3 Electrochemical behavior of α-Tetralone compound

3.1.3.1 Cyclic voltammetry of blank solution

Cyclic voltammogram of blank solution was performed in the potential window of 1.000 to -3.000 V vs Ag/AgCl which there was no peak, indicating that there was no significant impurities.

3.1.3.2 Redox behavior of α-Tetralone compound

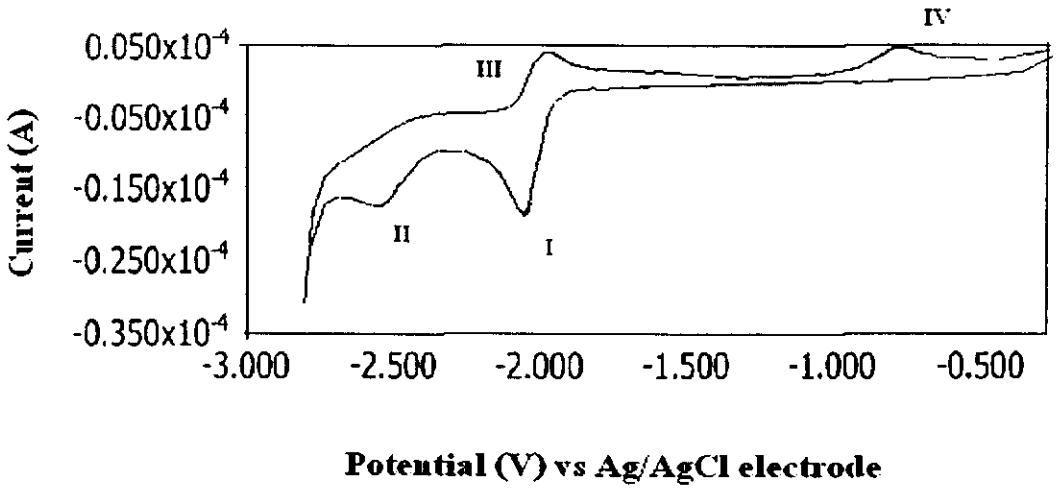

Figure 15 Cyclic voltammogram of 1.0 x 10^{-3} M α-Tetralone at GCE in 50 ml CH_3CN which 0.1 M TBAP as a supporting electrolyte with scan rate of 100 mV/s and resting potential is -0.216 V vs Ag/AgCl.

The first reduction peak appears at -2.182 V vs Ag/AgCl and when the scan is furthered to more negative potential, the second reduction potential of occurs at -2.487 V vs Ag/AgCl. If the potential scan is switched at -2.800 V, the second oxidation peak (IV) occurs at Epa_2 is equal -0.785 V vs Ag/AgCl. This oxidation is the couple of Epc_2 due to the fact that if the switching potential is at -1.500 V, the reduction does not appear which is shown in Figure 15.

The first couple (I and III) occurs at $E_1^{\circ\prime}$= -1.749 V vs NHE (E = 0.222 vs NHE), the minimum reduction potential of all ketones. This couple is not completely chemically reversible ($Ipa_1/Ipc_1 \neq 1$). This suggests that the ketyl radical of α-Tetralone is quite unstable and can partially further react. This behavior is different from that of Benzophenone, This is probably due to the unability of the electron of ketyl radical to delocalize between two phenyl groups as in Benzophenone.

The $\triangle Ep_1$(73 mV) is somewhat higher than the theoretical value, reflecting that the electron transfer is quite slow at this scan rate. Slow electron transfer causes the peak separation to increase.

Both reduction and oxidation are purely diffusion controlled. It exhibits a linear relationship between peak currents and square root of scan rate which shown in Figure 16. Detailed studies reveal that its electron transfer follows: Randles-Sevcik equation.

Table 16 The relationship of square root of scan rate and current peaks of α-Tetralone

Scan rate (mV/s)	Square root of scan rate $(mV/s)^{1/2}$	Ipc_1 (A)	Ipc_2 (A)	Ipa_1 (A)	Ipa_2 (A)
100	10.00	1.088×10^{-5}	4.850×10^{-7}	5.215×10^{-6}	1.840×10^{-6}
200	14.14	1.374×10^{-5}	8.000×10^{-7}	6.909×10^{-6}	2.480×10^{-6}
300	17.32	1.623×10^{-5}	1.328×10^{-6}	8.504×10^{-6}	2.540×10^{-6}
400	20.00	1.793×10^{-5}	1.745×10^{-6}	9.197×10^{-6}	2.740×10^{-6}
500	22.36	1.997×10^{-5}	1.694×10^{-6}	9.724×10^{-6}	2.960×10^{-6}
600	24.29	2.213×10^{-5}	2.242×10^{-6}	1.111×10^{-5}	3.220×10^{-6}

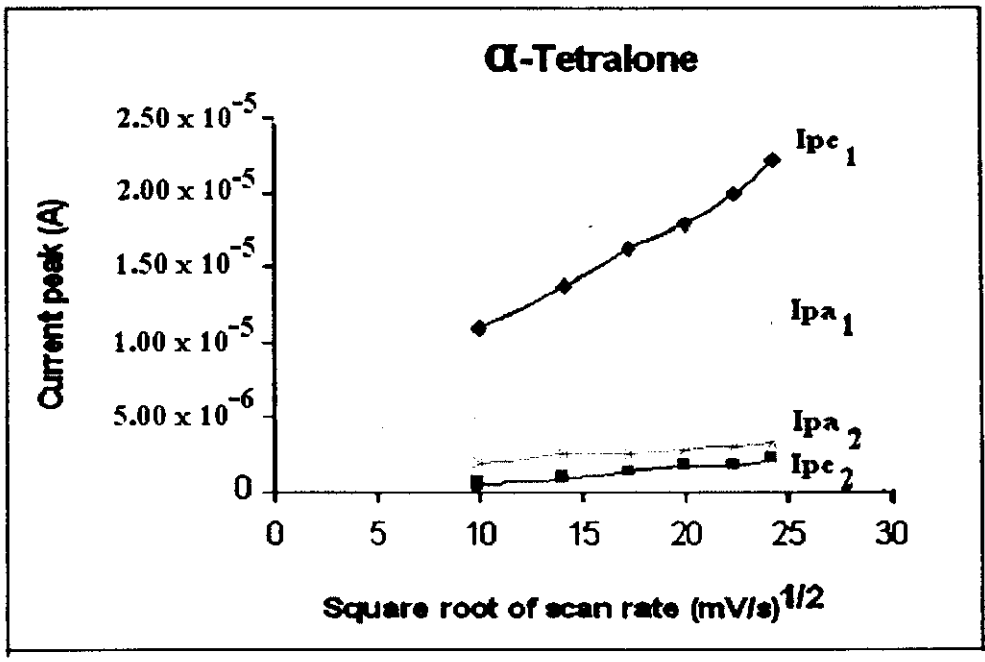

Figure 16 The plotting between square root of scan rate with current peaks (Ipc_1, Ipa_1, Ipc_2 and Ipa_2) of α-Tetralone

Discussion

The formation of ketyl radical occurs at more negative potential because of less possibility of resonance effect of α–Tetralone hence less stability of the product than that of Benzophenone. This also increases the electron density at phenyl group and implements the different behavior from Benzophenone, i.e, the second oxidation is able to occur. Due to the fact that there is only one carbonyl group, α–Tetralone can not exhibit the second reduction of the second carbonyl group as in quinones. Instead, the second reduction which occurs at very negative potential must be due to the phenyl group.

The height of this peak (II) is comparable with the first peak (I), suggesting that peak (II) involves one electron. In addition, the product is somewhat unstable and electron transfer process is quite slow because the couple Epc_2 and Epa_2 is

electrochemical quasi-reversible with $\triangle Ep_2$ = 1.780 V vs Ag/AgCl. The most important characteristic is that second couple occurs independently from the first couple so that they do not disturb each other. The reactions of α–Tetralone can be summarized in Scheme 2.

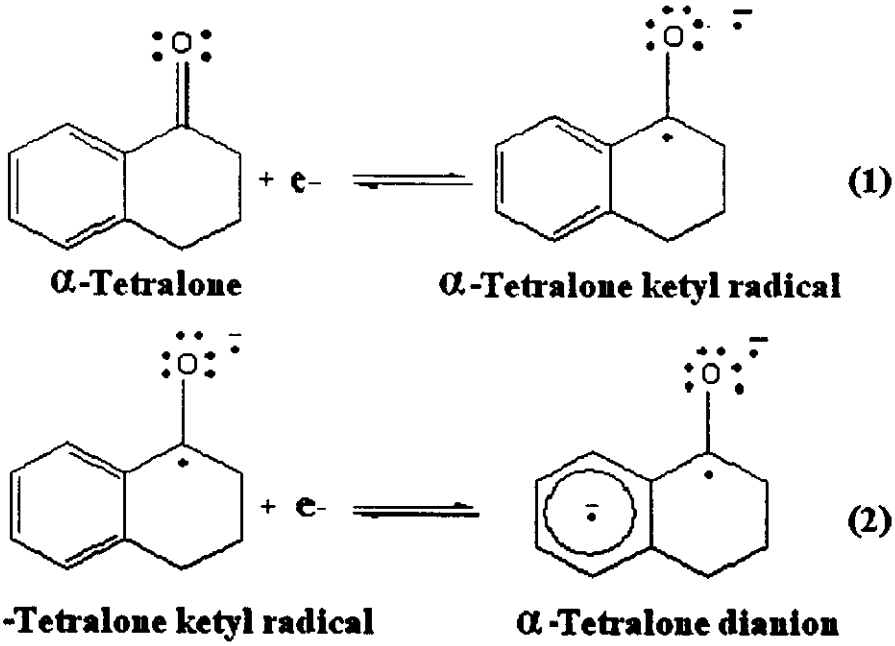

Scheme 2 Redox reactions of α–Tetralone

3.1.4 Electrochemical behavior of Anthrone compound

3.1.4.1 Cyclic voltammetry of blank solution

Blank cyclic voltammogram was recorded in the potential window of -2.000 V to 0.000 V vs Ag/AgCl. Indicating that there are no significant impurities.

3.1.4.2 Redox behavior of Anthrone

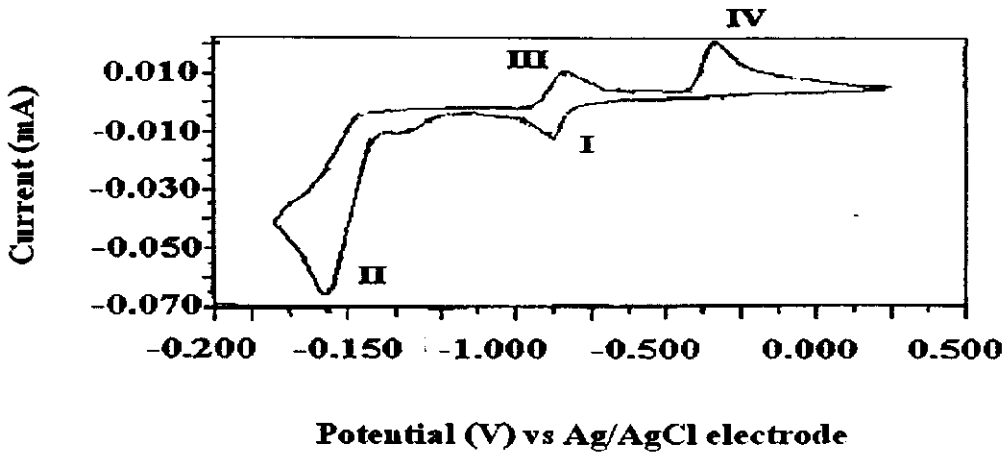

Figure 17 Cyclic voltammogram of 1.0 x 10^{-3} M Anthrone at GCE in 50 ml CH_3CN which 0.1 M TBAP as supporting electrolyte with scan rate of 100 mV/s and resting potential is -1.680 V.

The first redox couple is chemically reversible due to the fact that Ipa_1/Ipc_1 = 0.940. It is also electrochemically reversible since ΔEp_1 = 0.047 V, This behavior is diffusion controlled. Detailed studies reveal that its electron transfer follows Randles-Sevcik equation. Anthrone exhibits a linear relationship between peak current and square root of scan rate as shown in Figure 18 and 19 respectively.

Table 17 The data of the current peaks and square root of scan rate of Anthrone

Scan rate (mV/s)	Square root of scan rate $(mV/s)^{1/2}$	Ipc_1 (A)	Ipc_2 (A)	Ipa_1 (A)	Ipa_2 (A)
100	10.00	1.826 x 10^{-5}	5.148 x 10^{-6}	1.473 x 10^{-5}	2.331 x 10^{-5}
200	14.14	2.264 x 10^{-5}	1.366 x 10^{-5}	1.873 x 10^{-5}	5.754 x 10^{-5}
300	17.32	2.628 x 10^{-5}	2.101 x 10^{-5}	2.388 x 10^{-5}	7.732 x 10^{-5}
400	20.00	3.022 x 10^{-5}	2.644 x 10^{-5}	2.766 x 10^{-5}	9.441 x 10^{-5}

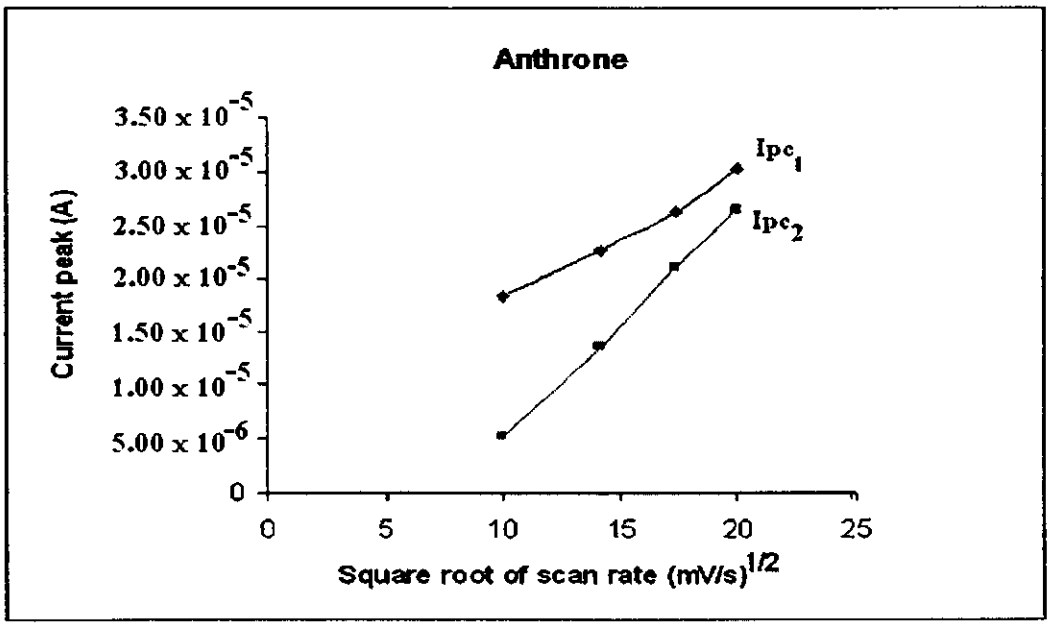

Figure 18 The plotting between square root of scan rate with the first reduction current peak (Ipc_1) and the second reduction current peak (Ipc_2) of Anthrone

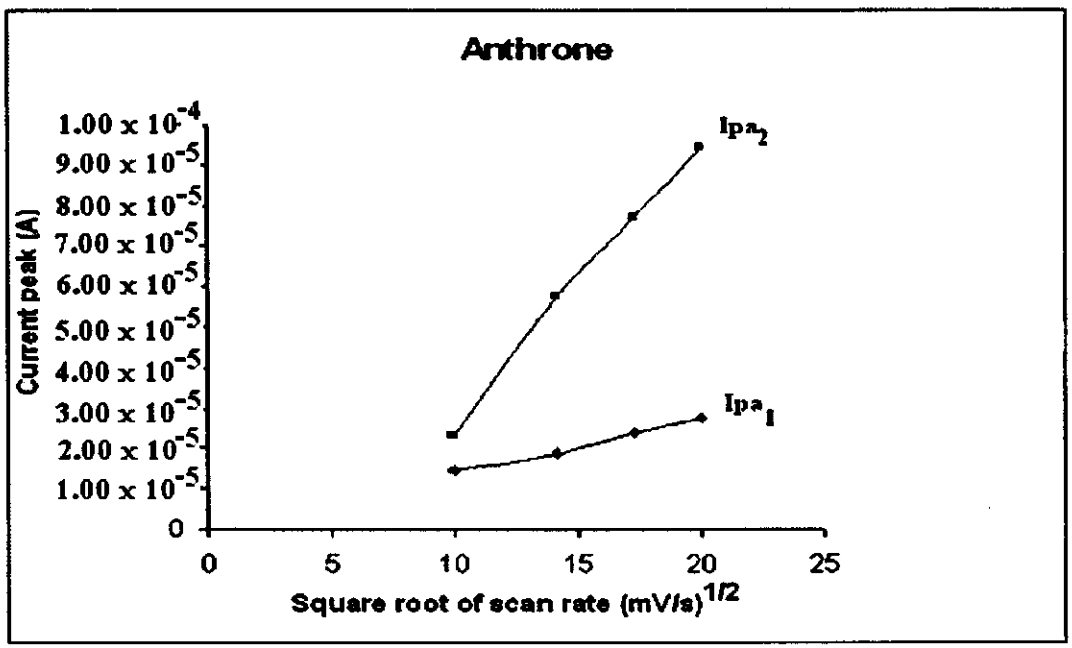

Figure 19 The plotting between square root of scan rate with the first oxidation current peak (Ipa_1) and the second reduction current peak (Ipa_2) of Anthrone

Discussion

Anthrone behaves in a quite similar way to α–Tetralone; i.e., the first reduction couple (I, III) due to the formation of ketyl radical and the second reduction (II) due to phenyl group.

However, the first couple (I, III) occurs at much more positive potential (better reduction compared with Benzophenone), clearly reflecting the effect of the second phenyl group in addition to the presence of connecting carbon to facilitate electron delocalzation in the radical product and hence increasing its stability. This also implements facile kinetics and chemical reversibility as can be seen from Ipa_1/Ipc_1 is equal to 1.128 V and $\Delta Ep_1 = 0.054$ V vs Ag/AgCl, very close to theoretical value, the distinctive behavior of Anthrone compared with α–Tetralone. By Randels-Sevcik Relationship, this first process is also diffusion controlled.

The increase of the second reduction peak (II) is very high, compared with the first peak due to the presence of one more phenyl group is the proof that this peak corresponds to the reduction of phenyl group and suggests that the reduction can occur at both phenyl groups and the total number of electron is multiple. Nevertheless, the product is unstable and the process of electron transfer is quite slow ($Ipa_2/Ipc_2 = 1.796$ V, $\Delta Ep_2 = 1.284$ V). The reaction and resonance form of the product are shown in Scheme 3.

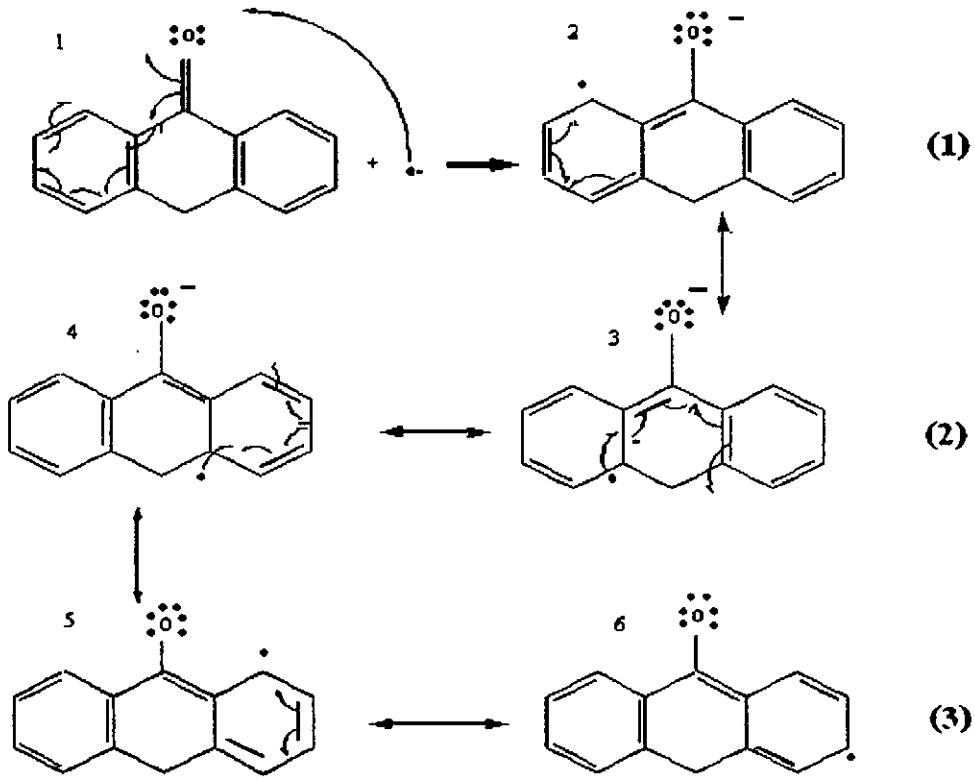

Scheme 3 The first reduction of Anthrone and resonance forms of the product

The formal potential of the first of Anthrone ($E_1^{O'}$ = -0.640 V vs NHE) is very close to that of Anthraquinone ($E_1^{O'}$ = -0.656 V vs NHE). This is due to the fact that the resonance forms of the product of Anthrone and Anthraquinone are quite similar with the same number of possible resonance forms (6). The resonance form of Anthraquinone product is shown in Scheme 4.

Scheme 4 The first reduction of Anthraquinone and resonance forms of the product.

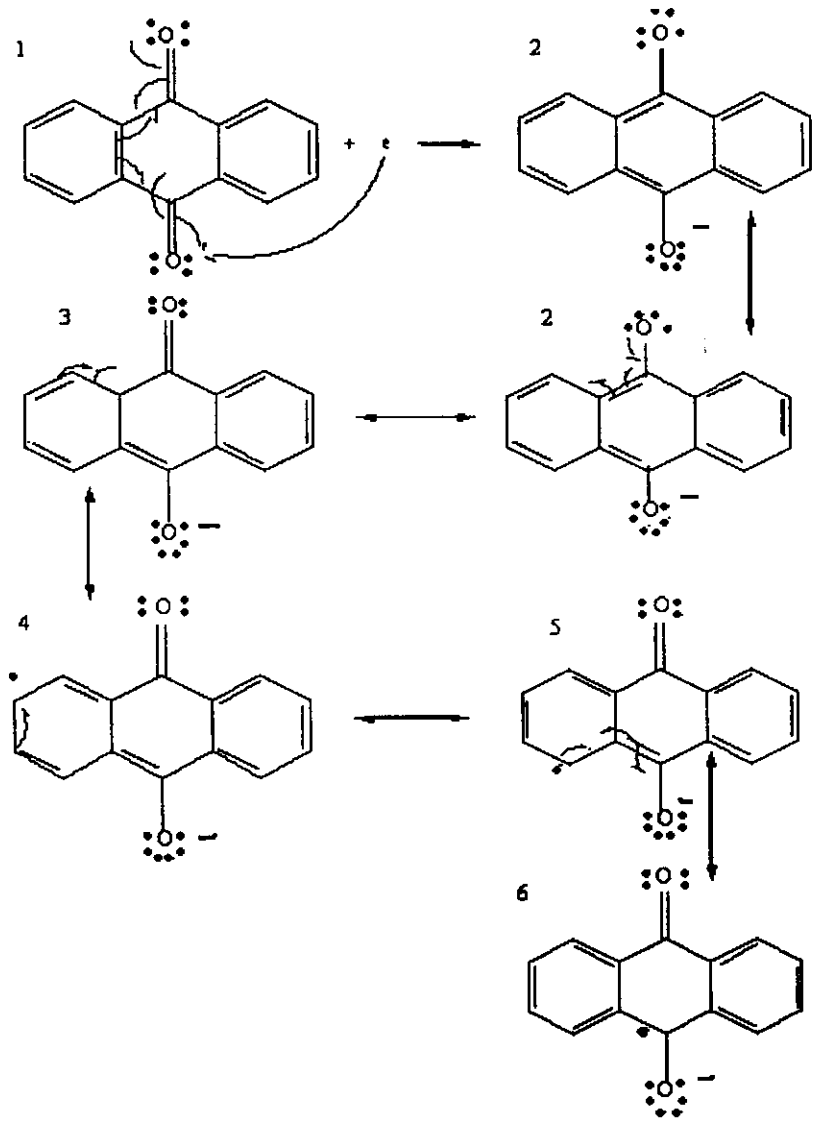

Scheme 4 The resonance of Anthraquinone

The result also indicates that the present of additional carbonyl group is not significant to the stability of reduction product. This is supported by the fact that there is no resonance form which radical appears at the lower carbonyl group.

3.1.5 Electrochemical behavior of 9-Xanthone compound

3.1.5.1 Cyclic voltammetry of blank solution

Cyclic voltammogram of blank solution was recorded in the the potential window of -3.000 to 0.500 V vs Ag/AgCl with indicating that there are no significant impurities.

3.1.5.2 Redox behavior of 9-Xanthone compound

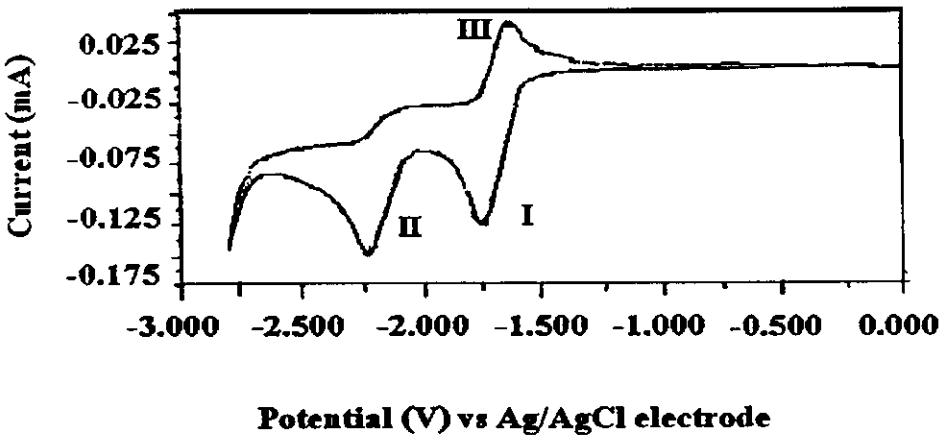

Figure 20 Cyclic voltammogram of 1.0 x 10^{-2} M 9-Xanthone at GCE in 50 ml CH_3CN which 0.1 M TBAP as supporting electrolyt with scan rate of 100 mV/s and resting potential is -0.006 V.

Xanthone exhibits two steps of reduction which show in Figure 20. The first reduction peak occurs at -1.889 V and oxidation peak is -1.552 V vs Ag/AgCl. There is one independence reduction peak which occurs at -2.230 V vs Ag/AgCl. This peak is electrochemical irreversible and is no oxidation couple.

The redox reaction diffusion controlled reflected by linear graph in Figure 21. Detailed studies reveal that its electron transfer follows the Randles-Sevcik equation.

Table 18 The relationship of square root of scan rate and current peaks of Xanthone

Scan rate (mV/s)	Square root of scan rate $(mV/s)^{1/2}$	Ipc_1 (A)	Ipc_2 (A)	Ipa_1 (A)
100	10.00	8.800×10^{-5}	7.414×10^{-5}	6.050×10^{-5}
200	14.14	1.080×10^{-4}	9.410×10^{-5}	6.860×10^{-5}
300	17.32	1.250×10^{-4}	1.093×10^{-4}	7.889×10^{-5}
400	20.00	1.390×10^{-4}	1.205×10^{-4}	8.558×10^{-5}
500	22.36	1.470×10^{-4}	1.291×10^{-4}	9.223×10^{-5}

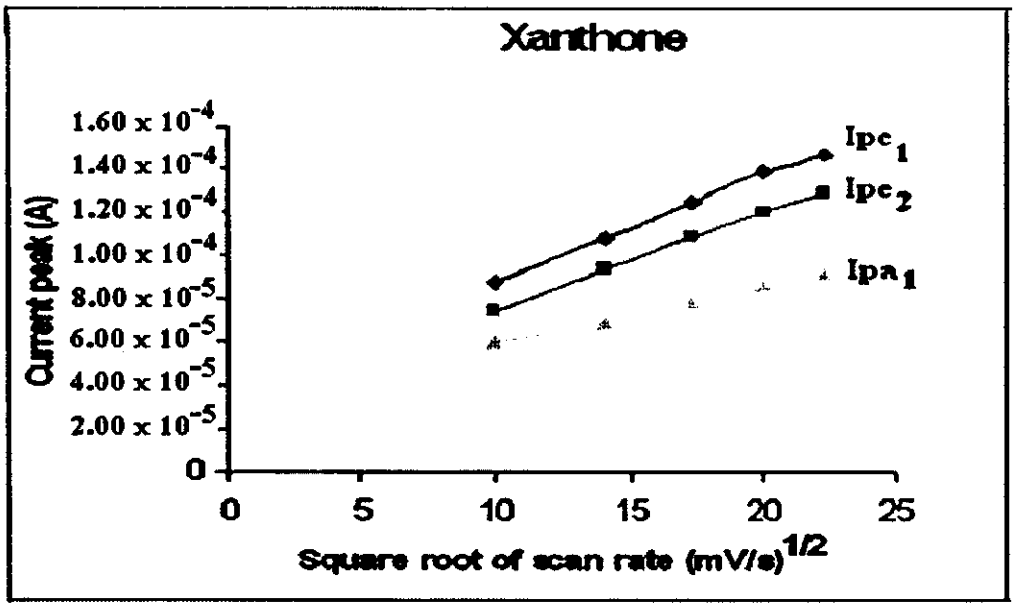

Figure 21 The plotting between square root of scan rate with reduction current peak (Ipc_1 and Ipc_2) and oxidation current peak (Ipa_1) of Xanthone.

Discussion

The electrochemical behavior of Xanthone is so much similar to that of Benzophenone as shown in Figure 13, the first electrochemically quasi-reversible

couple (I, III) is due to the reduction of carbonyl group. The fact that the second reduction peak (II) has somewhat less height, although there are two phenyl groups, without any corresponding (coupling) oxidation strongly indicates that this is due to the formation of dianion by carbonyl group, not the phenyl one. The reaction scheme of Xanthone is therefore the same as that of Benzophenone. The redox couple exhibits not completely chemically reversible due to the fact that Ipa_1/Ipc_1 is equal to 0.629.

The reason that the second oxidation can not occur at the phenyl position -0.334 V vs Ag/AgCl, which is different from α–Tetralone and Anthrone, is probably that there is no connection (carbon with hydrogen only) between the phenyl group which make the delocalization of electron impossible. Therefore, the next project should be the investigation of the electrochemical behavior compounds that have similar structure.

Conclusion of the electrochemical behavior of ketones

The redox reaction of Cyclohexanone does not exhibit any significant peak because it can not delocalize electron in the structure. In the case of Benzophenone shows two reduction and one oxidation process which involving with one electron transfer in each step of reaction.

Anthrone behaves in a quite similar way to α –Tetralone which exhibits two redox couple in CH_3CN solution; i.e., the first reduction couple due to the formation of ketyl radical and the second reduction due to phenyl group.

The electrochemical behavior of Xanthone is so much similar to that of Benzophenone. The first electrochemically and chemically quasi-reversible couple (I, III) is due to the reduction of carbonyl group. The fact that the second reduction peak (II) has somewhat less height, although there are two phenyl groups, without any corresponding (coupling) oxidation strongly indicates that this is due to the formation

of dianion by carbonyl group, not the phenyl one. The reason that the second oxidation can not occur at the phenyl position, which is different from α –Tetralone and Anthrone, is probably that there is no connection (carbon with hydrogen only) between the phenyl group. This can make the delocalization of electron impossible.

Ketones can be classified into two groups: those with two consecutive reductions both on the carbonyl group and on the carbonyl group followed by the phenyl group. The formal potential of the first couple of the ketones, the number of couples, separation peak and the first oxidation current peak to reduction current peak are summarized in Table 19.

Table 19 The formal potentials of the first couple of the ketones under investigation in CH_3CN with 0.1 mol/l of TBAP at GCE with scan rate is 100 mV/s.

Compounds	$E_1°'$ (V) vs Ag/AgCl	Number of couples	ΔEp_1 (mV)	Ipa_1/Ipc_1
Cyclohexanone	-	-	-	-
Benzophenone	-1.758	1	80	0.956
α - Tetralone	-2.020	2	73	0.479
Anthrone	-0.875	2	63	1.100
Xanthone	-1.687	1	127	0.629

From the Table 19 We found that the formal potential of the first couple of Anthrone is highest and α – Tetralone is lowest. The separation peak of all ketones is somewhat higher than theoretical value (> 59 mV) which indicates that the electron transfer is quite slow at 100 mV/s. All ketones exhibit not completely chemically reversible except Benzophenone due to Ipa_1/Ipc_1 is not equal to 1.

3.2 The electrochemical behavior of quinone compounds

3.2.1 Electrochemical behavior of *p*-Benzoquinone compound

3.2.1.1 Cyclic voltammetry of blank

Cyclic voltammogram of blank solution was performed in the potential window of 0.000 to -2.500 V vs Ag/AgCl. Found that there are no significant impurities.

3.2.1.2 Redox behavior of *p*-Benzoquinone

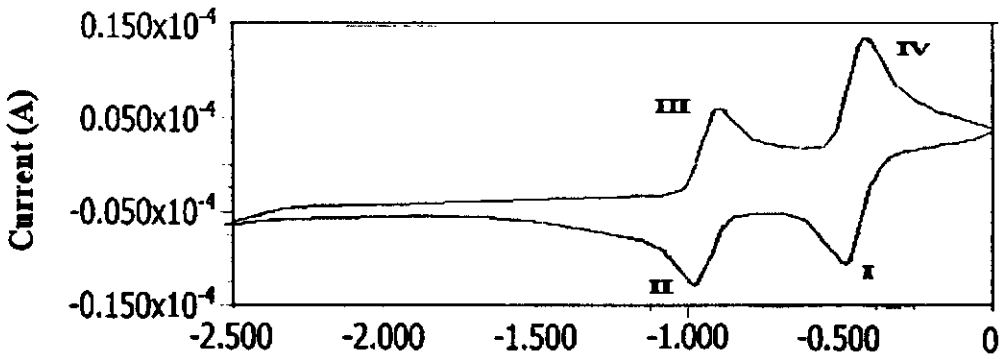

Figure 22 Cyclic voltammogram of 1.0 x 10^{-3} M *p*-Benzoquinone at GCE in 50 ml CH_3CN which 0.1 M TBAP as supporting electrolyte with scan rate of 100 mV/s and resting potential is -0.0011 V.

Discussion

p-Benzoquinone exhibits two redox couples which show in Figure 22. The first redox couple occurs at Epc_1 = -0.479 V and Epa_1 = -0.417 V. The second redox couple occurs at Epc_2 = -0.974 V and Epa_2 = 0.906 V. Both reduction and oxidation are purely diffusion controlled. The ΔEp (62 mV) is somewhat higher than the theoretical value

(ΔEp = 59 mV), indicate that the electron transfer is slow at 100 mV/s. Slow electron transfer causes the peak separation to increase. The first couple (I and IV) occurs at $E_1°'$= -0.448 V vs Ag/AgCl.

p-Benzoquinone is diffusion control of the current. It exhibits a linear relationship between peak currents and square root of scan rate as shown in Figure 23.

Table 20 The relationship of square root of scan rate and current peaks of *p*-Benzoquinone

Scan rate (mV/s)	Square root of scan rate $(mV/s)^{1/2}$	Ipc_1 (A)	Ipc_2 (A)	Ipa_1 (A)	Ipa_2 (A)
100	10.00	9.260×10^{-6}	7.493×10^{-6}	1.120×10^{-5}	7.393×10^{-6}
200	14.14	1.272×10^{-5}	9.698×10^{-6}	1.297×10^{-5}	1.001×10^{-5}
300	17.32	1.567×10^{-5}	1.180×10^{-5}	1.554×10^{-5}	1.237×10^{-5}
400	20.00	1.777×10^{-5}	1.326×10^{-5}	1.796×10^{-5}	1.422×10^{-5}
500	22.36	1.990×10^{-5}	1.518×10^{-5}	2.172×10^{-5}	1.577×10^{-5}
600	24.49	2.196×10^{-5}	1.616×10^{-5}	2.548×10^{-5}	1.732×10^{-5}

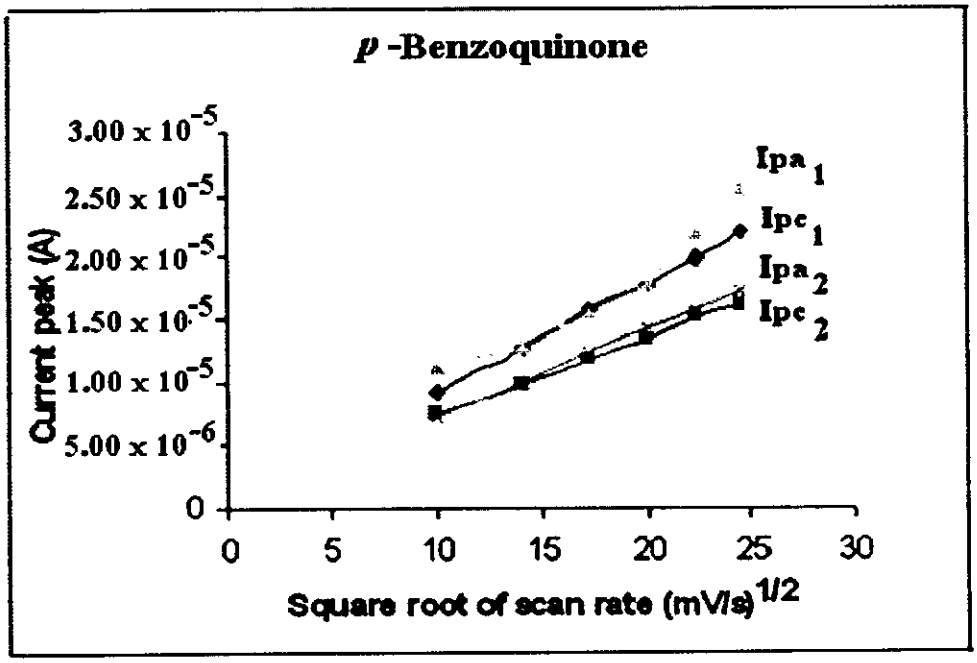

Figure 23 The plotting between square root of scan rate and current peaks of *p*-Benzoquinone.

The first reduction of Benzoquinone to its semiquinone ($Q^{\bullet -}$) in CH_3CN is electrochemically reversible due to is diffusion control from graph of Randles-sevcik equation and chemically reversible ($Ipa_1/Ipc_1 = 0.999$).

The semiquinone ($Q^{\bullet -}$) can be reduced to form quinone dianion in the second reduction step (Janell *et al.*, 1998) which show mechanism in Scheme 5.

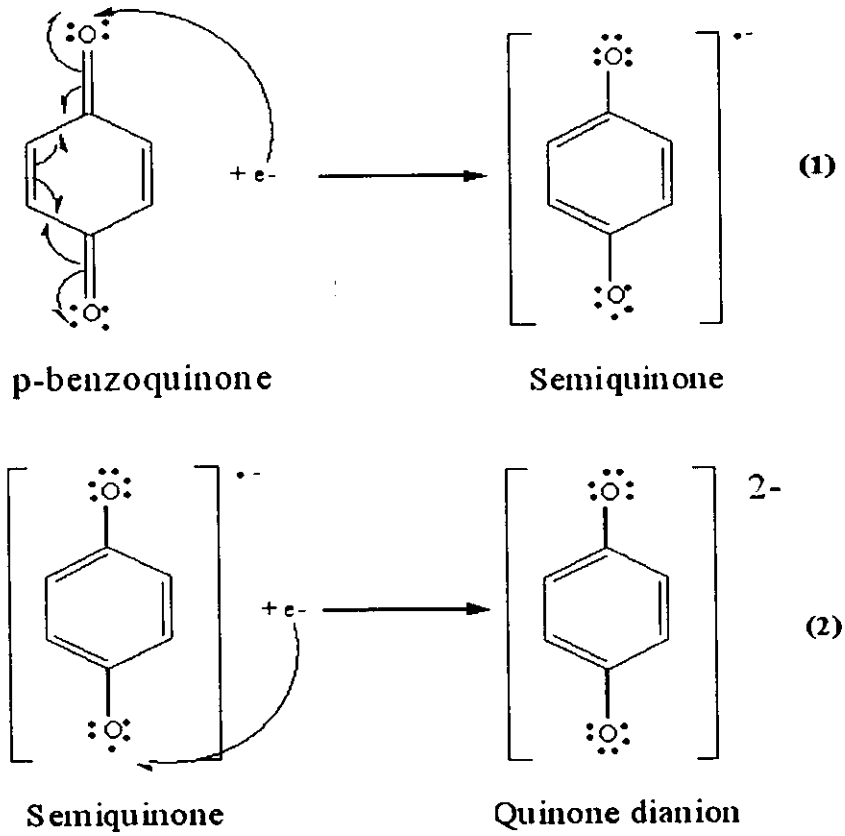

Scheme 5 The redox reaction of *p*-Benzoquinone (Janell *et al.*, 1998)

3.2.2 Electrochemical behavior of Tetrahydroxybenzoquinone compound

3.2.2.1 Cyclic voltammetry of blank

Cyclic voltammogram of blank solution was performed in the potential window from -0.250 to 2.750 V vs Ag/AgCl. Found that there are no significant impurities.

3.2.2.2 Redox behavior of Tetrahydroxy-1,4-benzoquinone compound

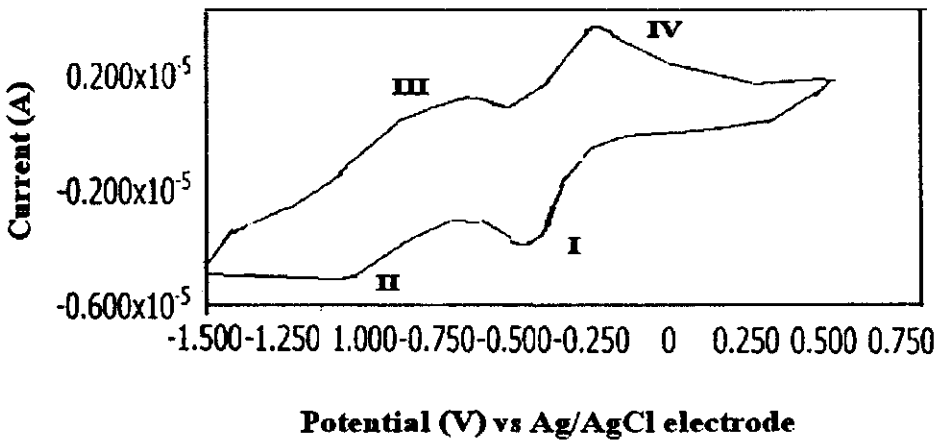

Figure 24 Cyclic voltammogram of 1.0 x 10^{-3} M Tetrahydroxybenzoquinone at glassy carbon electrode in 50 ml CH_3CN which 0.1 M TBAP as supporting electrolyte with scan rate of 100 mV/s and resting potential is -0.118 V.

Discussion

Tetrahydroxybenzoquinone exhibits two redox couples as shown in Figure 24. The first redox couple occurs at Epc_1 = - 0.422 V and Epa_1 = -0.251 V vs Ag/AgCl. The second redox couple occurs at Epc_2 = -1.150 V and Epa_2 = -0.630 V vs Ag/AgCl respectively. The ΔEp_1 (171 mV) is somewhat higher than the theoretical value ($\Delta Ep > 59$ mV), indicate that the electron transfer is slow at 100 mV/s. The first couple (I and IV) occurs at $E_1°'$= -0.337 V vs Ag/AgCl, the maximum reduction potential of all quinones. The first redox couple is not completely chemically reversible (Ipa_1/Ipc_1 = 0.285) and the second couple is not completely chemically reversible also (Ipa_2/Ipc_2 = 0.716). The both redox reactions of test solution are not diffusion controled and has adsorption behavior at GCE. It exhibits not linear relationship between peak currents and square root of scan rate which shown in Figure 25 and 26 respectively. Detailed studies reveal that its electron transfer follows Randles-sevcik equation.

Table 21 The relationship of square root of scan rate and current peaks of Tetrahydroxybenzoquinone

Scan rate (mV/s)	Square root of scan rate $(mV/s)^{1/2}$	Ipc_1 (A)	Ipc_2 (A)	Ipa_1 (A)	Ipa_2 (A)
100	10.00	6.291×10^{-7}	2.790×10^{-7}	2.330×10^{-6}	2.000×10^{-7}
200	14.14	8.362×10^{-7}	5.530×10^{-7}	3250×10^{-6}	1.610×10^{-7}
300	17.32	1.175×10^{-6}	6.720×10^{-7}	4.060×10^{-6}	1.340×10^{-7}
400	20.00	4.200×10^{-6}	9.270×10^{-7}	3.720×10^{-6}	0.000
500	22.36	1.629×10^{-5}	9.830×10^{-7}	5.192×10^{-6}	1.760×10^{-7}
600	24.49	4.905×10^{-5}	1.912×10^{-6}	5.723×10^{-6}	3.930×10^{-7}

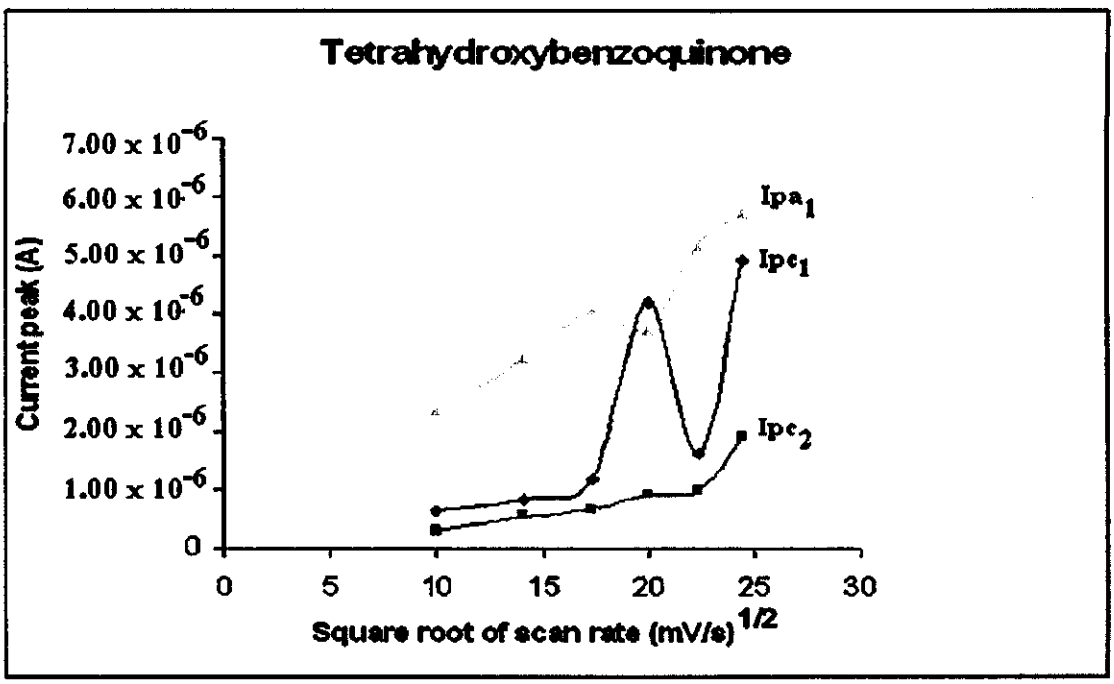

Figure 25 The plotting between square root of scan rate and current peaks (Ipc_1, Ipc_2 and Ipa_1) of Tetrahydroxybenzoquinone

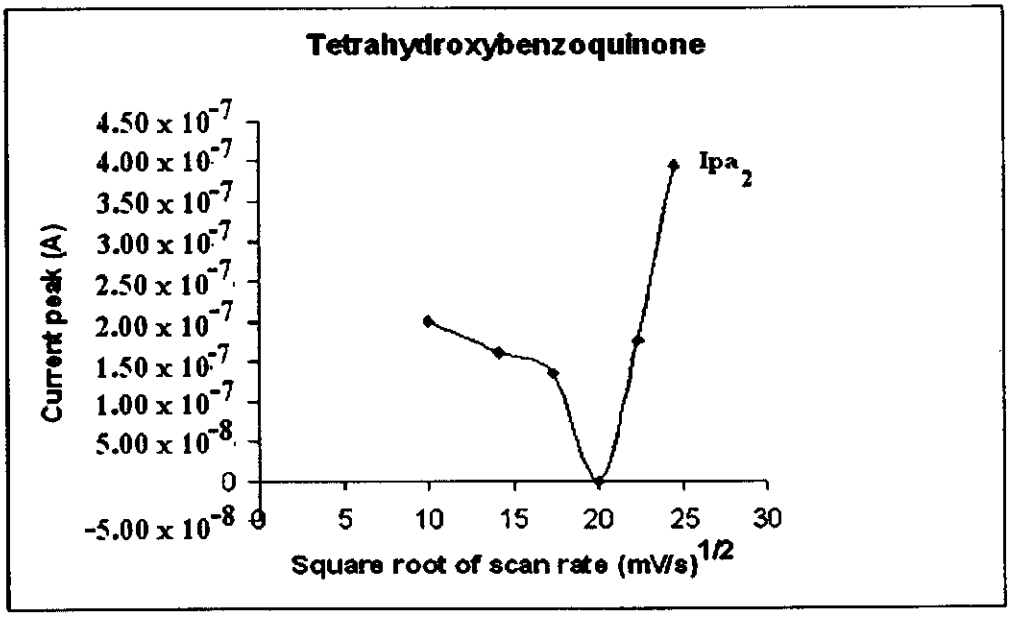

Figure 26 The plotting between square root of scan rate and oxidation current peak I (Ipa_2) of Tetrahydroxybenzoquinone

The first reduction reaction corresponds to the transformation of quinone (Q) into semiquinone ($Q^{\bullet-}$) and the second to the transformation of semiquinone ($Q^{\bullet-}$) into quinine dianion (Q^{2-}) which this behavior is similar with p-Benzoquinone.

The first formal potential is equal to -0.337 V vs NHE. The presence of electron withdrawing group such as hydroxyl group helps stabilize the reduction product (Janell *et al.*, 1998), hence the more positive reduction potentials as can be clearly seen in the case of Tetrahydroxybenzoquinone compared with those of Benzoquinone or dihydroxy derivatives compared with the parent Anthraquinone compound.

3.2.3 Electrochemical behavior of 1,4-Naphthoquinone compound

3.2.3.1 Cyclic voltammetry of blank

Cyclic voltammogram of blank solution was performed in the potential window from -0.250 to 2.750 V vs Ag/AgCl. Found that there are no significant impurities.

3.2.3.2 Redox behavior of 1,4-Naphthoquinone

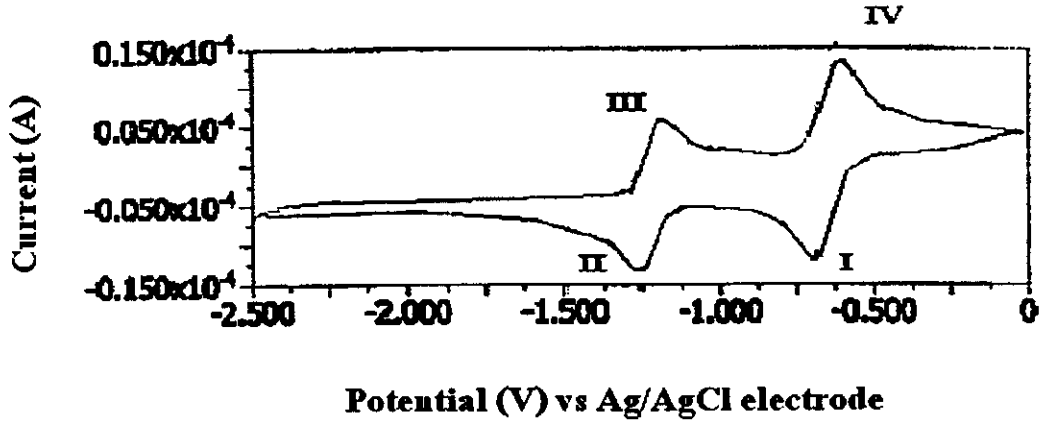

Figure 27 Cyclic voltammogram of 1.0 x 10^{-3} M 1,4-Naphthoquinone at GCE in 50 ml CH_3CN which 0.1 M TBAP as a supporting electrolyte with scan rate of 100 mV/s and resting potential is -0.0011 V.

Discussion

The electrochemical behavior of 1,4-Naphthoquinone is so much similar to that *p*-Benzoquinone which the first reduction potential (Epc_1) occurs at -0.686 V vs Ag/AgCl and the first oxidation (Epa_1) is -0.620 V vs Ag/AgCl. The first formal potential ($E_1^{O'}$) is equal to -0.693 V vs Ag/AgCl. The second reduction and oxidation potential appears at -1.260 V and -1.189 V vs Ag/AgCl respectively. The first couple is chemically reversible (Ipa_1/Ipc_1 = 0.970). Both reduction and oxidation are purely diffusion controlled. The relationship between peak currents and square root of scan rate is linear as shown in Figure 28. Detailed studies reveal that its electron transfer follows: Randles-sevcik equation.

Table 22 The relationship of square root of scan rate and current peaks of 1,4-Naphthoquinone

Scan rate (mV/s)	Square root of scan rate $(mV/s)^{1/2}$	Ipc_1 (A)	Ipc_2 (A)	Ipa_1 (A)	Ipa_2 (A)
100	10.00	1.050×10^{-5}	1.204×10^{-5}	8.135×10^{-6}	1.055×10^{-5}
200	14.14	1.470×10^{-5}	1.530×10^{-5}	1.105×10^{-5}	1.475×10^{-5}
300	17.32	1.820×10^{-5}	1.849×10^{-5}	1.371×10^{-5}	1.826×10^{-5}
400	20.00	2.110×10^{-5}	2.177×10^{-5}	1.606×10^{-5}	2.118×10^{-5}
500	22.36	2.450×10^{-5}	2.510×10^{-5}	1.867×10^{-5}	2.448×10^{-5}
600	24.49	2.680×10^{-5}	2.750×10^{-5}	2.074×10^{-5}	2.678×10^{-5}

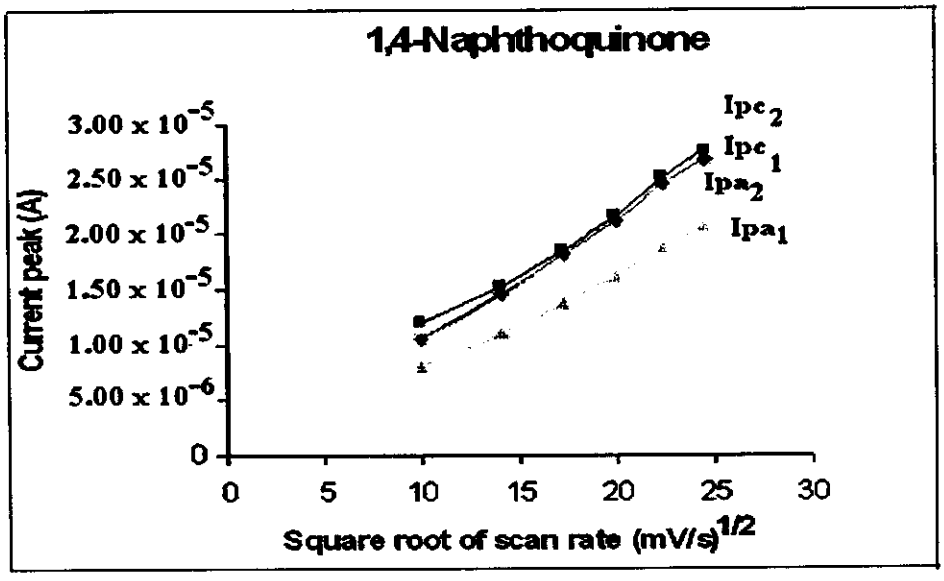

Figure 28 The plotting between square root of scan rate and current peaks (Ipc_1, Ipc_2, Ipa_1 and Ipa_2) of 1,4-Naphthoquinone

The difference of the first couple peak potential of this compound (66 mV) is somewhat higher than theoretical value (> 59 mV) which indicates that the electron transfer is quite slow at 100 mV/s. In the case of electrochemical reduction of 1,4-NQ, redox couples of $NQ/NQ^{\bullet -}$ and $NQ^{\bullet -}/NQ^{2-}$ are observed in extremely proton-deficient media such as CH_3CN. The first electron transfer step, NQ to $NQ^{\bullet -}$, exhibits a well-defined reversible voltammetric wave. On the other hand, the second redox wave of NQ is more sensitive to proton sources than the first one. The second electron transfer, $NQ^{\bullet -}$ to NQ^{2-}, is generally regarded as a quasi-reversible wave.

3.2.4 Electrochemical behavior of Anthraquinone compound

3.2.4.1 Cyclic voltammetry of blank

Cyclic voltammogram of blank solution was performed in the potential window from -0.250 to 2.750 V vs Ag/AgCl. Found that there are no significant impurities.

3.2.4.2 Redox behavior of Anthraquinone

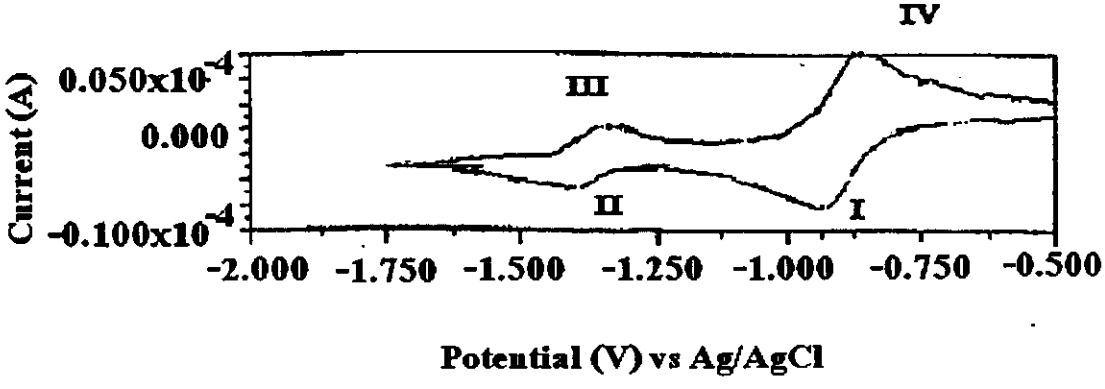

Figure 29 Cyclic voltammogram of 1.0 x 10^{-3} M Anthraquinone at GCE in 50 ml CH_3CN which 0.1 M TBAP as a supporting electrolyte with scan rate of 100 mV/s and resting potential is -0.0011 V.

Discussion

The electrochemical behavior of Anthraquinone is similar with *p*-Benzoquinone which contain two redox couples in the reaction. The first reduction potential (Epc_1) occurs at -0.935 V vs Ag/AgCl and the first oxidation is -0.861 V vs Ag/AgCl. The first couple (I and IV) occurs at $E_1°' = -0.898$ V vs Ag/AgCl , the minimum reduction potential of all quinones. For the second reduction and oxidation potential appears at -1.403 V and -1.370 V vs Ag/AgCl respectively. The first redox couple is chemically reversible ($Ipa_1/Ipc_1 = 1.082$) and the second couple is chemically reversible also ($Ipa_2/Ipc_2 = 1.299$). The ΔEp_1 of Anthraquinone (74 mV) is somewhat higher than the theoretical value ($>$ 59 mV) which indicate that the electron transfer is quite slow at this scan rate (100 mV/s). Both reduction and oxidation are purely diffusion controlled which shown in Figure 30.

Table 23 The relationship of square root of scan rate and current peaks of Anthraquinone

Scan rate (mV/s)	Square root of scan rate $(mV/s)^{1/2}$	Ipc_1 (A)	Ipc_2 (A)	Ipa_1 (A)	Ipa_2 (A)
100	10.00	6.608×10^{-6}	1.838×10^{-6}	7.151×10^{-6}	2.388×10^{-6}
200	14.14	1.004×10^{-5}	3.366×10^{-6}	1.019×10^{-5}	4.200×10^{-6}
300	17.32	1.281×10^{-5}	4.786×10^{-6}	1.256×10^{-5}	5.715×10^{-6}
400	20.00	1.543×10^{-5}	6.357×10^{-6}	1.477×10^{-5}	7.349×10^{-6}
500	22.36	1.787×10^{-5}	7.554×10^{-6}	1.708×10^{-5}	8.790×10^{-6}
600	24.49	2.046×10^{-5}	9.124×10^{-6}	1.955×10^{-5}	1.050×10^{-5}

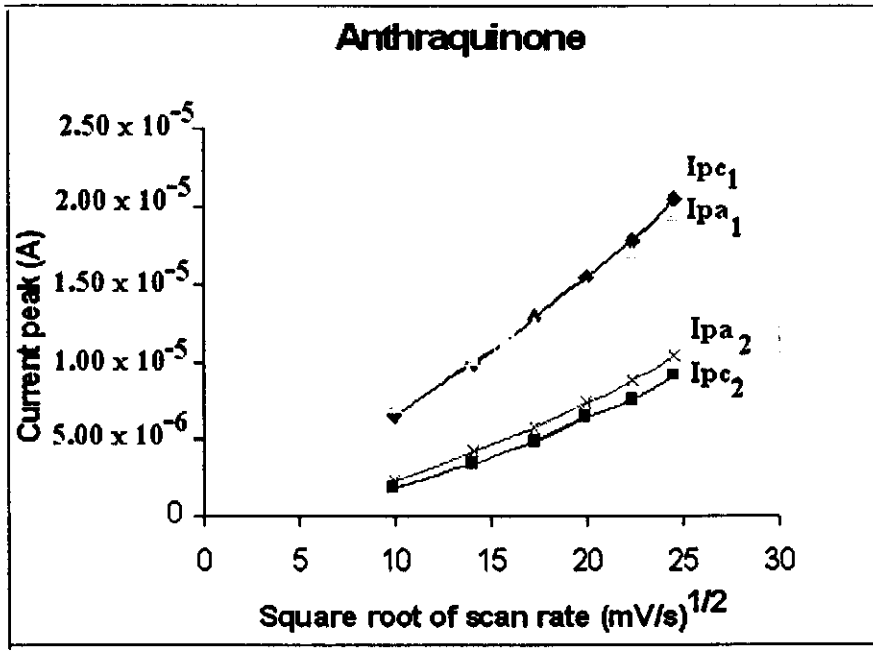

Figure 30 The plotting between square root of scan rate and current peaks of Anthraquinone

The first reduction reaction corresponds to the transformation of Anthraquione (AQ) into semiquinone ($AQ^{\bullet-}$) and the second to the transformation of semiquinone ($AQ^{\bullet-}$) into quinone dianion (AQ^{2-}) which this behavior is similar with p-Benzoquinone.

3.2.5 Electrochemical behavior of 1,2-Dihydroxyanthraquinone compound

3.2.5.1 Cyclic voltammetry of blank

Cyclic voltammogram of blank solution was performed in the potential window from -0.250 to 2.750 V vs Ag/AgCl. Found that there are no significant impurities.

3.2.5.2 Redox behavior of 1,2-Dihydroxyanthraquinone

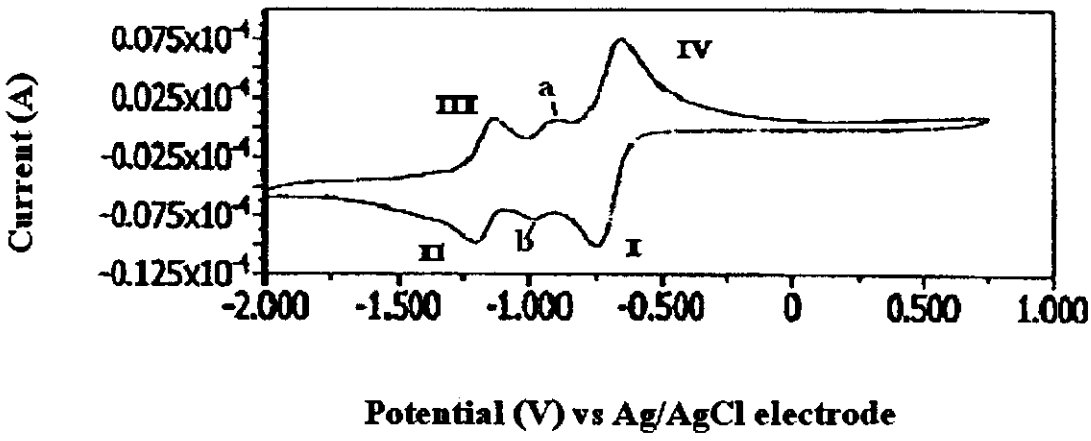

Figure 31 Cyclic voltammogram of 1.0 x 10^{-3} M 1,2-Dihydroxyanthraquinone at GCE in 50 ml CH_3CN which 0.1 M TBAP as supporting electrolyte with scan rate of 100 mV/s and resting potential is -0.0011 V.

Discussion

The electrochemical behavior of 1,2-Dihydroxyanthraquinone is so much similar to that p-Benzoquinone which the first reduction potential (Epc_1) occurs at -0.750 V vs Ag/AgCl and the first oxidation (Epa_1) is –0.657 V vs Ag/AgCl. The first formal potential ($E_1^{o'}$) is equal to -0.703 V vs Ag/AgCl. The second cathodic peak and its corresponding anodic peak which appears at -1.243 V and -1.172 V vs Ag/AgCl respectively. The first couple is chemically reversible (Ipa_1/Ipc_1 = 1.086) and the second couple is chemically reversible also (Ipa_2/Ipc_2 = 1.164).

The small peaks (a and b) are showder or interference peaks which occur due to 1,2-Dihydroxyanthraquinone compound is impurity (96% purity).

The ΔEp_1 of 1,2-Dihydroxyanthraquinone (93 mV) is somewhat higher than the theoretical value ($>$ 59 mV) which indicate that the electron transfer is quite slow

at this scan rate (100 mV/s) and slow electron transfer causes the peak separation to increase of the first couple.

1,2-Dihydroxyanthraquinone is diffusion control of the current due to it exhibits a linear graph between peak currents and square root of scan rate which shown in Figure 32. The test solution does not occur absorption phenomena at surface of the electrode. Detailed studies reveal that its electron transfer follows Randles-sevcik equation.

Table 24 The relationship of square root of scan rate and current peaks of 1,2-Dihydroxyanthraquinone

Scan rate (mV/s)	Square root of scan rate $(mV/s)^{1/2}$	Ipc_1 (A)	Ipc_2 (A)	Ipa_1 (A)	Ipa_2 (A)
100	10.00	2.231×10^{-6}	3.172×10^{-6}	8.063×10^{-6}	3.693×10^{-6}
200	14.14	3.084×10^{-6}	4.804×10^{-6}	1.170×10^{-5}	5.866×10^{-6}
300	17.32	3.631×10^{-6}	6.441×10^{-6}	1.538×10^{-5}	7.452×10^{-6}
400	20.00	4.245×10^{-6}	7.935×10^{-6}	1.872×10^{-5}	8.509×10^{-6}
500	22.36	5.022×10^{-6}	9.537×10^{-6}	2.177×10^{-5}	9.739×10^{-6}
600	24.49	5.464×10^{-6}	1.068×10^{-5}	2.463×10^{-5}	1.101×10^{-5}

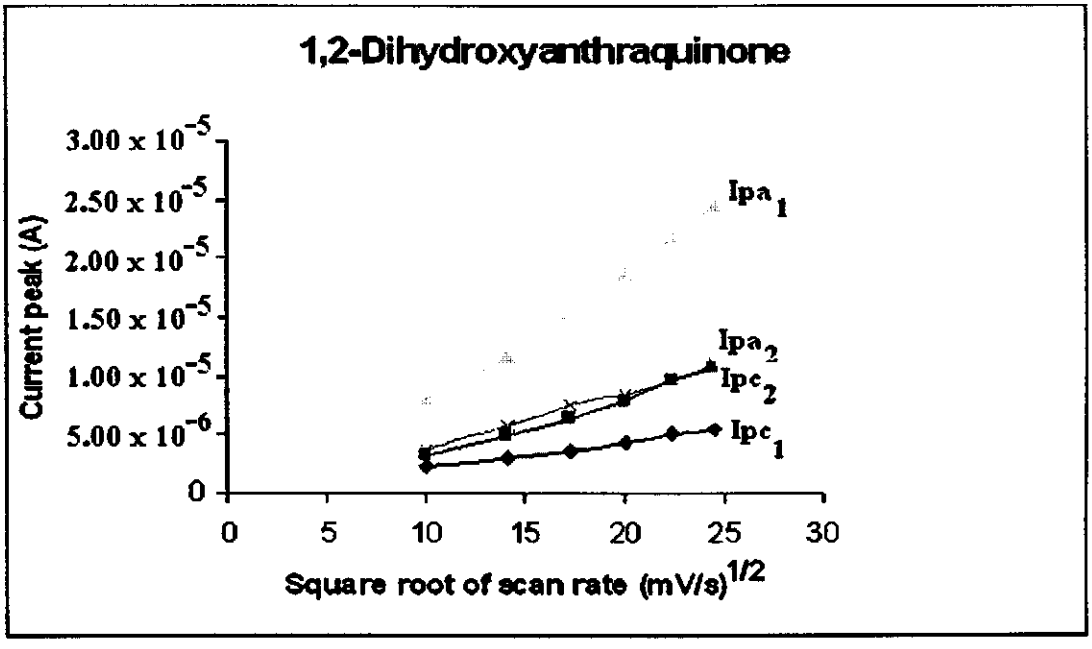

Figure 32 The plotting between square root of scan rate and current peaks of 1,2-Dihydroxyanthraquinone

The first reduction reaction corresponds to the transformation of 1,2-Dihydroxyanthraquione into semiquinone and the second to the transformation of semiquinone into quinone dianion which this behavior is similar to p-Benzoquinone.

3.2.6 Electrochemical behavior of 1,4-Dihydroxyanthraquinone compound

3.2.6.1 Cyclic voltammetry of blank

Blank Cyclic voltammogram which in the potential window of 0.000 to -2.500 V vs Ag/AgCl which there is no peak, indicating that there are no significant impurities.

3.2.6.2 Redox behavior of 1,4-Dihydroxyanthraquinone

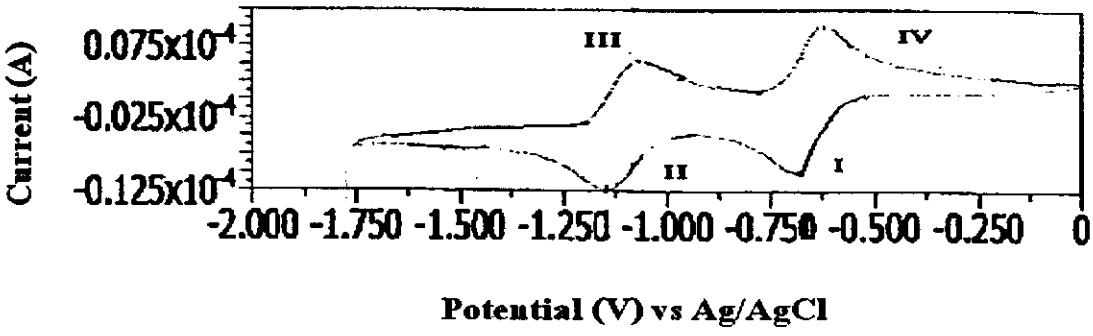

Figure 33 Cyclic voltammogram of 1.0 x 10^{-3} M 1,4-Dihydroxyanthraquinone at GCE in 50 ml CH_3CN which 0.1 M TBAP as a supporting electrolyte with scan rate of 100 mV/s and resting potential is -0.0011 V.

Discussion

The cyclic voltammogram of 1,4-Dihydroxyanthraquinone shows two redox couples in CH_3CN as in Figure 33. It undergo two successive and distinct reduction/oxidantion process The first reduction/oxidation occur at -0.683 V and -0.615 V vs Ag/AgCl respectively. This behavior shows the second reduction at -1.150 V and the second oxidation at -1.080 V vs Ag/AgCl. The first couple (I and IV) occurs at $E_1°' = -0.653$ V vs Ag/AgCl.

Both reduction and oxidation are diffusion control of the current. It exhibits a linear relationship between peak currents and square root of scan rate which shown in Figure 34. Detailed studies reveal that its electron transfer follows Randles-sevcik equation.

Table 25 The relationship of square root of scan rate and current peaks of 1,4-Dihydroxyanthraquinone

Scan rate (mV/s)	Square root of scan rate $(mV/s)^{1/2}$	Ipc_1 (A)	Ipc_2 (A)	Ipa_1 (A)	Ipa_2 (A)
100	10.00	8.549×10^{-6}	9.946×10^{-6}	9.427×10^{-6}	8.868×10^{-6}
200	14.14	1.282×10^{-5}	1.393×10^{-5}	1.477×10^{-5}	1.250×10^{-5}
300	17.32	1.624×10^{-5}	1.709×10^{-5}	1.963×10^{-5}	1.576×10^{-5}
400	20.00	1.917×10^{-5}	2.039×10^{-5}	2.384×10^{-5}	1.876×10^{-5}
500	22.36	2.133×10^{-5}	2.251×10^{-5}	2.660×10^{-5}	2.084×10^{-5}
600	24.49	2.368×10^{-5}	2.493×10^{-5}	3.040×10^{-5}	2.307×10^{-5}

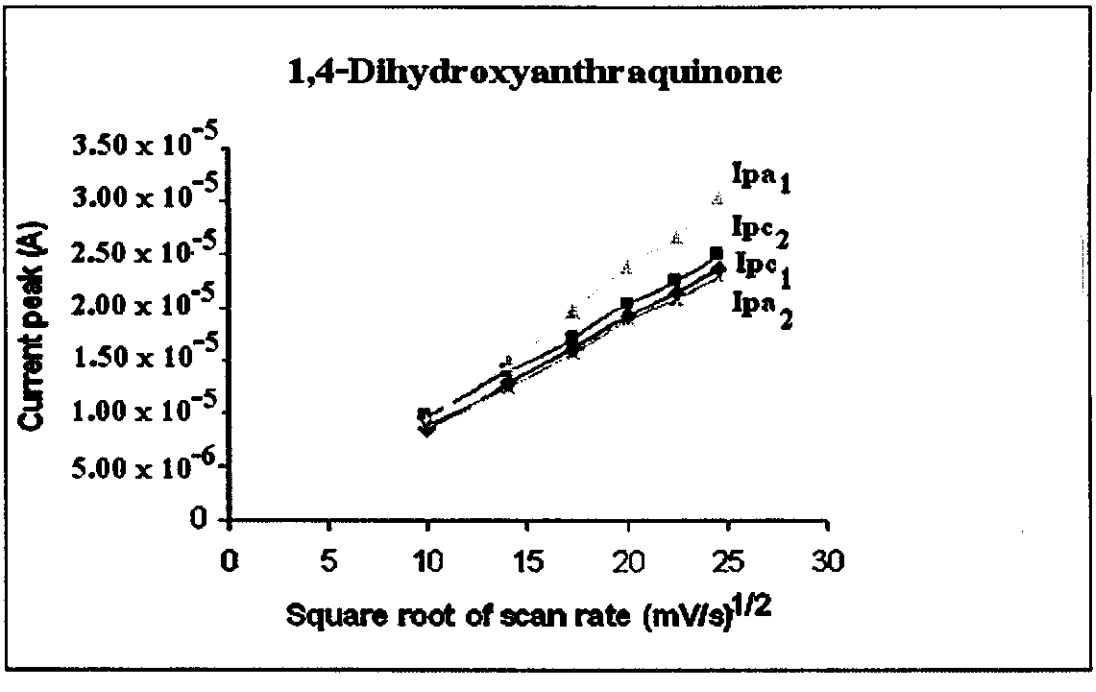

Figure 34 The plotting between square root of scan rate and current peaks of 1,4-Dihydroxyanthraquinone

Both couples are electrochemically reversible and chemically reversible (Ipa_1/Ipc_1 = 1.050) and (Ipa_2/Ipc_2 = 1.066). The ΔEp_1 of 1,4-dihydroxyanthraquinone (63 mV) is somewhat higher than the theoretical value (> 59 mV) which indicate that the electron transfer is quite slow at this scan rate (100 mV/s) and slow electron transfer causes the peak separation to increase of the first couple.The first reduction reaction corresponds to the transformation of 1,4-Dihydroxyanthraquione into semiquinone and the second to the transformation of semiquinone into quinone dianion.

3.2.7 Electrochemical behavior of 1,8-Dihydroxyanthraquinone compound

3.2.7.1 Cyclic voltammetry of blank

Cyclic voltammogram of blank solution was performed in the potential window from -0.250 to 2.750 V vs Ag/AgCl. Found that there are no significant impurities.

3.2.7.2 Redox behavior of 1,8-Dihydroxyanthraquinone

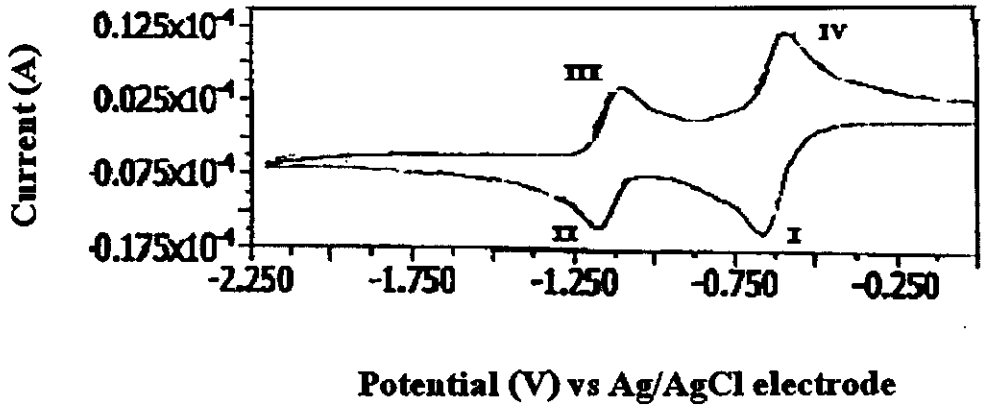

Figure 35 Cyclic voltammogram of 1.0 x 10^{-3} M 1,8-Dihydroxyanthraquinone at GCE in 50 ml CH_3CN which 0.1 M TBAP as a supporting electrolyte with scan rate of 100 mV/s and resting potential is -0.0011 V.

Discussion

The cyclic voltammogram of 1,8-Dihydroxyanthraquinone shows two redox couples in CH_3CN as in Figure 35. It undergo two successive and distinct reduction/oxidantion process The first reduction/oxidation occur at -0.657 V and -0.593 V vs Ag/AgCl respectively. This behavior shows the second reduction at -1.150 V and the second oxidation at -1.089 V vs Ag/AgCl.

Both reduction and oxidation are diffusion control of the current. It exhibits a linear relationship between peak currents and square root of scan rate which shown in Figure 36. Detailed studies reveal that its electron transfer follows Randles-sevcik equation.

Table 26 The relationship of square root of scan rate and current peaks of 1,8-Dihydroxyanthraquinone

Scan rate (mV/s)	Square root of scan rate $(mV/s)^{1/2}$	Ipc_1 (A)	Ipc_2 (A)	Ipa_1 (A)	Ipa_2 (A)
100	10.00	1.213×10^{-5}	7.258×10^{-6}	1.132×10^{-5}	7.644×10^{-6}
200	14.14	1.592×10^{-5}	1.084×10^{-5}	1.615×10^{-5}	1.051×10^{-5}
300	17.32	1.986×10^{-5}	1.312×10^{-5}	2.075×10^{-5}	1.286×10^{-5}
400	20.00	2.319×10^{-5}	1.536×10^{-5}	2.463×10^{-5}	1.499×10^{-5}
500	22.36	2.628×10^{-5}	1.716×10^{-5}	2.823×10^{-5}	1.675×10^{-5}
600	24.49	2.939×10^{-5}	1.932×10^{-5}	3.080×10^{-5}	1.878×10^{-5}

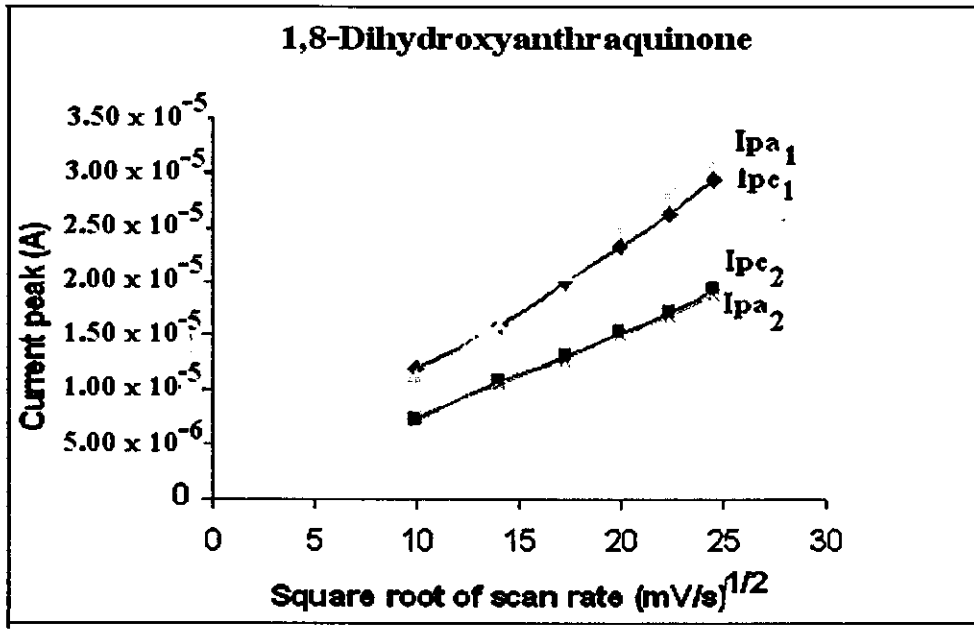

Figure 36 The plotting between square root of scan rate and current peaks of 1,8-Dihydroxyanthraquinone

Both couples are electrochemically reversible and chemically reversible (Ipa_1/Ipc_1 = 1.014) and (Ipa_2/Ipc_2 = 0.969). The formal potential of the first couple ($E^{O'}$) is equal to -0.608 V vs Ag/AgCl which has $E^{O'}$ is higher than 1,2-Dihydroxyanthraquinone and 1,4-Dihydroxyanthraquinone.

The ΔEp_1 of 1,8-Dihydroxyanthraquinone (64 mV) is somewhat higher than the theoretical value (> 59 mV) which indicate that the electron transfer is quite slow at this scan rate (100 mV/s) and slow electron transfer causes the peak separation to increase of the first couple.

The first reduction reaction corresponds to the transformation of 1,8-Dihydroxyanthraquione into semiquinone and the second to the transformation of semiquinone into quinone dianion which this electrochemical behavior is similar with all quinone.

3.2.8 Electrochemical behavior of Dammacanthal compound

3.2.8.1 Cyclic voltammetry of blank

Cyclic voltammogram of blank solution was performed in the potential window from -0.250 to 2.750 V vs Ag/AgCl. Found that there are no significant impurities.

3.2.8.2 Redox behavior of Dammacanthal

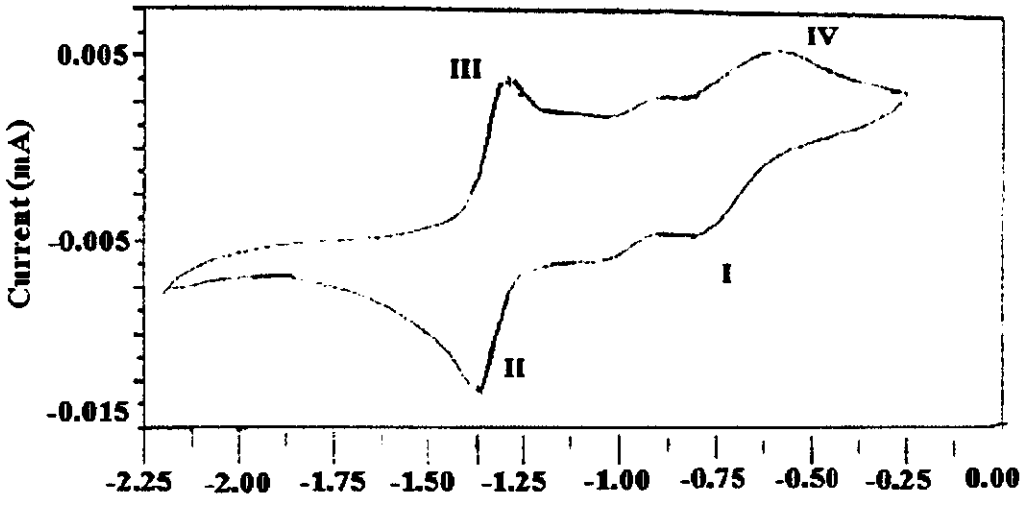

Figure 37 Cyclic voltammogram of 1.0 x 10^{-3} M Dammacanthal at GCE in 50 ml CH_3CN which 0.1 M TBAP as a supporting electrolyte with scan rate of 100 mV/s and resting potential is -0.0011 V.

Discussion

The cyclic voltammogram of Damnacanthal shows two redox couples in CH_3CN as in Figure 37. It undergo two successive and distinct reduction/oxidantion

process The first reduction/oxidation occur at -0.833 V and -0.579 V vs Ag/AgCl respectively. This behavior shows the second reduction at -1.370 V and the second oxidation at -1.287 V vs Ag/AgCl. The formal potential of the first couple ($E_1^{O'}$) is equal to -0.706 V vs Ag/AgCl.

The behavior of Damnacanthal is not diffusion control of the current due to occurs absorption behavior at glassy carbon electrode which it exhibits not linear relationship between peak currents and square root of scan rate which shown in Figure 38, 39 respectively. The both of peak couples are quasi-reversible which can see from Figure 37 and the graph of Randle equation is not linear.

Table 27 The relationship of square root of scan rate and current peaks of Damnacanthal

Scan rate (mV/s)	Square root of scan rate $(mV/s)^{1/2}$	Ipc_1 (A)	Ipc_2 (A)	Ipa_1 (A)	Ipa_2 (A)
100	10.00	1.087×10^{-7}	6.543×10^{-6}	2.251×10^{-6}	1.322×10^{-6}
200	14.14	0.000	8.454×10^{-6}	3.412×10^{-6}	9.800×10^{-7}
300	17.32	0.000	1.022×10^{-5}	4.129×10^{-6}	9.500×10^{-7}
400	20.00	1.465×10^{-7}	1.321×10^{-5}	4.701×10^{-6}	1.148×10^{-6}
500	22.36	1.261×10^{-7}	1.485×10^{-5}	5.183×10^{-6}	1.261×10^{-6}
600	24.49	9.544×10^{-8}	1.710×10^{-5}	5.730×10^{-6}	1.130×10^{-6}

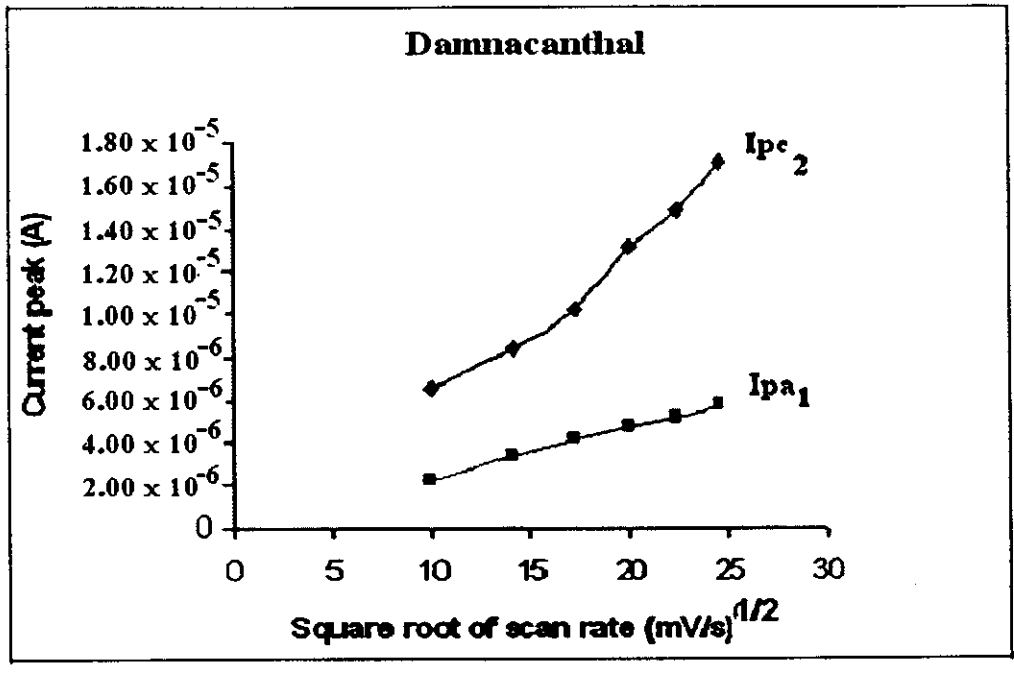

Figure 38 The plotting between square root of scan rate and the current peaks (Ipc_2 and Ipa_1) of Damnacanthal

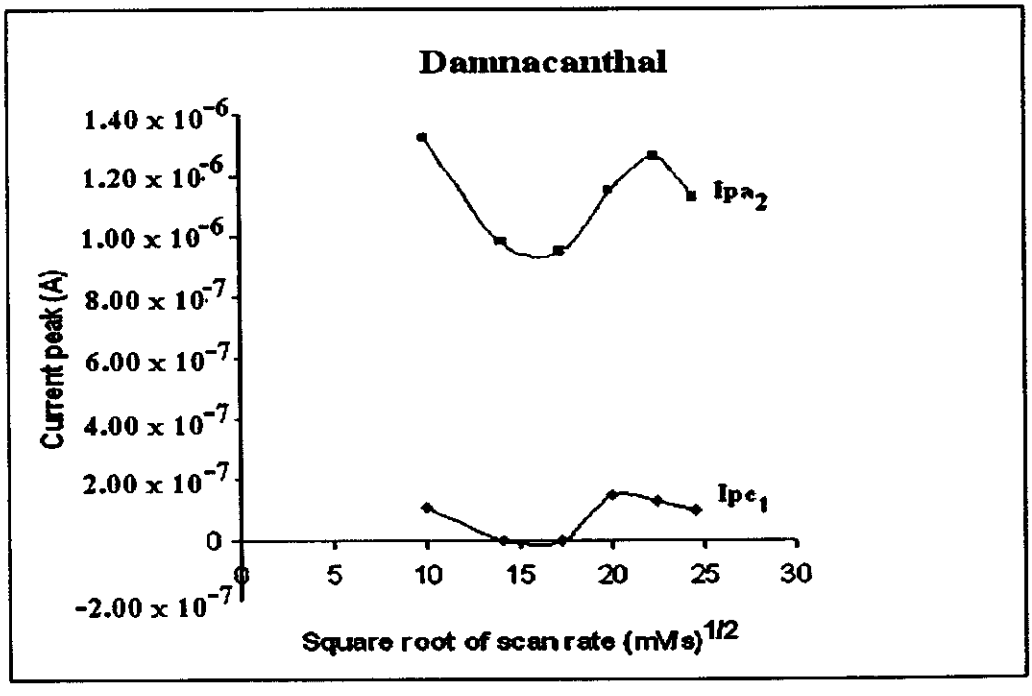

Figure 39 The plotting between square root of scan rate and the current peaks (Ipa_2 and Ipc_1) of Damnacanthal

The first couples is not completely electrochemically reversible and the second couples is chemically irreversible ($Ipa_1/Ipc_1 = 0.460$) and ($Ipa_2/Ipc_2 = 7.741$).

The formal potential of the first couple ($E_1^{O'}$) is equal to -0.706 V vs Ag/AgCl. The ΔEp_1 of Damnacanthal (254 mV) is somewhat higher than the theoretical value ($>$ 59 mV) which indicate that the electron transfer is quite slow at this scan rate (100 mV/s).

The first reduction reaction corresponds to the transformation of Damnacanthal into semiquinone and the second to the transformation of semiquinone into quinone dianion which this electrochemical behavior is similar with all quinone.

Conclusion of the electrochemical behavior of quinones

They all exhibit typical two reversible couple, which presents two consecutive one-electron reversible waves (I-IV and II-III), related to reactions (1) and (2). The first reduction reaction corresponds to the transformation of Q into semiquinone (Q•-) and the second to the transformation of Q•- into quinone dianion (Q^{2-}) (Mark and Dennis, 2001).

$$Q + e^- \leftrightarrow Q^{\bullet -} \quad (1)$$

$$Q^{\bullet -} + e^- \leftrightarrow Q^{2-} \quad (2)$$

All quinones exhibit the same behavior, i.e., two redox couples. The presence of electron withdrawing group such as hydroxyl group helps stabilize the reduction product, hence the more positive reduction potentials as can be clearly seen in the case of Tetrahydroxybenzoquinone compared with Benzoquinone or dihydroxy derivatives compared with the parent Anthraquinone compound (Table 28).

The ΔEp_1 of all quinones is somewhat higher than the the theoretical value (>59 mV), reflecting that the electron transfer is quite slow at this scan rate (100 mV). Slow electron transfer at the electrode causes the peak separation to increase of the first couple.

The first couple exhibits chemically reversible ($Ipa_1/Ipc_1 = 1$) for all quinones except in the case of Tetrahydroxybenzoquinone and Damnacanthal are not completely chemical reversible. The formal potential and separation peak of quinones were shown in Table 28.

Table 28 Peak potentials of 1.0×10^{-3} M of quinones vs Ag /AgCl in acetonitrile

Quinones	$E_1^{o'}$	$E_2^{o'}$	ΔEp_1 (mV)	ΔEp_2 (mV)
p-Benzoquinone	-0.448	-0.940	62	68
Tetrahydroxybenzoquinone	-0.337	-0.890	171	520
1,4-Naphthoquinone	-0.693	-1.224	66	71
Anthraquinone	-0.898	-1.370	74	66
1,2-Dihydroxyanthraquinone	-0.703	-1.208	93	71
1,4-Dihydroxyanthraquinone	-0.653	-1.109	63	78
1,8-Dihydroxyanthraquinone	-0.608	-1.119	64	61
Damnacanthal	-0.706	-1.328	254	83

3.3 Electrochemical behavior of silver ion

3.3.1 Cyclic voltammetry of blank

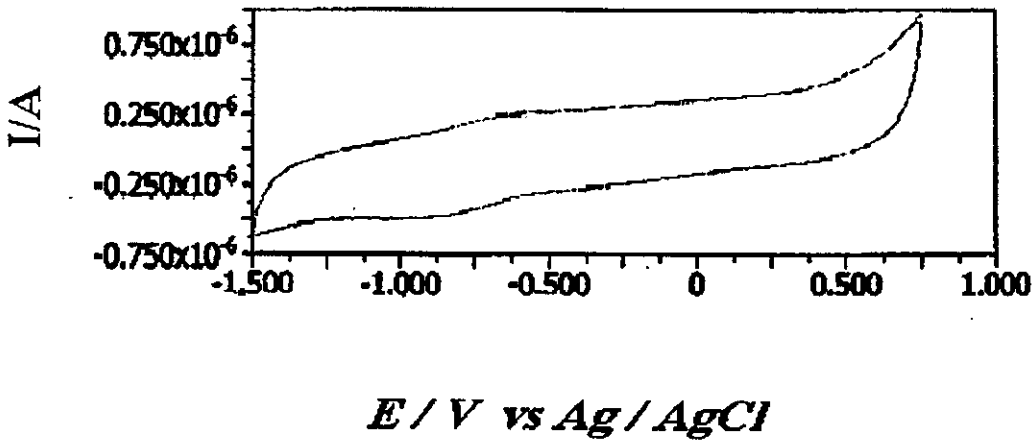

Figure 40 Cyclic voltammogram of blank solution in 50 ml acetonitrile at GCE with scan rate is 100 mV/s and scan from -1.500 to 0.750 V vs Ag/AgCl.

3.3.2 Cyclic voltammetry of silver ion in CH_3CN

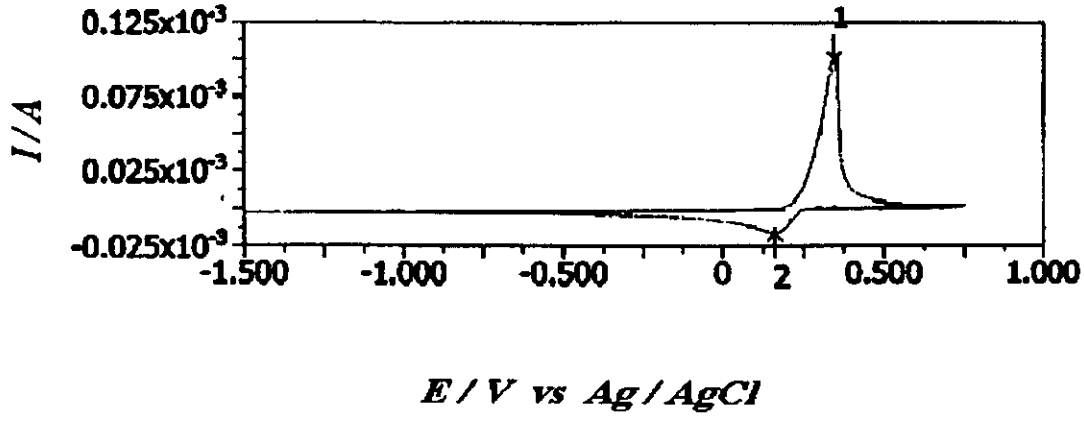

Figure 41 Cyclic voltammogram of 1.0 x 10^{-3} M $AgNO_3$ at GCE in 50 ml CH_3CN which 0.1 M TBAP as a supporting electrolyte with scan rate of 100 mV/s within the potential window of -1.500 to 0.750 V and the resting potential is -0.0011V.

Discussion

The result is that there is no significant peak but instrument indicates that there is the peak at -1.168 V with the peak height which is due to trace impurities. When silver ion is added with the concentration 1 x 10^{-2} M and start the scan form -1.50 to 0.75 V. There is an oxidation peak with Epa_1 = 0.160 V vs Ag/AgCl and Ipa_1 = 1.611 x 10^{-5}A. When the scan is reversed. The reduction peak occurs with Epc_1 = 0.346 V vs Ag/AgCl and Ipc_1 = 1.009 x 10^{-4} A as shown Figure 41. This behavior is chemically irreversible (Ipa_1/Ipc_1 = 0.159). The formal potential of the first couple ($E_1^{O'}$) is equal to 0.253 V vs Ag/AgCl. The reactions involved are as follows :

$Ag^+(aq) + e^-$	$\longrightarrow$	Ag (s)	Deposition	(1)
Ag (s)	$\longrightarrow$	$Ag^+(aq) + e^-$	Stripping	(2)

Due to the fact that the scan is started at -1.50 V which is negative enough to drive the reduction of $Ag^+(aq)$ i.e, $Ag^+(aq) + e^- \longrightarrow Ag$ (s). Silver ion in the solution takes electron and becomes Ag at the surface of GCE after that the oxidation reaction $Ag\ (s) \longrightarrow Ag^+(aq) + e^-$ occurs. Silver atom loses electron to become $Ag^+(aq)$ back to the solution.

3.4 The investigation of mole ratio of ketones with silver ion

3.4.1 The mole ratio of Cyclohexanone with silver ion

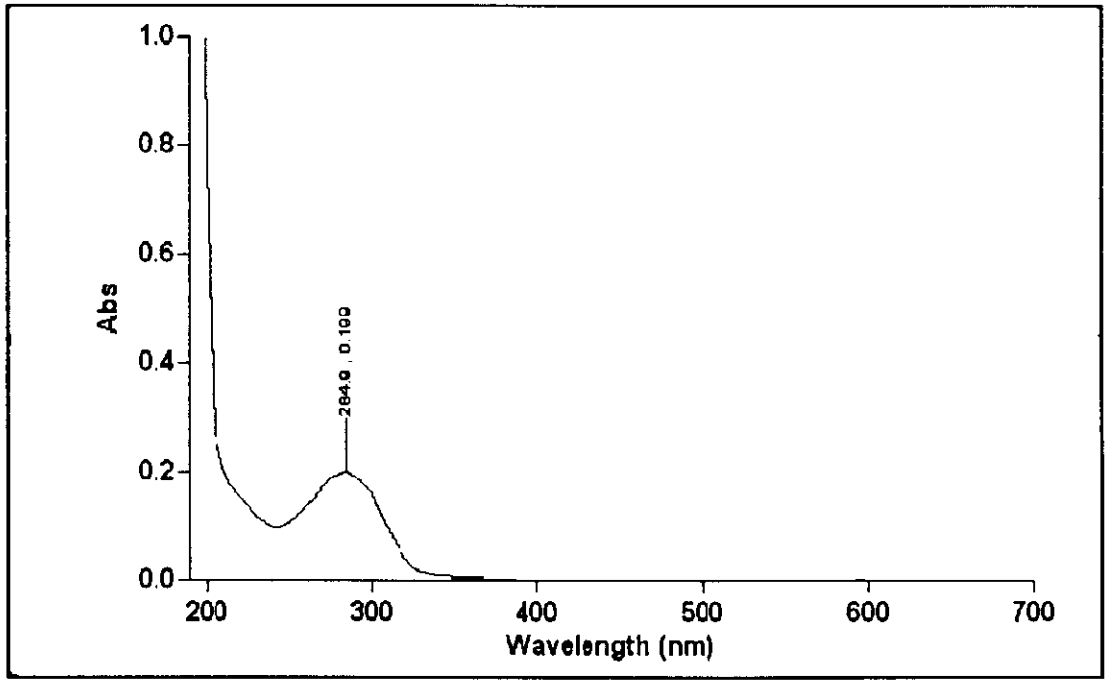

Figure 42 UV-Visible spectra of 1.0×10^{-2} M of Cyclohexanone in CH_3CN

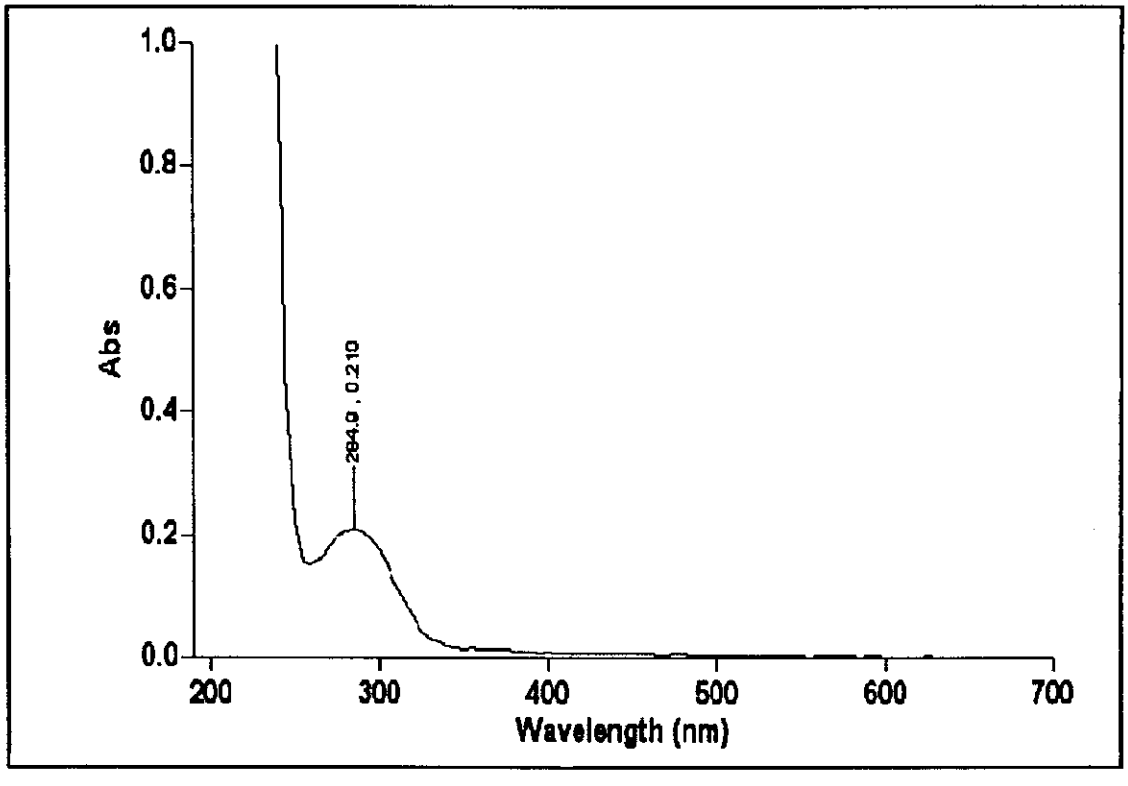

Figure 43 UV-Visible spectrum of Cyclohexanone and silver ion in the ratio 1 to 1

The carbonyl compound consist with one sigma electron, one π electron and anti bonding electron which Cyclohexanone exhibits absorption band at 284.0 nm in the UV region contains $n \longrightarrow \pi^*$ band or near UV region within 200-350 nm and absorbance is 0.210 (Figure 42). UV-VIS spectrum at various ligand : metal ratios is presented in Figure 43. The position and the intensity of the 284.9 nm band in the Ag^+-Cyclohexanone system remains practically unchanged. These results indicate that the Cyclohexanone does not interact significanthly with silver ions.

Table 29 The relationship between mole ratio of Cyclohexanone with silver ion and absorbance

Mole ratio of Cyclohexanone with silver ion	Absorbance
6 to 1	0.211
5 to 1	0.211
4 to 1	0.211
3 to 1	0.211
2 to 1	0.210
1.5 to 1	0.210
1 to 1	0.210
0.7 to 1	0.210
0.5 to 1	0.210
0.3 to 1	0.210

Plots of absorbance vs Ag^+ : Cyclohexanone mole ratio indicate that there are no formation of complex between Cyclohexanone and silver ion (Figure 44).

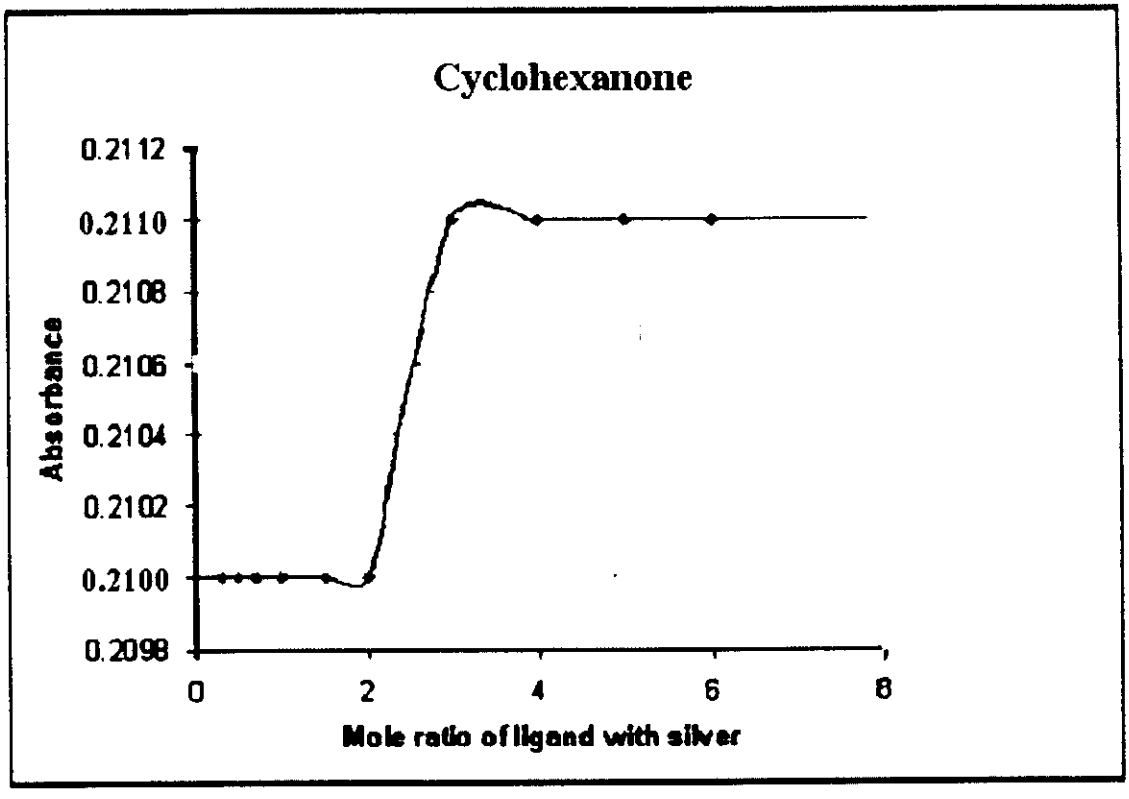

Figure 44 Mole ratio plot of complex of Cyclohexanone with silver ion

3.4.2 The mole ratio of Benzophenone with silver ion

The carbonyl compound consist with one sigma electron, one π electron and anti bonding electron which Benzophenone exhibits absorption band at 195.0 nm in the UV region contains $\pi \longrightarrow \pi^*$ band within far UV region (100-200 nm) and second peak of Benzophenone appears at the wavelength is 249.9 nm due to occurs transition of $n \longrightarrow \pi^*$ band within near UV region (200-300 nm) and absorbance is 0.322 (Figure 45).

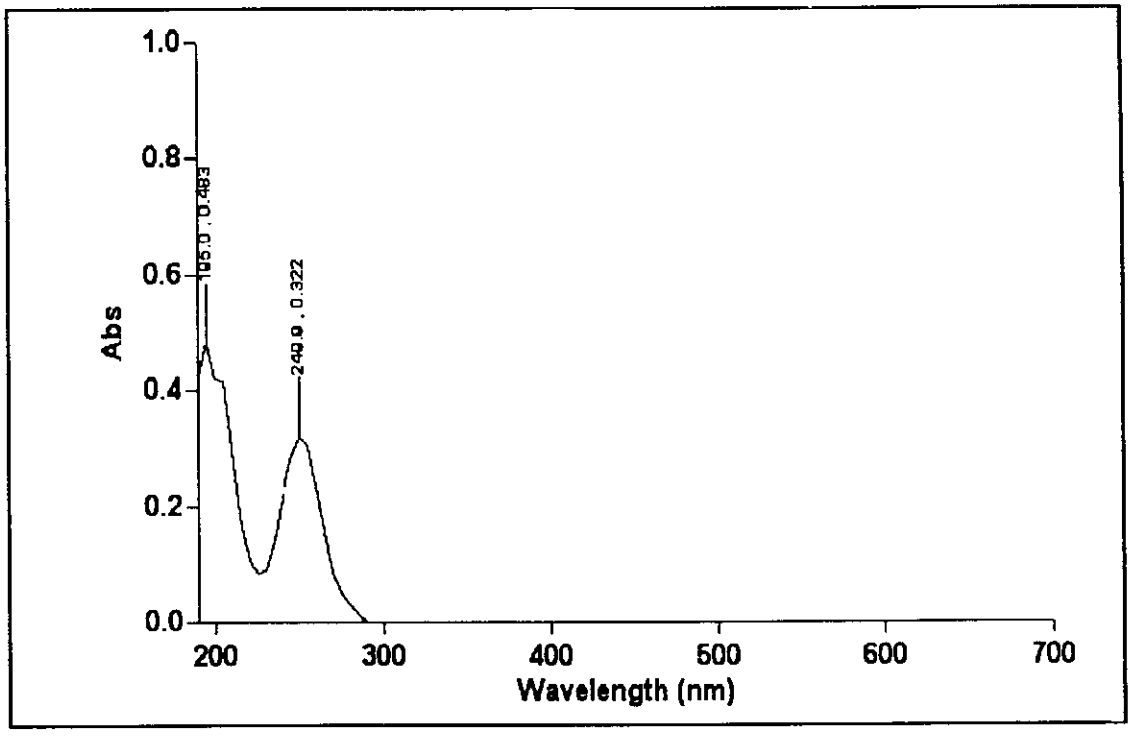

Figure 45 UV-Visible spectrum of 2.0 x 10^{-5} M Benzophenone in CH_3CN

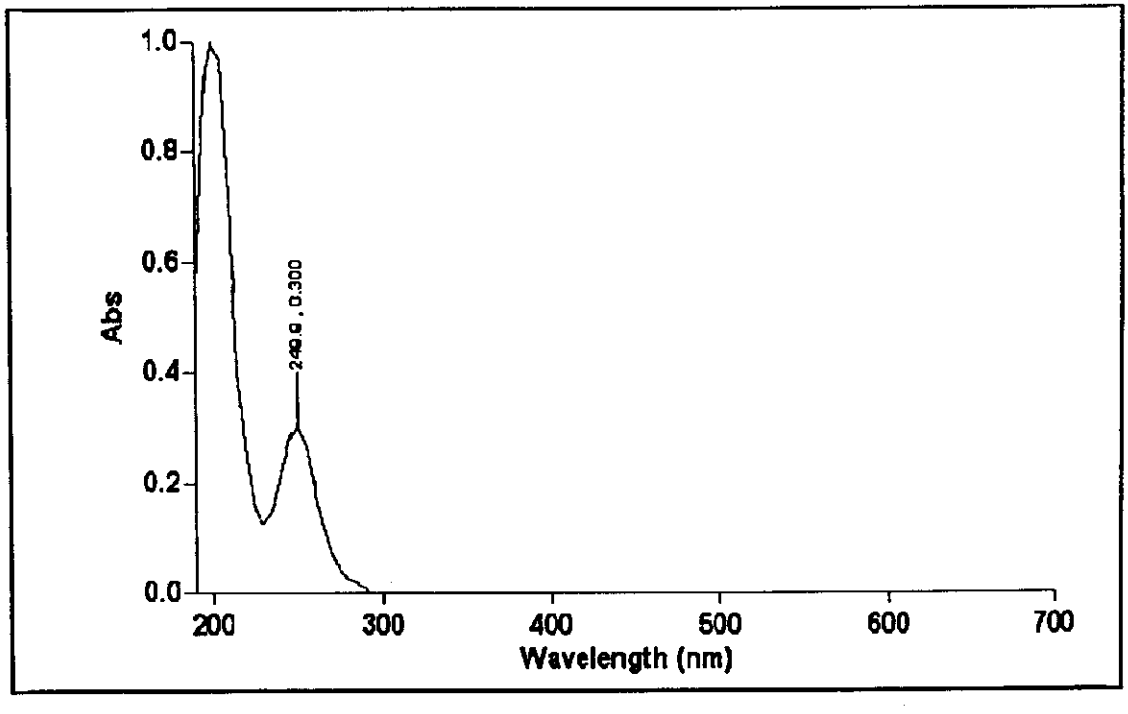

Figure 46 UV-Visible spectrum of Benzophenone and silver ion in the ratio 0.5 to 1

UV-VIS spectra at the ratio of 0.5 ligand : 1 metal ratios is presented in Figure 46.

Table 30 The relationship between mole ratio of Benzophenone with silver ion and absorbance

Mole ratio of Benzophenone with silver ion	Absorbance
6 to 1	0.319
5 to 1	0.319
4 to 1	0.319
3 to 1	0.319
2 to 1	0.316
1.5 to 1	0.313
0.9 to 1	0.307
0.8 to 1	0.305
0.6 to 1	0.302
0.5 to 1	0.300

Another interesting aspect is the ratio of silver ion and various ligands in the complexes. The intersection between two straight lines in the plot of absorbance of the complex and mole ratio indicates the stoichiometry in the complex which is shown in Figure 10 (Douglas *et al.*, 1996).

A typical series of UV–VIS spectra at various ligand : metal ratios is presented in Figure 47. Plots of absorbance *vs.* Ag^{+} : Benzophenone mole ratio indicate the formation of 1 : 1 complex (Figure 47).

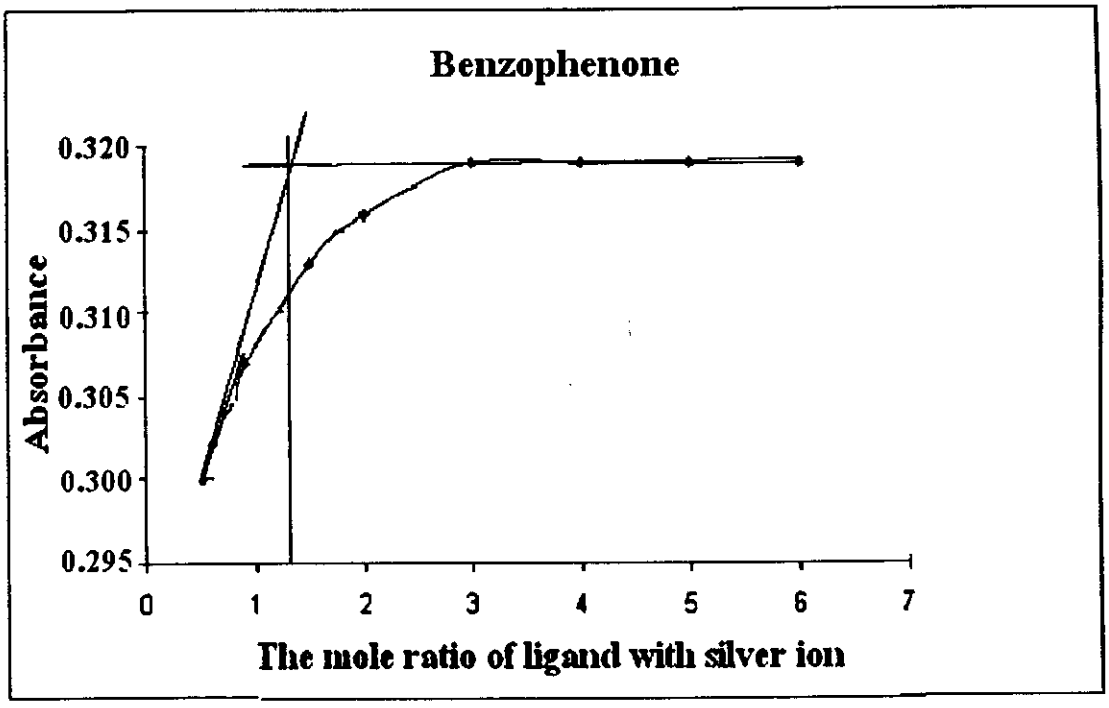

Figure 47 Mole ratio plot of complex of Benzophenone with silver ion.

3.4.3 The mole ratio of α-Tetralone with silver ion

The carbonyl compound consist with one sigma electron, one π electron and anti bonding electron which α-Tetralone exhibits absorption band at 246.0 nm and 290.1 nm in the UV region contains n⟶ π* band within near UV region (200-300 nm) and absorbance is 0.112 and 0.322 respectively. (Figure 48). A typical series of UV-VIS spectra at various ligand : metal ion ratios is presented in Figure 49

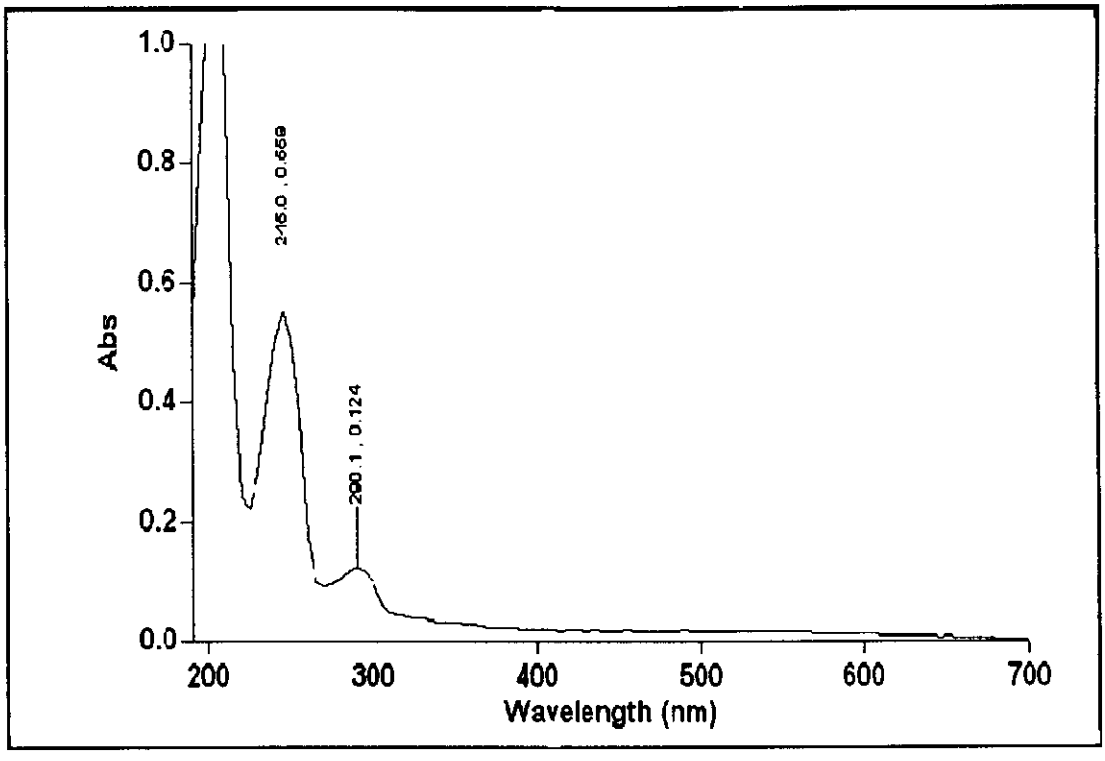

Figure 48 UV-Visible spectrum of 3 x 10^{-5} M of α-Tetralone in CH_3CN

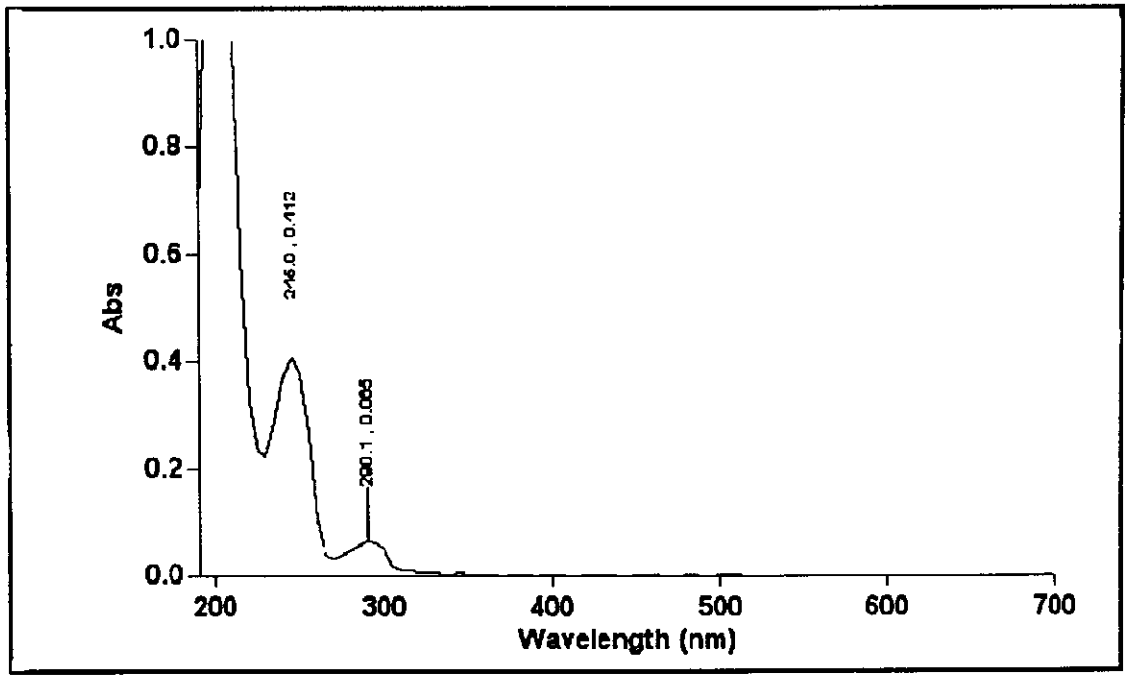

Figure 49 UV-Visible spectrum between 3 x 10^{-5} M of α-Tetralone and 1 x 10^{-4} M silver ion in the ratio 0.6 to 1

Table 31 The relationship between mole ratio of α-Tetralone with silver ion and absorbance

Mole ratio of α-Tetralone with silver ion	Absorbance
6 to 1	0.078
5 to 1	0.077
4 to 1	0.076
3 to 1	0.075
2.5 to 1	0.074
2 to 1	0.073
1.5 to 1	0.072
1 to 1	0.071
0.9 to 1	0.069
0.8 to 1	0.067
0.6 to 1	0.065

Another interesting aspect is the ratio of silver ion and various ligands in the com-plexes. The intersection between two straight lines in the plot of absorbance of the complex and mole ratio indicates the stoichiometry in the complex (Douglas *et al.*, 1996) as shown in the case of α-Tetralone (Figure 50). Plots of absorbance *vs.* Ag^{+} : α-Tetralone mole ratio indicate the formation of 1 : 1 complex.

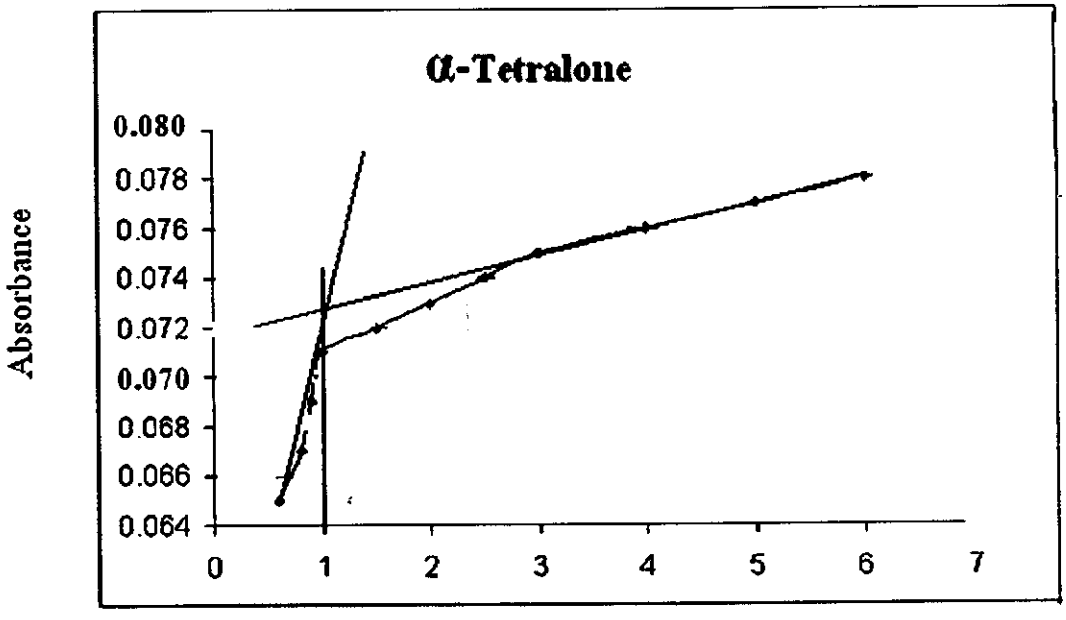

Figure 50 Mole ratio plot of complex of α-Tetralone with silver ion

3.4.4 The mole ratio of Anthrone with silver ion

The UV-VIS spectrum of Anthrone in the UV region contains $\pi \longrightarrow \pi^*$ band which peak of Anthrone appears at the wavelength is 260.1 nm and absorbance is 0.211 (Figure 51). A typical series of UV-VIS spectra at various ligand : metal ion ratios is presented in Figure 52.

Another interesting aspect is the ratio of silver ion and various ligands in the complexes. The intersection between two straight lines in the plot of absorbance of the complex and mole ratio indicates the stoichiometry in the complex (Douglas *et al.*, 1996) as shown in case of Anthrone (Figure 53).

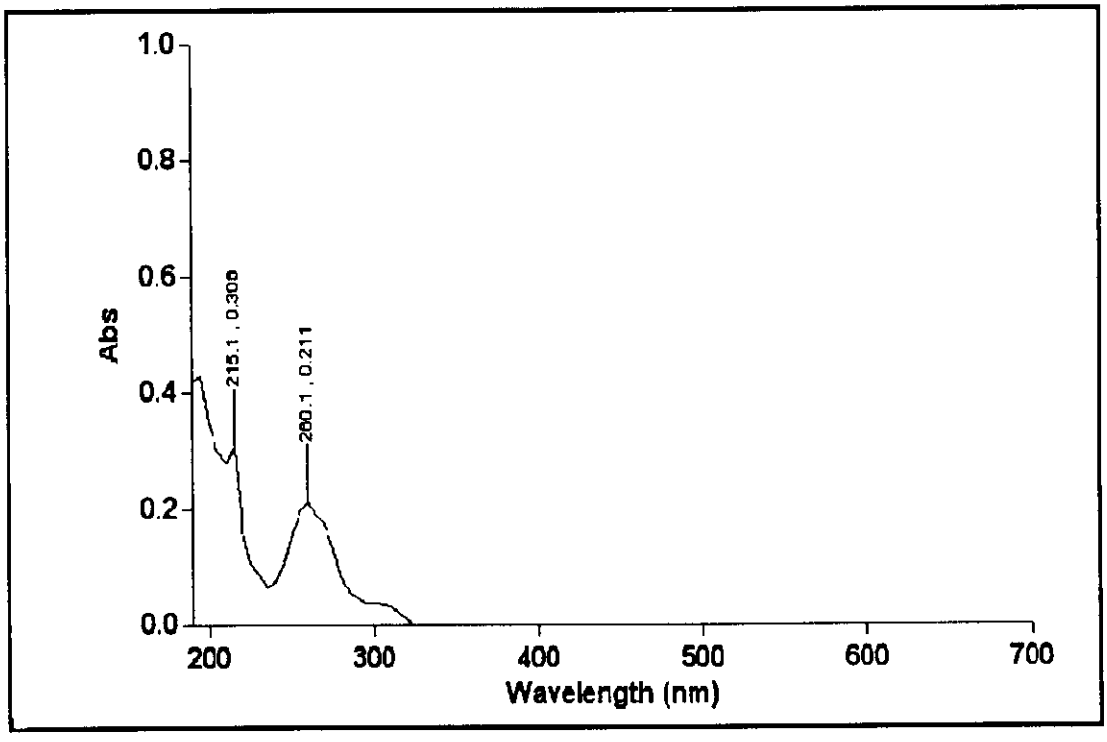

Figure 51 UV-Visible spectrum between 1 x 10^{-5} M of Anthrone in CH_3CN

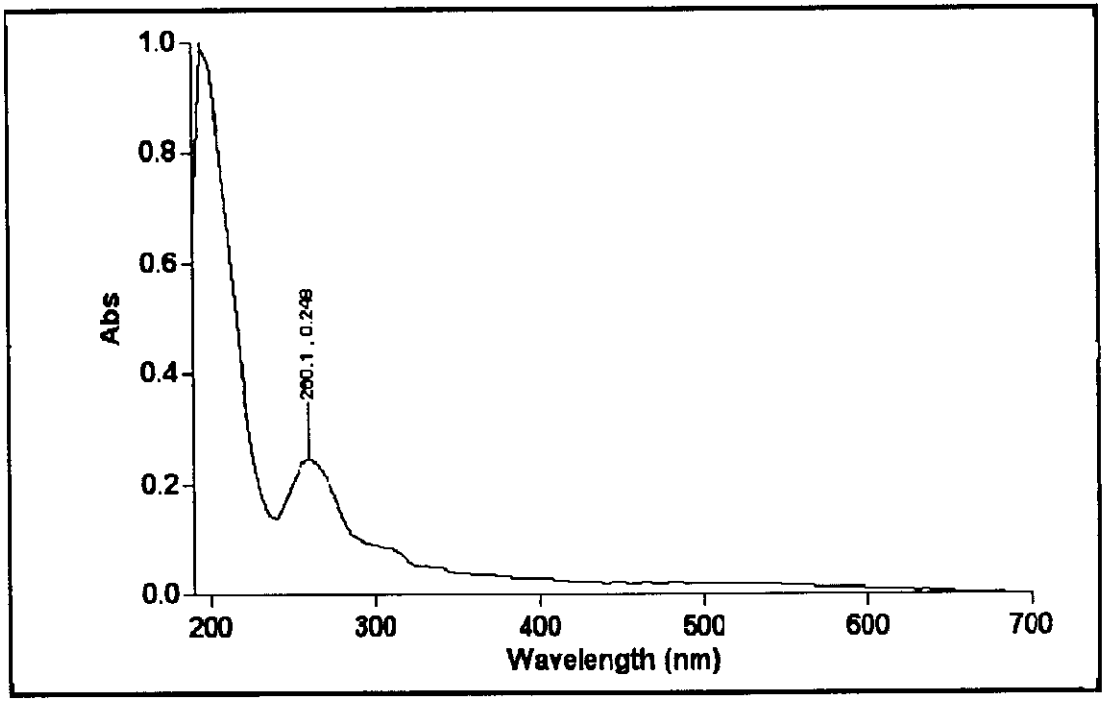

Figure 52 UV-Visible spectrum between 1 x 10^{-5} M of Anthrone and 1 x 10^{-4} M silver ion in the ratio 0.3 to 1

Table 32 The relationship between mole ratio of Anthrone with silver ion and absorbance

Mole ratio of Anthrone with silver ion	Absorbance
6 to 1	0.293
5 to 1	0.293
4 to 1	0.293
3 to 1	0.293
2 to 1	0.290
1.5 to 1	0.287
1 to 1	0.282
0.8 to 1	0.277
0.6 to 1	0.272
0.5 to 1	0.265
0.4 to 1	0.259
0.3 to 1	0.248

There are only few reports about more complex. In most cases, polar side-arm groups comprise ethers, amines, amides or carbocyclic ones (Tadeusz *et al.*, 2000)

Plots of absorbance *vs.* Ag^{+} : Anthrone mole ratio indicate the formation of 1 : 1 complex (Figure 53)

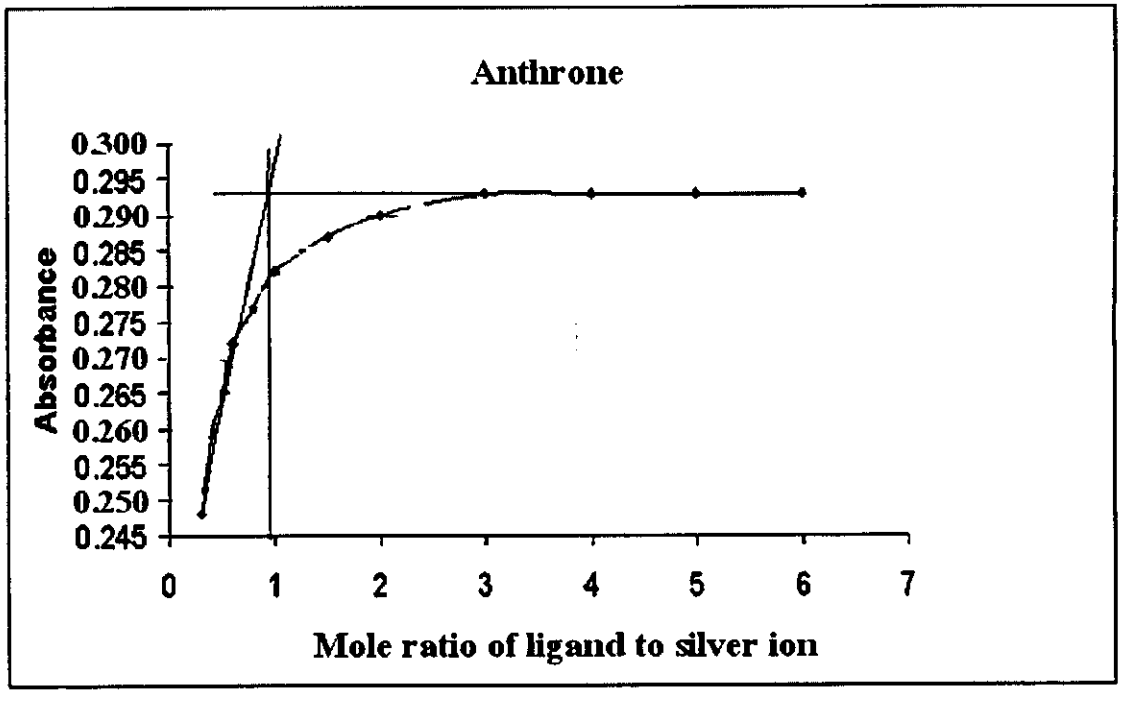

Figure 53 Mole ratio plot of complex of Anthrone with silver ion

3.4.5 The mole ratio of Xanthone with silver ion

The UV-VIS spectrum of Xanthone in the UV region contains $\pi \longrightarrow \pi^*$ band which peak of Xanthone appears at the wavelength is 340.0 nm and absorbance is 0.132 (Figure 54). A typical series of UV-VIS spectra at various ligand : metal ratios is presented in Figure 55.

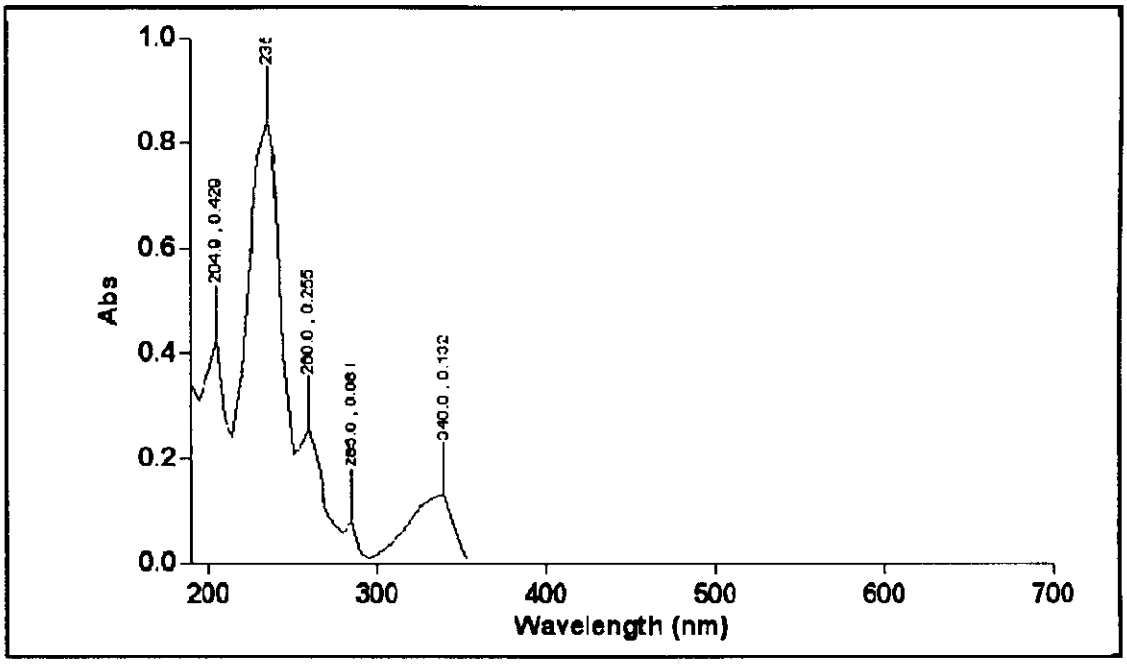

Figure 54 UV-Visible spectrum of 2 x 10^{-5} M of Xanthone in CH_3CN

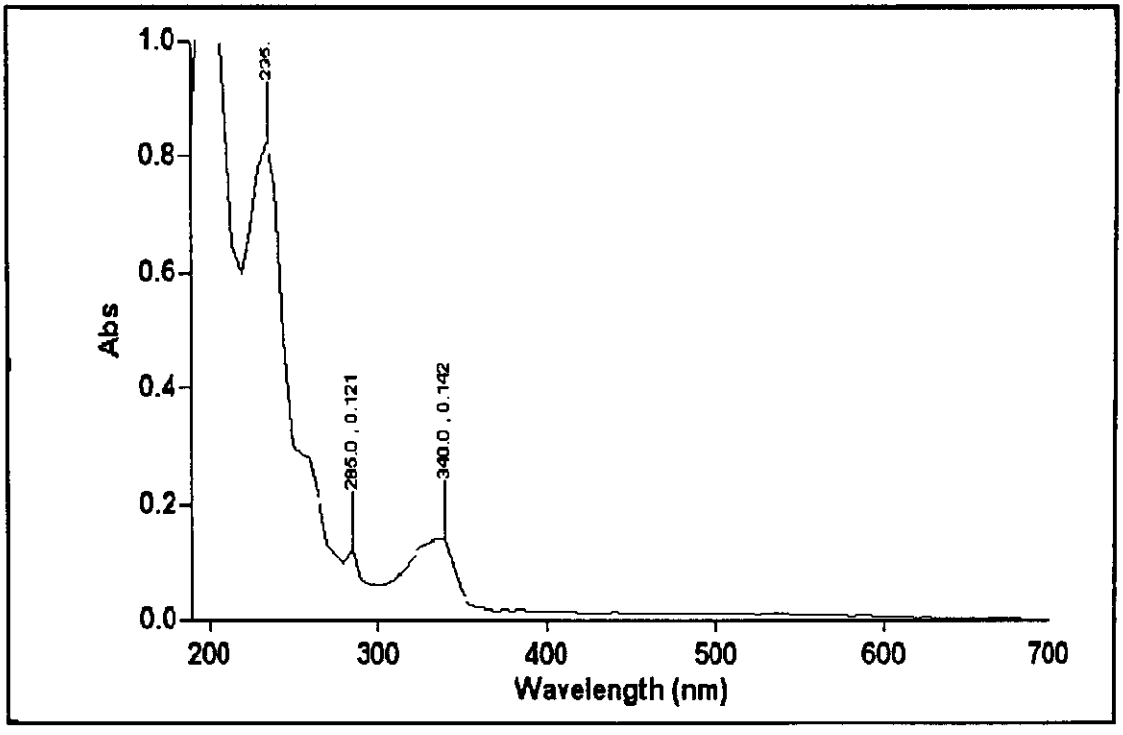

Figure 55 UV-Visible spectrum between 2 x 10^{-5} M of Anthrone and 1 x 10^{-4} M Silver ion in the ratio 0.4 to 1

Table 33 The relationship between mole ratio of Xanthone with silver ion and absorbance

Mole ratio of Xanthone with silver ion	Absorbance
6 to 1	0.179
5 to 1	0.179
4 to 1	0.179
3 to 1	0.175
2 to 1	0.172
1.5 to 1	0.168
1 to 1	0.163
0.8 to 1	0.158
0.6 to 1	0.152
0.5 to 1	0.146
0.4 to 1	0.142

Another interesting aspect is the ratio of silver ion and various ligands in the complexes. The intersection between two straight lines in the plot of absorbance of the complex and mole ratio indicates the stoichiometry in the complex (Douglas *et al.*, 1996) as shown in case of Xanthone (Figure 56).

Plots of absorbance *vs.* Ag^{+} : Xanthone mole ratio indicate the formation of 1 : 1 complex.

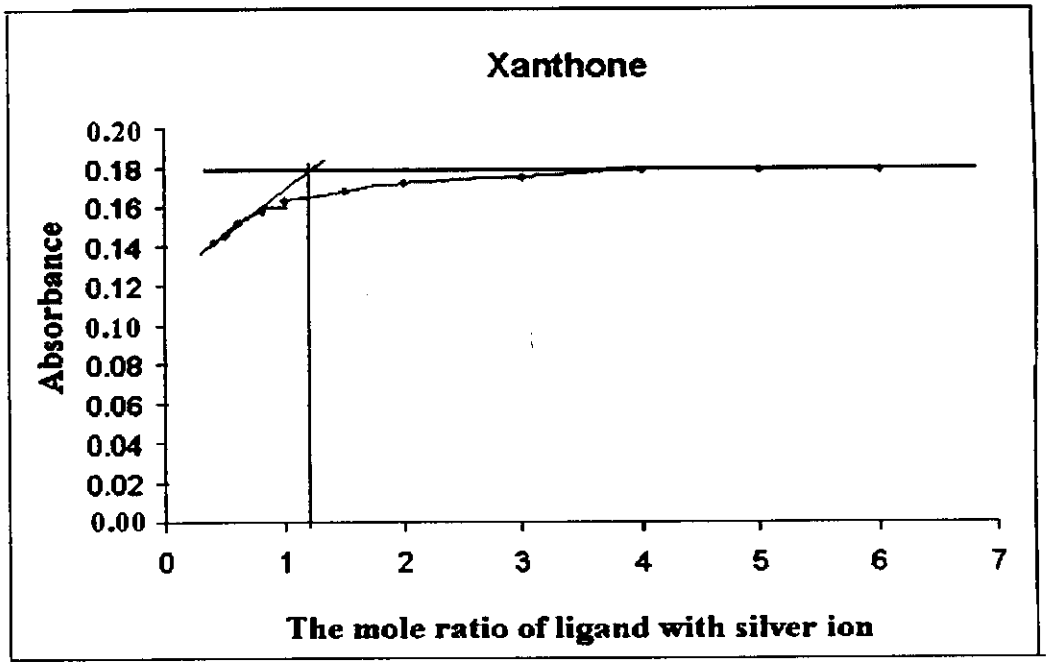

Figure 56 Mole ratio plot of complex of Xanthone with silver ion

Table 34 Summarize mole ratio of complex between ketones with silver ion in CH_3CN

Compounds	Mole ratio of complex (ligands to silver)
Cyclohexanone	No complex
Benzophenone	1 : 1
α-Tetralone	1 : 1
Anthrone	1 : 1
Xanthone	1 : 1

3.5 The investigation of mole ratio of quinones with silver ion

3.5.1 The mole ratio of *p*-Benzoquinone with silver ion

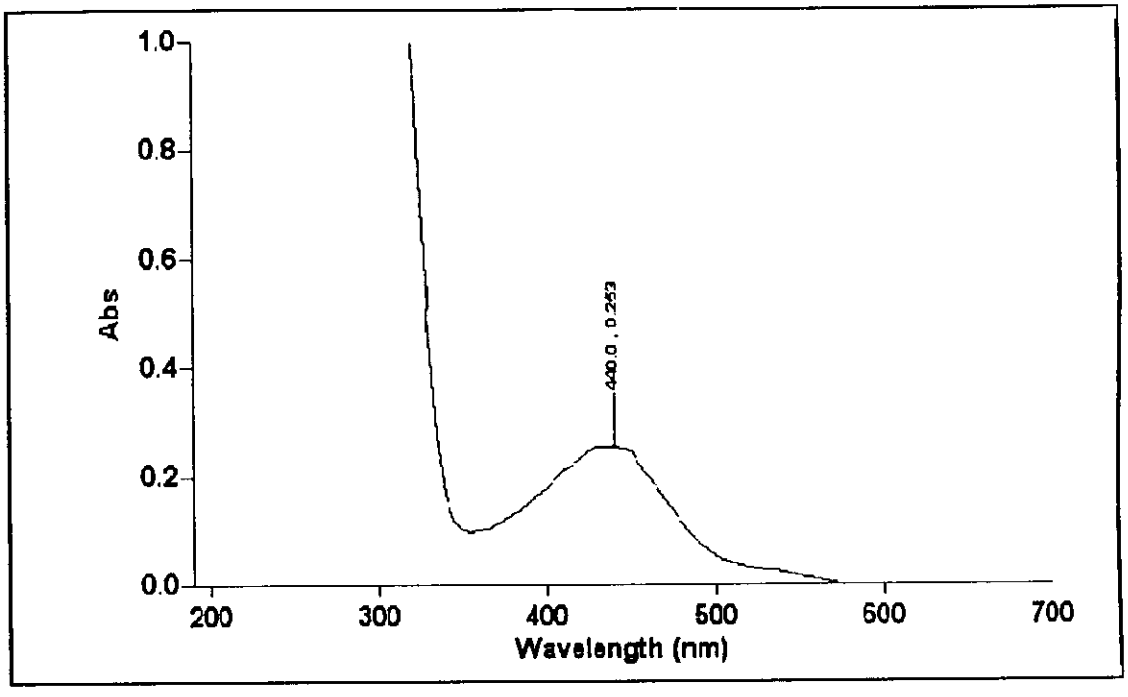

Figure 57 UV-Visible spectrum of 1 x 10^{-2} M of *p*-Benzoquinone in CH_3CN

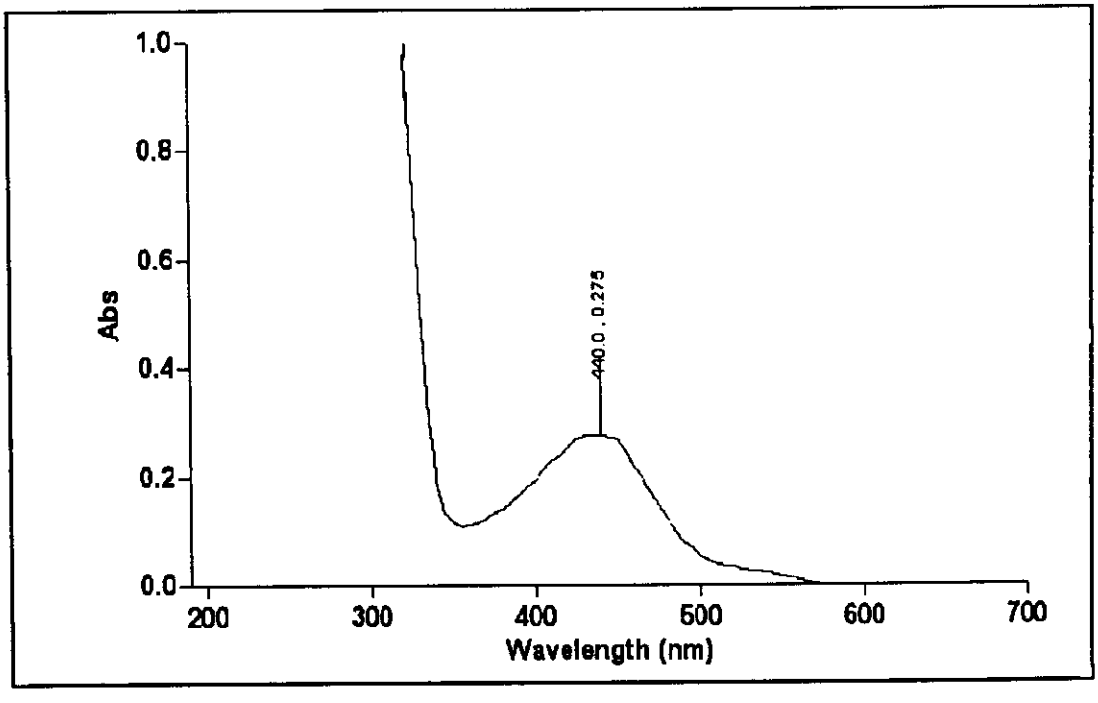

Figure 58 UV-Visible spectrum between 1 x 10^{-2} M of *p*-Benzoquinone and 0.1 M silver ion in the ratio 2 to 1

The UV-VIS spectrum of *p*-Benzoquinone in the visible region contains $n \longrightarrow \pi^*$ band within visible region (350-800 nm) which peak of *p*-Benzoquinone appears at the wavelength is 440 nm and absorbance is 0.253 (Figure 57). A typical series of UV-VIS spectra at various ligand : metal ion ratios is presented in Figure 58.

Another interesting aspect is the ratio of silver ion and various ligands in the complexes. The intersection between two straight lines in the plot of absorbance of the complex and mole ratio indicates the stoichiometry in the complex (Douglas *et al.*, 1996) as shown in case of *p*-Benzoquinone (Figure 59). Plots of absorbance *vs.* Ag^+ : *p*-Benzoquinone mole ratio indicate the formation of 1 : 2 complex.

Table 35 The relationship between mole ratio of *p*-Benzoquinone with silver ion and absorbance

Mole ratio of *p*-Benzoquinone with silver ion	Absorbance
0.25 to 1	0.255
0.5 to 1	0.261
0.9 to 1	0.267
1.3 to 1	0.272
2 to 1	0.275
2.5 to 1	0.277
3 to 1	0.278
4 to 1	0.279
5 to 1	0.279

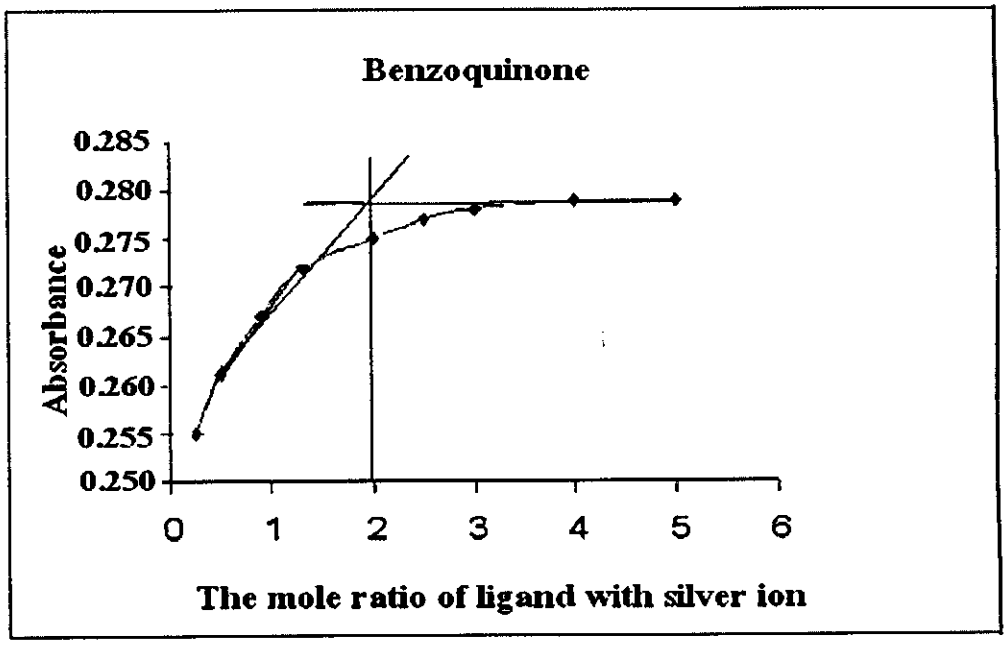

Figure 59 Mole ratio plot of complex of *p*-Benzoquinone with silver ion

3.5.2 The mole ratio of 1,4-Naphthoquinone with silver ion

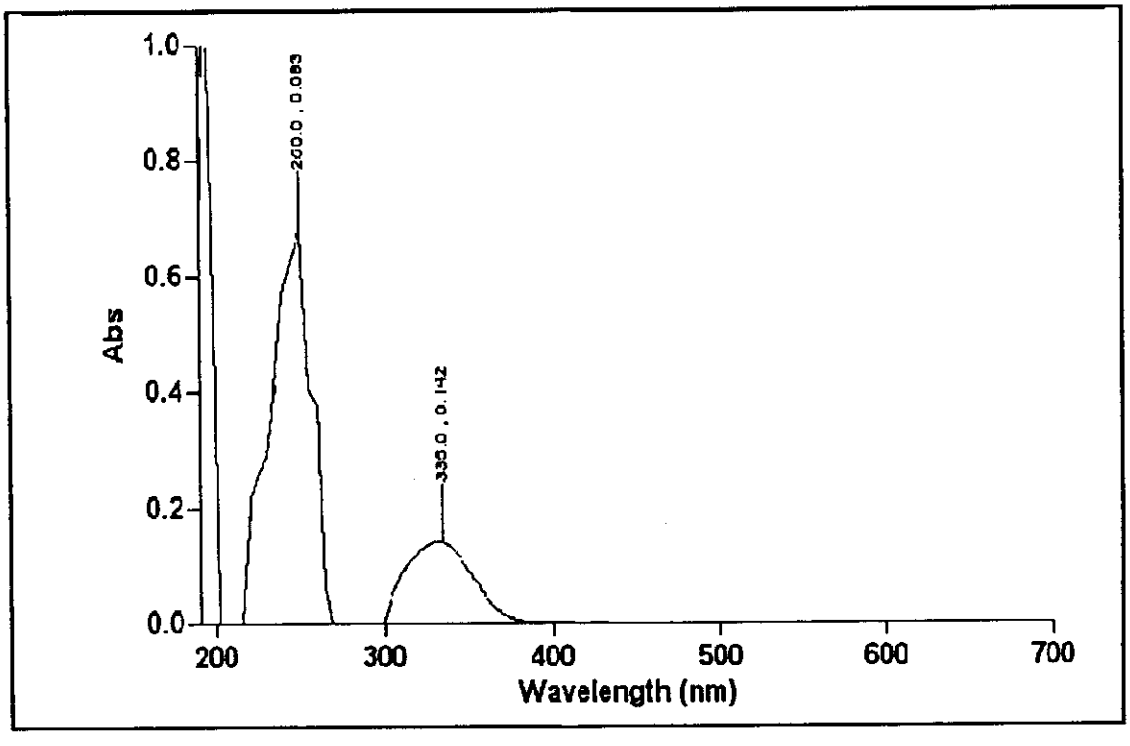

Figure 60 UV-Visible spectrum of 5×10^{-5} M of 1,4-Naphthoquinone in CH_3CN

The UV-VIS spectrum of 1,4-Naphthoquinone in the visible region contains $n \longrightarrow \pi^*$ band which peak of 1,4-Naphthoquinone appears at the wavelength is 335 nm and absorbance is 0.142 (Figure 60). A typical series of UV-VIS spectra at various ligand : metal ratios is presented in Figure 61.

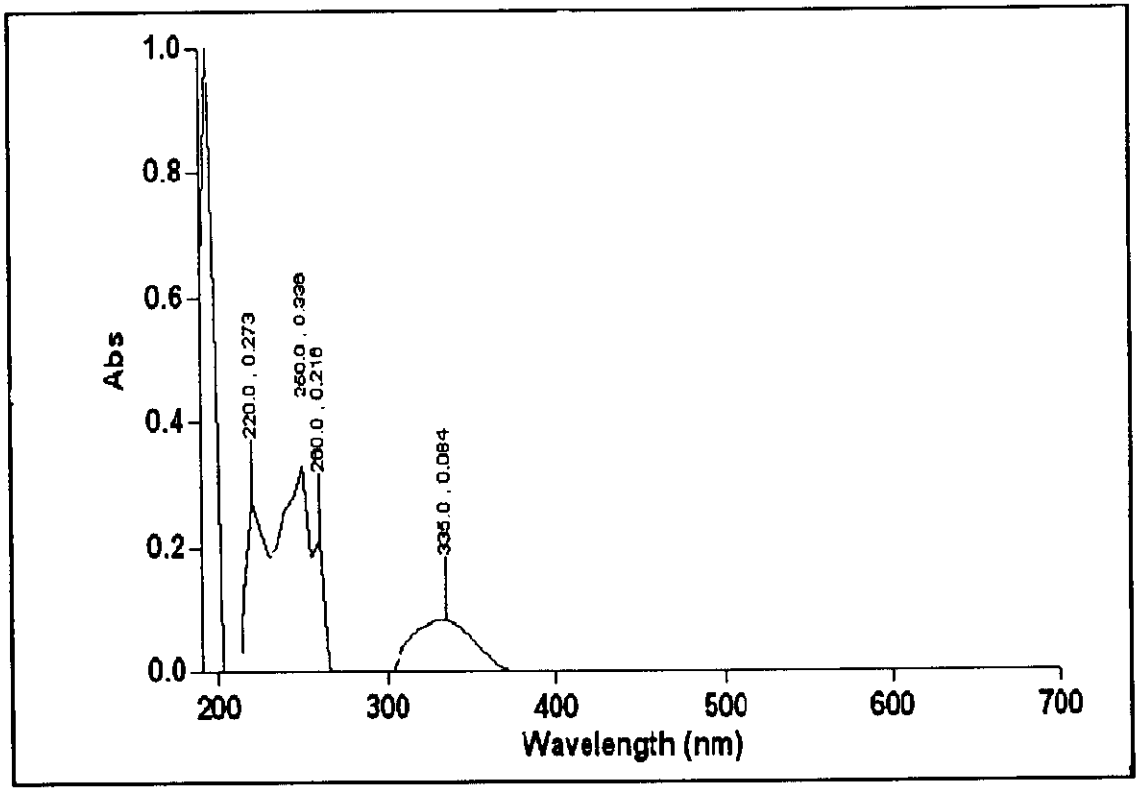

Figure 61 UV-Visible spectrum between 5 x 10^{-5} M of 1,4-Naphthoquinone and 1 x 10^{-4} M silver ion in the ratio 1 to 1

Another interesting aspect is the ratio of silver ion and various ligands in the complexes. The intersection between two straight lines in the plot of absorbance of the complex and mole ratio indicates the stoichiometry in the complex (Douglas *et al.*, 1996) as shown in the case of 1,4-Naphthoquinone (Figure 62). Plots of absorbance *vs.* Ag^+ : 1,4-Napthoquinone mole ratio indicate the formation of 1 : 2 complex.

Table 36 The relationship between mole ratio of 1,4-Naphthoquinone with silver ion and absorbance

Mole ratio of 1,4-Napthoquinone with silver ion	Absorbance
6 to 1	0.119
5 to 1	0.117
4 to 1	0.115
3.5 to 1	0.113
3 to 1	0.111
2.5 to 1	0.108
2 to 1	0.104
1.8 to 1	0.101
1.5 to 1	0.095
1.2 to 1	0.089
1 to 1	0.084

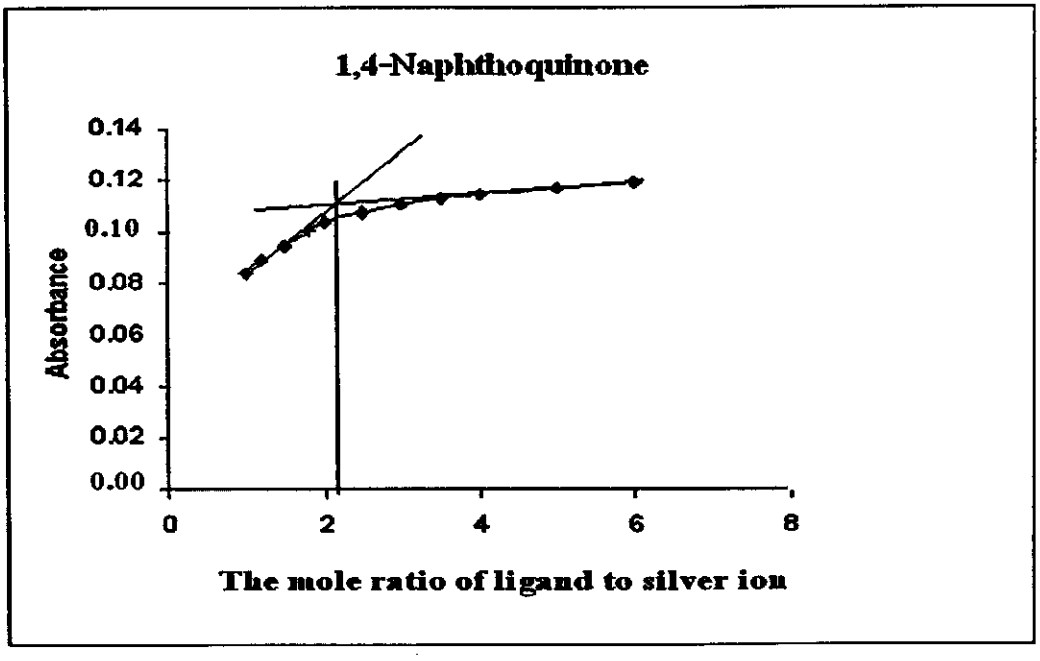

Figure 62 Mole ratio plot of complex of 1,4-Naphthoquinone with silver ion

3.5.3 The mole ratio of Tetrahydroxybenzoquinone with silver ion

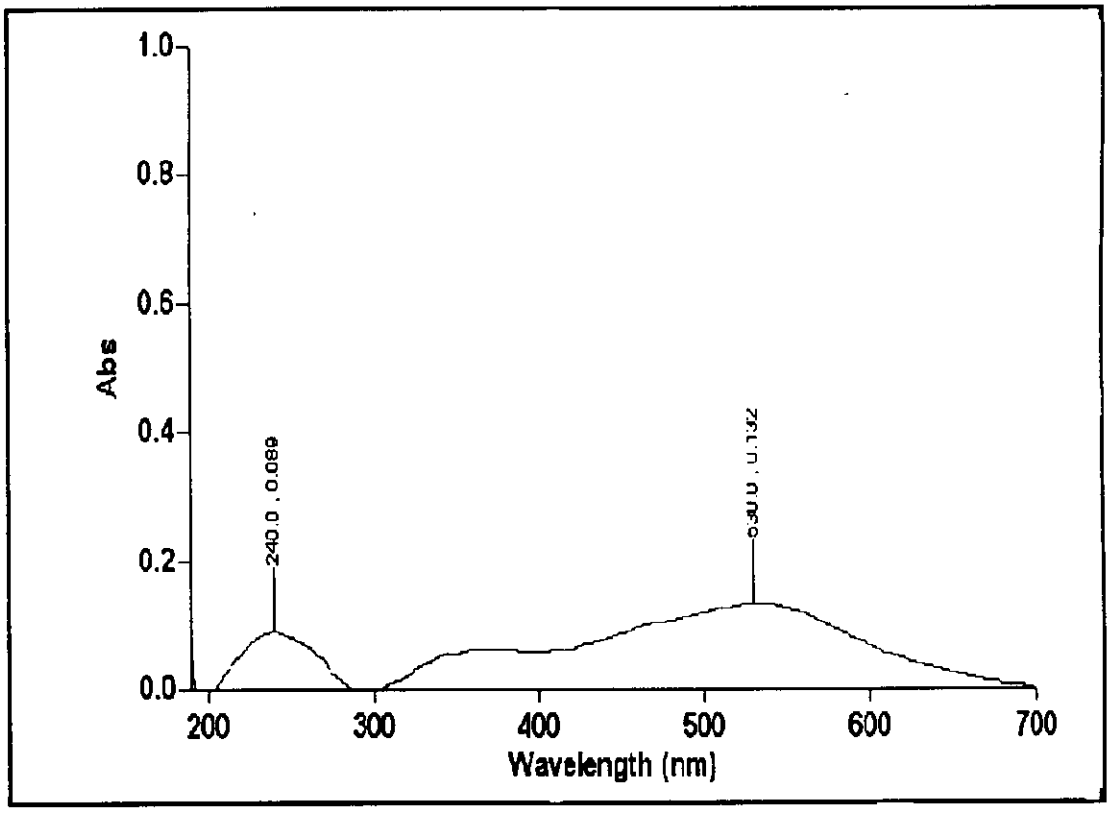

Figure 63 UV-Visible spectrum of 7 x 10^{-5} M of Tetrahydroxybenzoquinone in CH_3CN

The UV-VIS spectrum of Tetrahydroxybenzoquinone in the visible region contains $n \longrightarrow \pi^*$ band which peak of Tetrahydroxybenzoquinone appears at the wavelength is 530 nm and absorbance is 0.132 (Figure 63). A typical series of UV-VIS spectra at various ligand : metal ratios is presented in Figure 64.

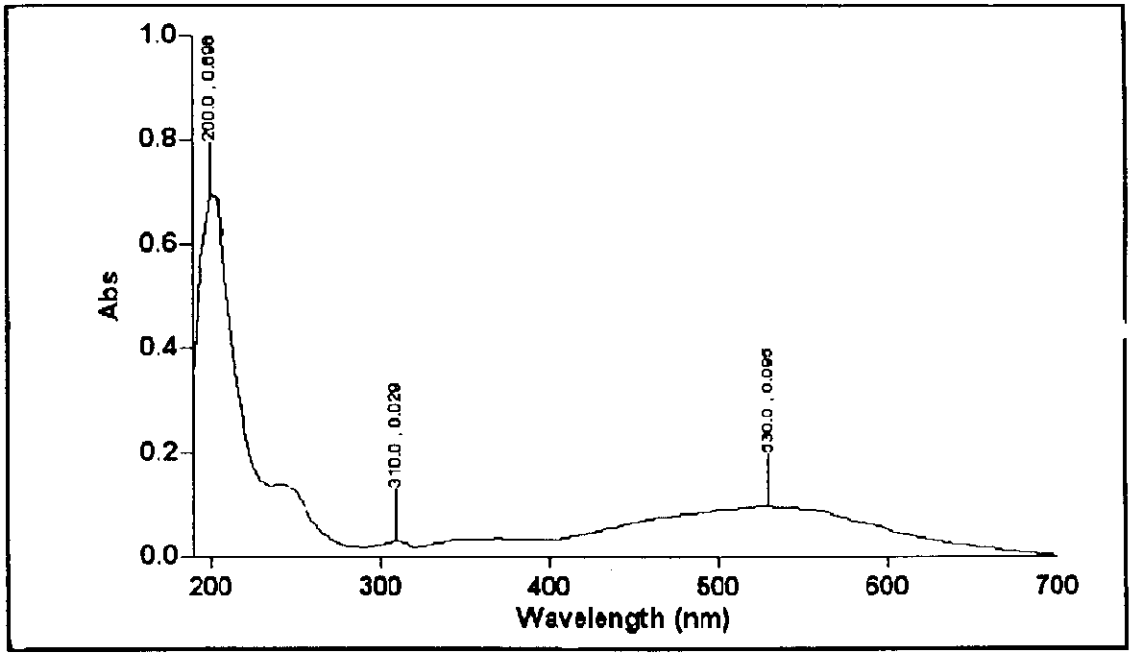

Figure 64 UV-Visible spectrum between 7 x 10^{-5} M of Tetrahydroxybenzoquinone and 1 x 10^{-4} M silver ion in the ratio 2 to 1

Table 37 The relationship between mole ratio of Tetrahydroxybenzoquinone with silver ion and absorbance

Mole ratio of Tetrahydroxybenzoquinone and silver ion	Absorbance
5 to 1	0.114
4 to 1	0.110
3 to 1	0.105
2.5 to 1	0.100
2 to 1	0.095
1.7 to 1	0.089
1.4 to 1	0.085
1.2 to 1	0.081

Another interesting aspect is the ratio of silver ion and various ligands in the complexes. The intersection between two straight lines in the plot of absorbance of the complex and mole ratio indicates the stoichiometry in the complex (Douglas *et al.*, 1996) as shown in the case of Tetrahydroxybenzoquinone (Figure 65).

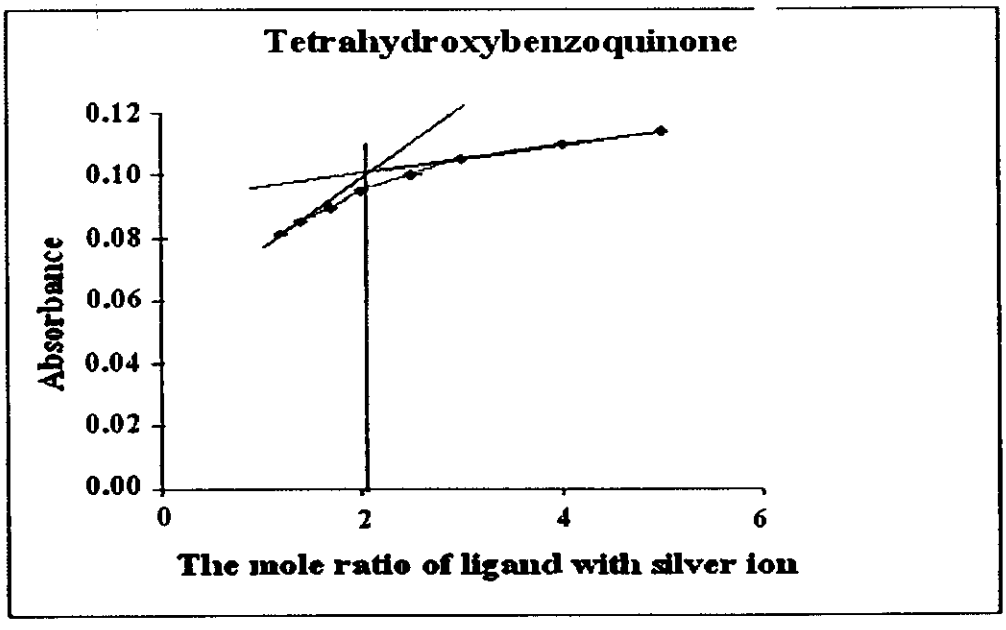

Figure 65 Mole ratio plot of complex of Tetrahydroxybenzophenone with silver ion

Plots of absorbance *vs.* Ag^+ : Tetrahydroxybenzophenone mole ratio indicate the formation of 1 : 2 complex.

3.5.4 The mole ratio of Anthraquinone with silver ion

The UV-VIS spectrum of Anthraquinone in the visible region contains $n \longrightarrow \pi^*$ band which peak of Anthraquinone appears at the wavelength is 321.0 nm and absorbance is 0.126 (Figure 66). A typical series of UV-VIS spectra at various ligand : metal ratios is presented in Figure 67.

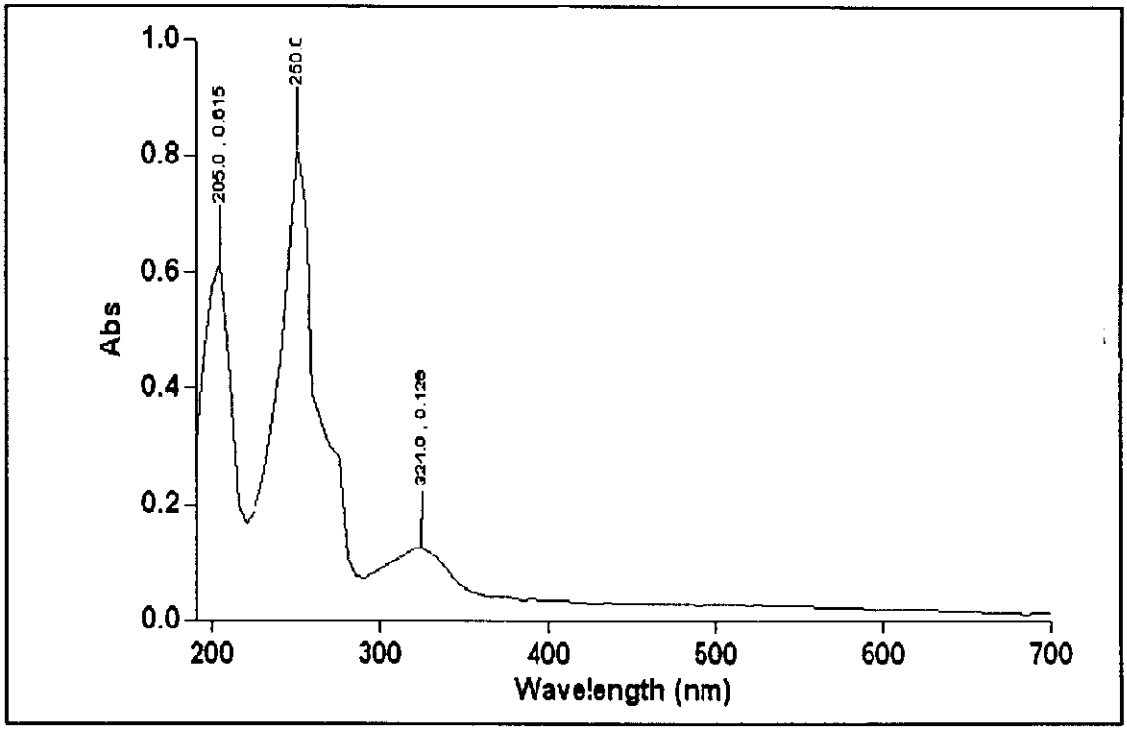

Figure 66 UV-Visible spectrum of 9 x 10^{-6} M of Anthraquinone in CH_3CN

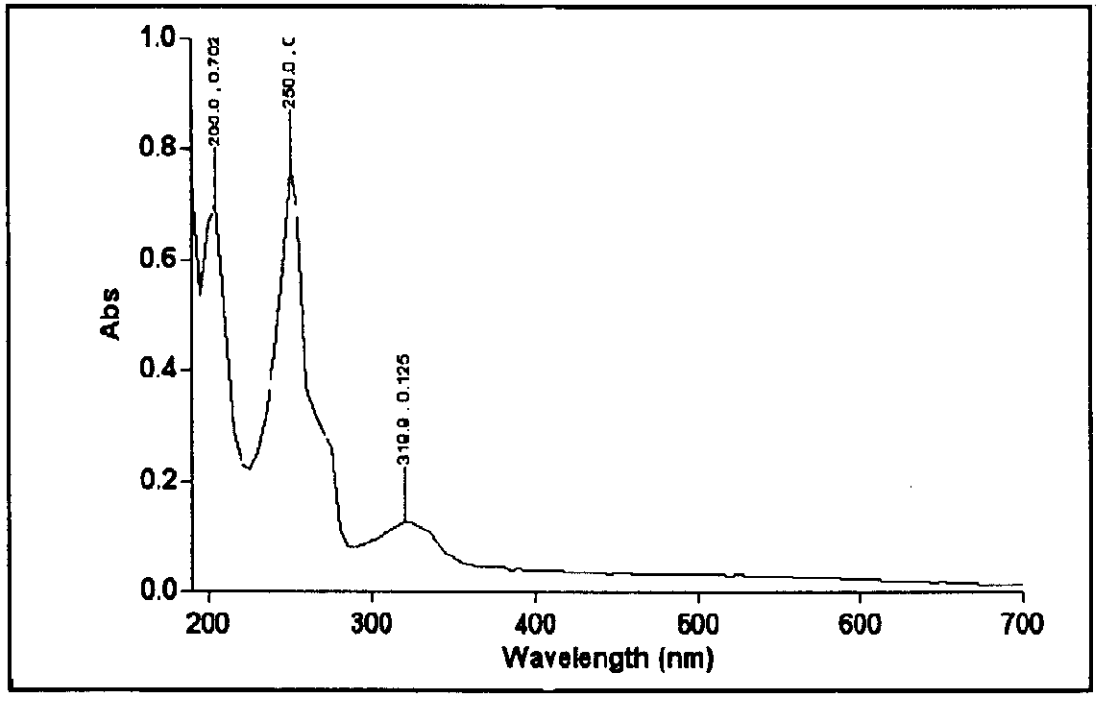

Figure 67 UV-Visible spectrum between 9 x 10^{-6} M of Anthraquinone and 1 x 10^{-4} M silver ion in the ratio 0.75 to 1

Table 38 The relationship between mole ratio of Anthraquinone with silver ion and absorbance

Mole ratio of Anthraquinone and silver ion	Absorbance
0.5 to 1	0.080
0.75 to 1	0.085
1 to 1	0.086
1.5 to 1	0.087
2 to 1	0.089
2.25 to 1	0.089
2.50 to 1	0.089
3 to 1	0.089
5 to 1	0.089

Another interesting aspect is the ratio of silver ion and various ligands in the complexes. The intersection between two straight lines in the plot of absorbance of the complex and mole ratio indicates the stoichiometry in the complex (Douglas *et al.*, 1996) as shown in the case of Anthraquinone (Figure 68).

Plots of absorbance *vs.* Ag^+ : Anthraquinone mole ratio indicate the formation of 1 : 2 complex

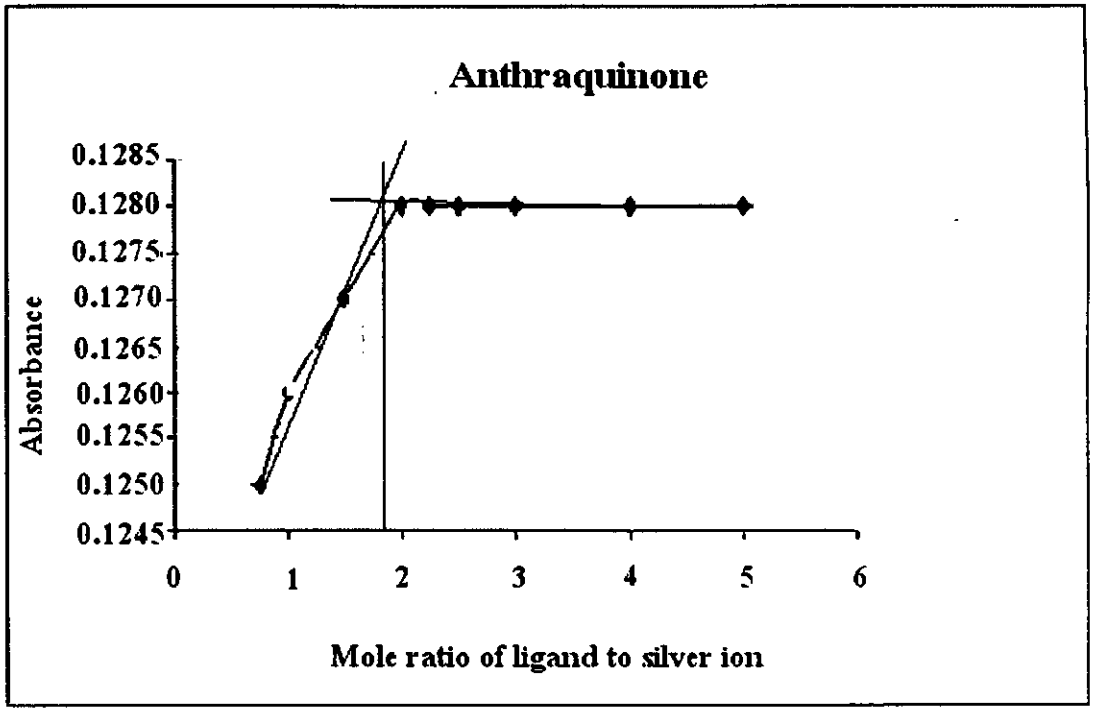

Figure 68 Mole ratio plot of complex of Anthraquinone with silver ion

3.5.5 The mole ratio of 1,2-Dihydroxyanthraquinone with silver ion

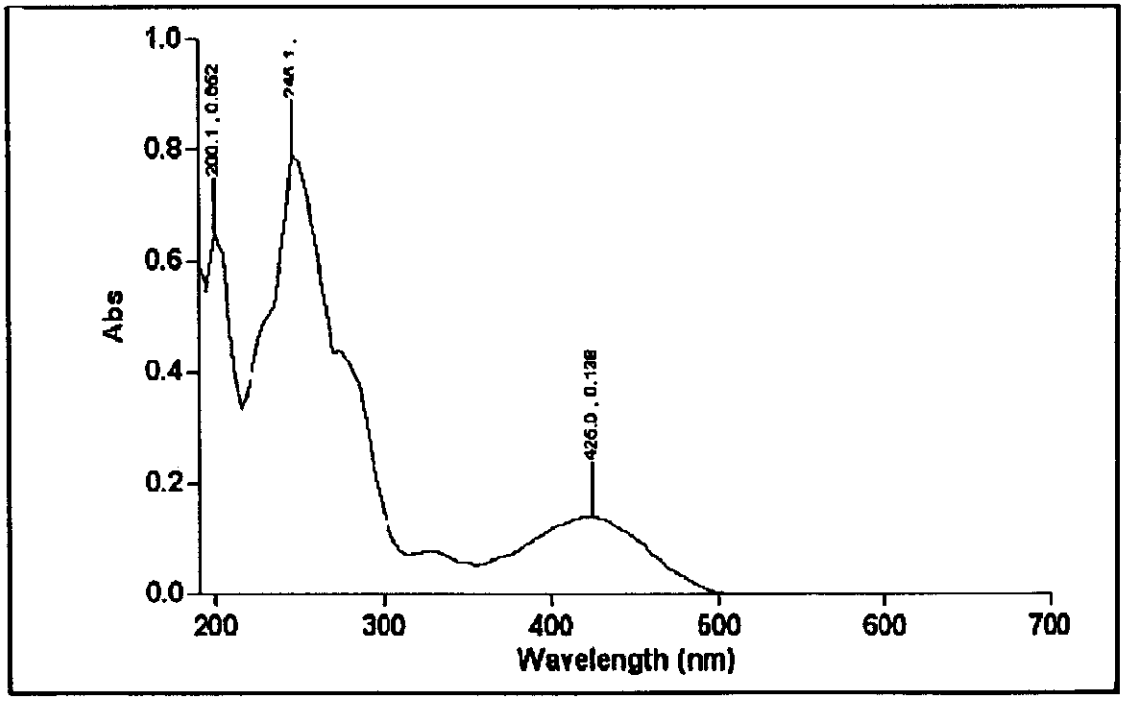

Figure 69 UV-Visible spectrum of 4×10^{-5} M of 1,2-Dihydroxyanthraquinone in CH_3CN

The UV-VIS spectrum of 1,2-Dihydroxyanthraquinone in the visible region contains $\Pi \longrightarrow \pi^*$ band which peak of 1,2-Dihydroxyanthraquinone appears at the wavelength is 425.5 nm and absorbance is 0.138 (Figure 69). A typical series of UV-VIS spectra at various ligand : metal ratios is presented in Figure 70.

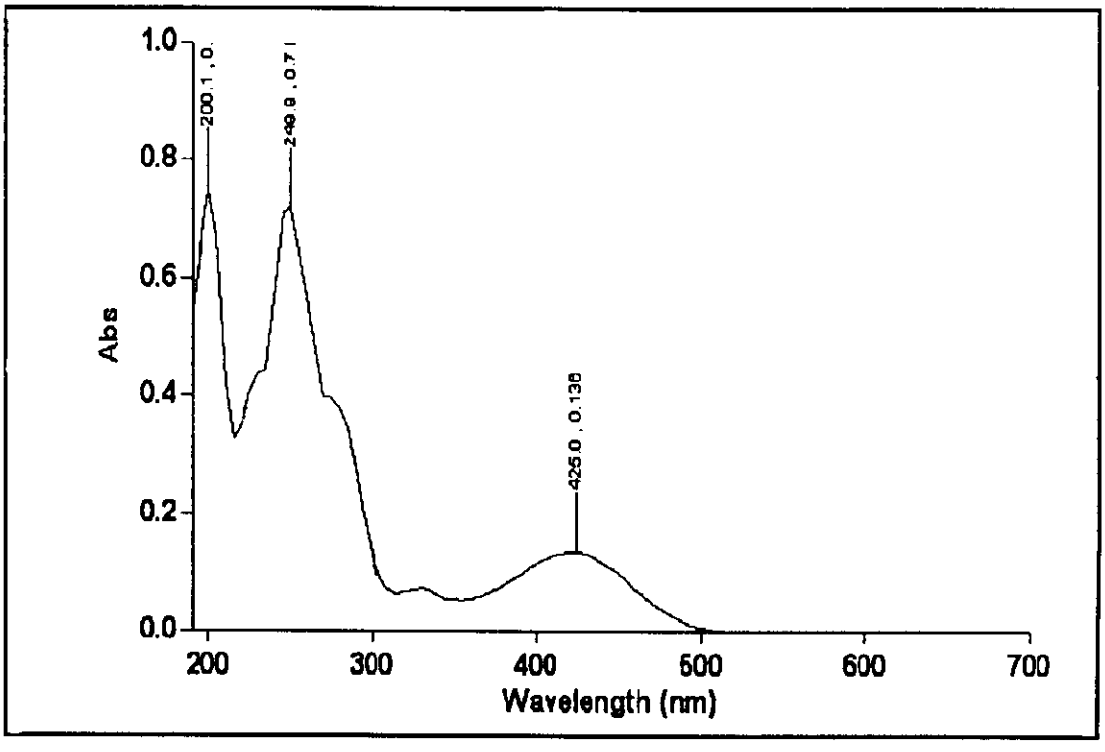

Figure 70 UV-Visible spectrum between 4 x 10^{-5} M of 1,2-Dihydroxyanthraquinone and 1 x 10^{-4} M silver ion in the ratio 6 to 1

Another interesting aspect is the ratio of silver ion and various ligands in the complexes. The intersection between two straight lines in the plot of absorbance of the complex and mole ratio indicates the stoichiometry in the complex (Douglas *et al.*, 1996) as shown in the case of 1,2-Dihydroxyanthraquinone (Figure 71).

Table 39 The relationship between mole ratio of 1,2-Dihydroxyanthraquinone with silver ion and absorbance

Mole ratio of 1,2-Dihydroxyanthraquinone and silver ion	Absorbance
6 to 1	0.136
5 to 1	0.136
4 to 1	0.136
3 to 1	0.136
1.7 to 1	0.135
1.2 to 1	0.133
0.6 to 1	0.130
0.1 to 1	0.126

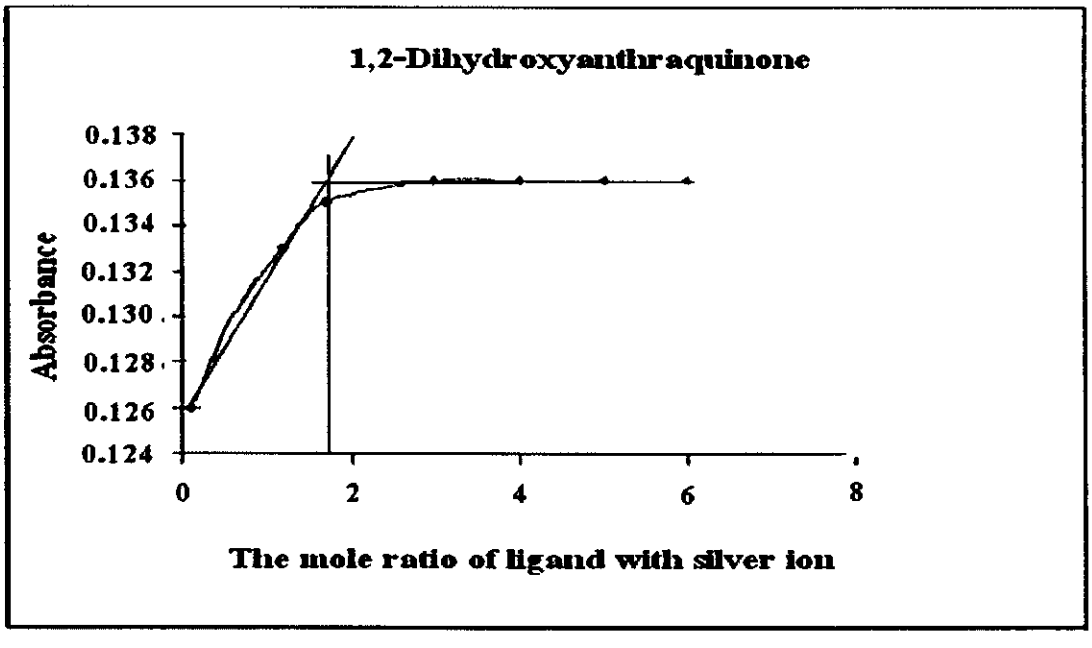

Figure 71 Mole ratio plot of complex of 1,2-Dihydroxyanthraqunone with silver ion

Plots of absorbance *vs.* Ag^{+} : 1,2-Dihydroxyanthraquinone mole ratio indicate the formation of 1 : 2 complex.

3.5.6 The mole ratio of 1,4-Dihydroxyanthraquinone with silver ion

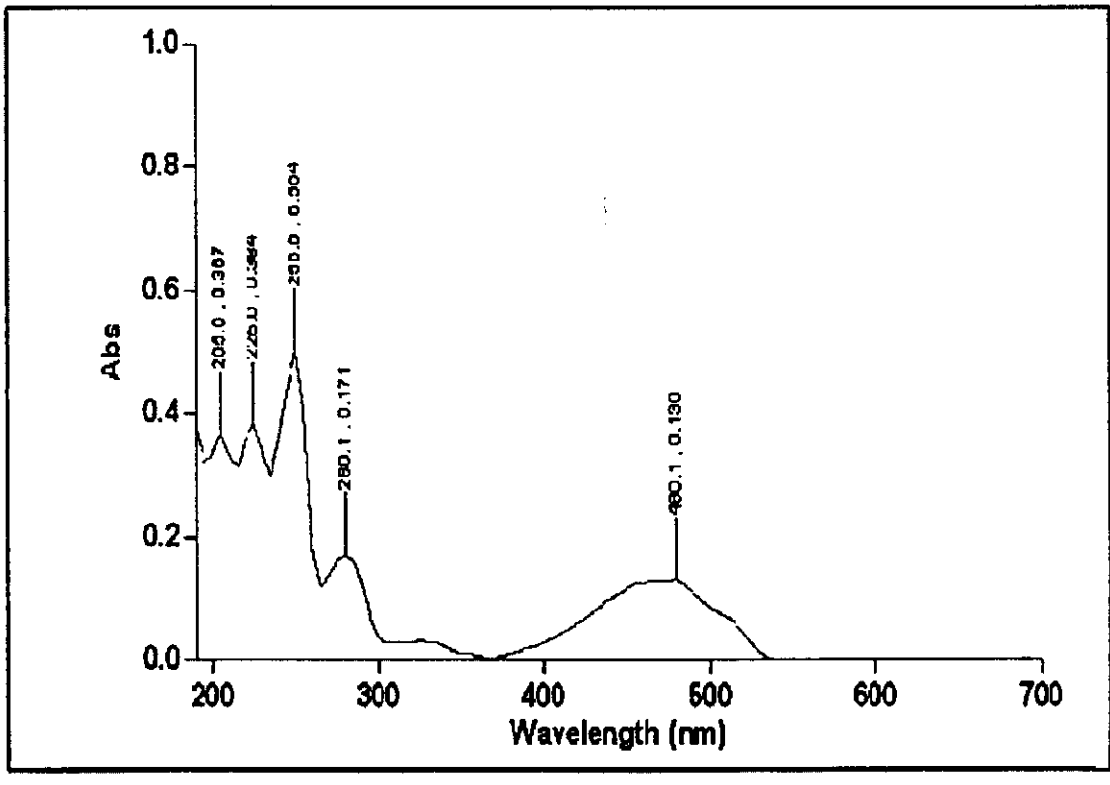

Figure 72 UV-Visible spectrum between 1x 10^{-5} M of 1,4-Dihydroxyanthraquinone

The UV-VIS spectrum of 1,4-Dihydroxyanthraquinone in the visible region contains $n \longrightarrow \pi^*$ band which peak of 1,4-Dihydroxyanthraquinone appears at the wavelength is 480.1 nm and absorbance is 0.130 (Figure 72). A typical series of UV-VIS spectra at various ligand : metal ratios is presented in Figure 73. The position and the intensity of the 470.0 nm band in the Ag^+- 1,4-Dihydroxyanthraquinone system remains practically changed.

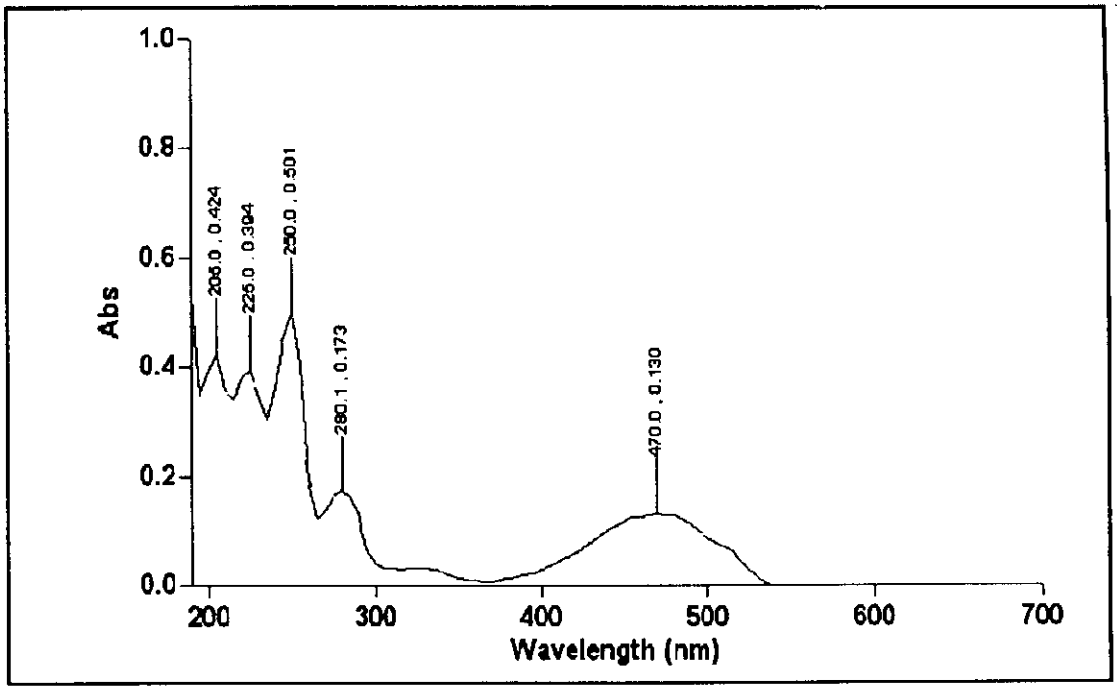

Figure 73 UV-Visible spectrum between 1x 10^{-5} M of 1,4-Dihydroxyanthraquinone and 1 x 10^{-4} M Silver ion in the ratio 1.7 to 1

Table 40 The relationship between mole ratio of 1,4-Dihydroxyanthraquinone with silver ion and absorbance

Mole ratio of 1,4-Dihydroxyanthraquinone and silver ion	Absorbance
0.5 to 1	0.126
1 to 1	0.127
1.5 to 1	0.128
2 to 1	0.129
2.5 to 1	0.129
3 to 1	0.129
3.5 to 1	0.129
4 to 1	0.129

Another interesting aspect is the ratio of silver ion and various ligands in the complexes. The intersection between two straight lines in the plot of absorbance of the complex and mole ratio indicates the stoichiometry in the complex (Douglas *et al.*, 1996) as shown in the case of 1,4-Dihydroxyanthraquinone (Figure 74).

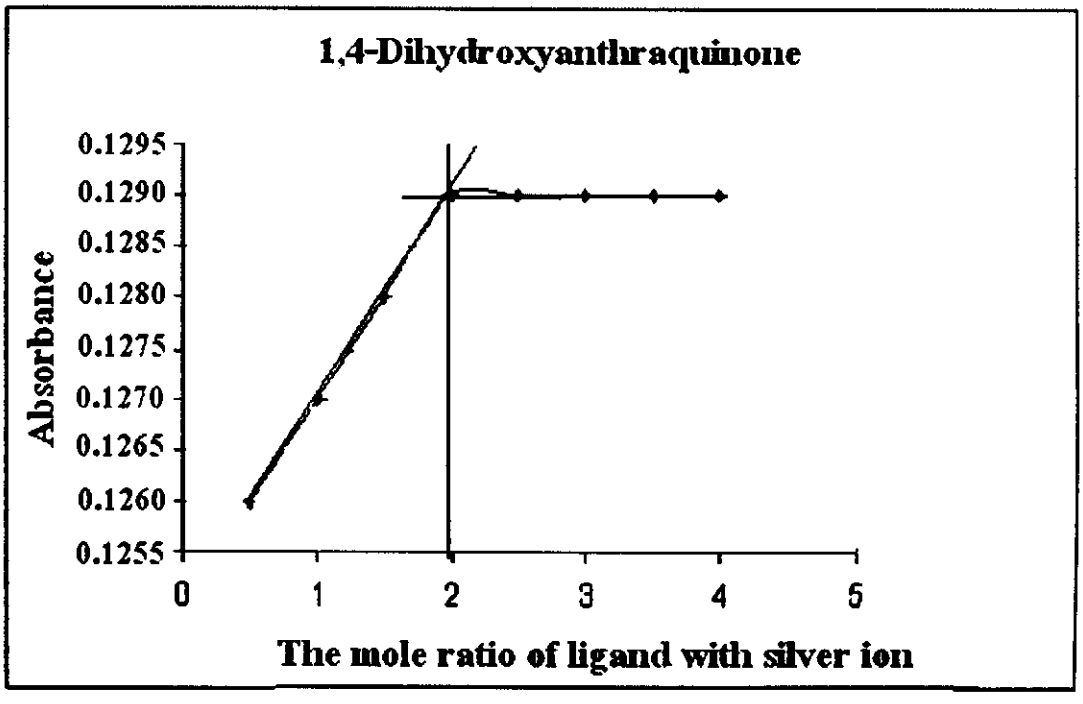

Figure 74 Mole ratio plot of complex of 1,4-Dihydroxyanthraquinone with silver ion

Plots of absorbance *vs.* Ag^+ : 1,4-Dihydroxyanthraquinone mole ratio indicate the formation of 1 : 2 complex.

3.5.7 The mole ratio of 1,8-Dihydroxyanthraquinone with silver ion

The UV-VIS spectrum of 1,8-Dihydroxyanthraquinone in the visible region contains $n \longrightarrow \pi^*$ band which peak of 1,8-Dihydroxyanthraquinone appears at the wavelength is 425.5 nm and absorbance is 0.212 (Figure 75).

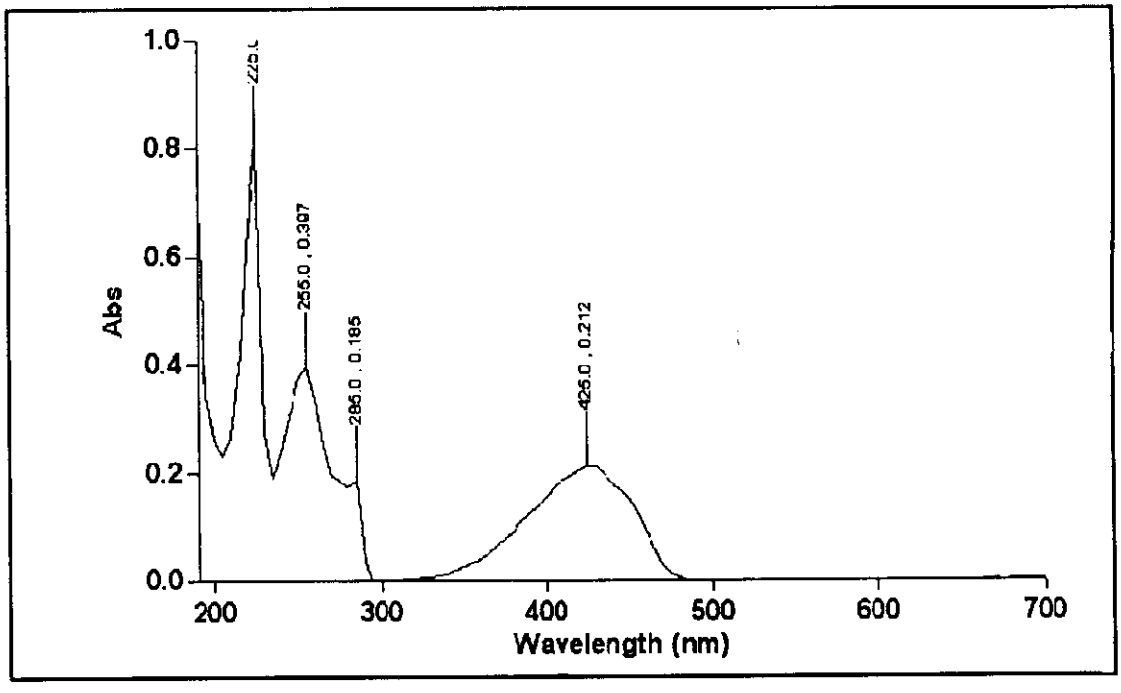

Figure 75 UV-Visible spectrum of 1 x 10^{-5} M of 1,8-Dihydroxyanthraquinone

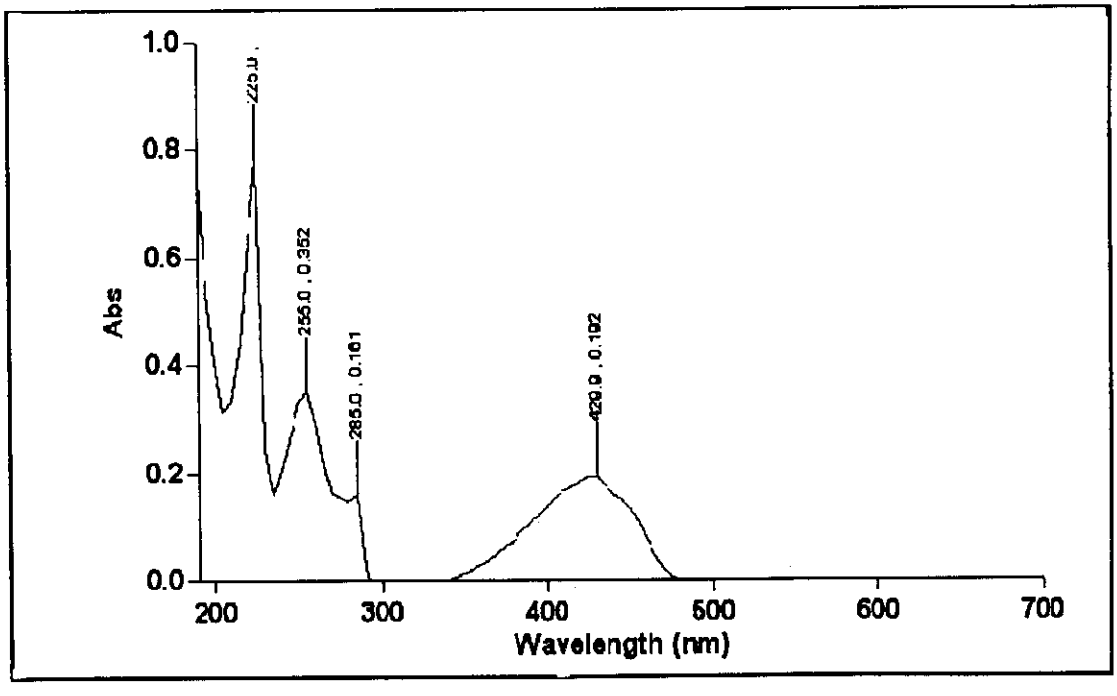

Figure 76 UV-Visible spectrum between 1 x 10^{-5} M of 1,8-Dihydroxyanthraquinone and 1 x 10^{-4} M silver ion in the ratio 1.5 to 1

A typical series of UV-VIS spectra at various ligand : metal ratios is presented in Figure 76. The position and the intensity of the 429.9 nm band in the Ag^{+}- 1,8-Dihydroxyanthraquinone system remains practically changed.

Another interesting aspect is the ratio of silver ion and various ligands in the complexes. The intersection between two straight lines in the plot of absorbance of the complex and mole ratio indicates the stoichiometry in the complex (Douglas *et al.*, 1996) as shown in the case of 1,8-Dihydroxyanthraquinone (Figure 77).

Plots of absorbance *vs.* Ag^{+}:1,8-Dihydroxyanthraquinone mole ratio indicate the formation of 1 : 2 complex

Table 41 The relationship between mole ratio of 1,8-Dihydroxyanthraquinone with silver ion and absorbance

Mole ratio of 1,8-Dihydroxyanthraquinone and silver ion	Absorbance
6 to 1	0.199
5 to 1	0.199
4 to 1	0.199
3 to 1	0.198
2.5 to 1	0.197
2 to 1	0.195
1.5 to 1	0.192
1.25 to 1	0.190
1 to 1	0.187

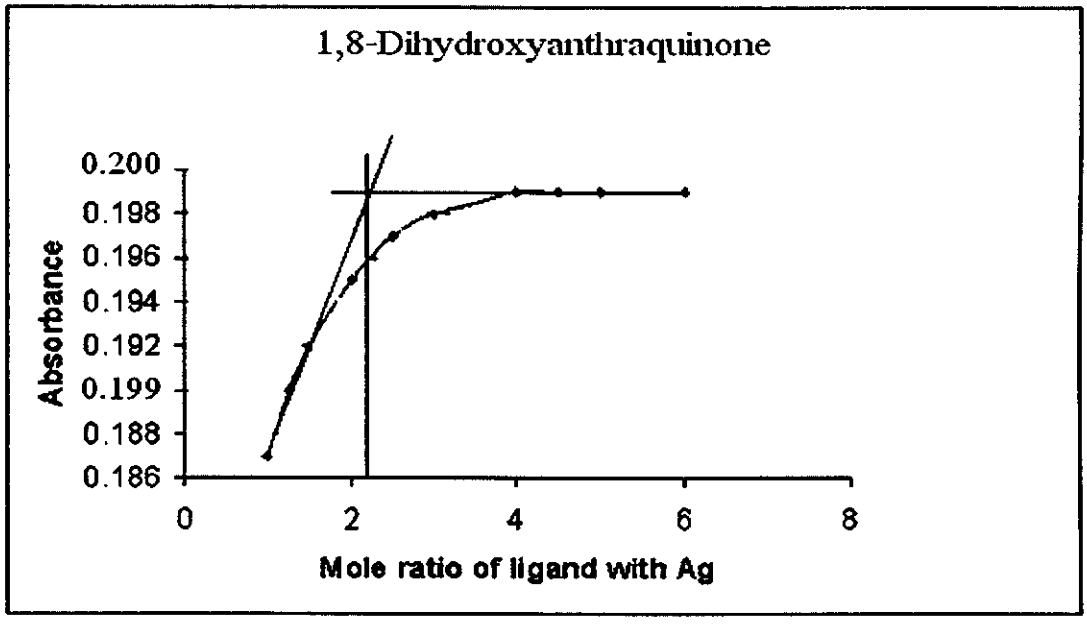

Figure 77 Mole ratio plot of complex of 1,8-Dihydroxyanthraquinone with silver ion

3.5.8 The mole ratio of Damnacanthal with silver ion

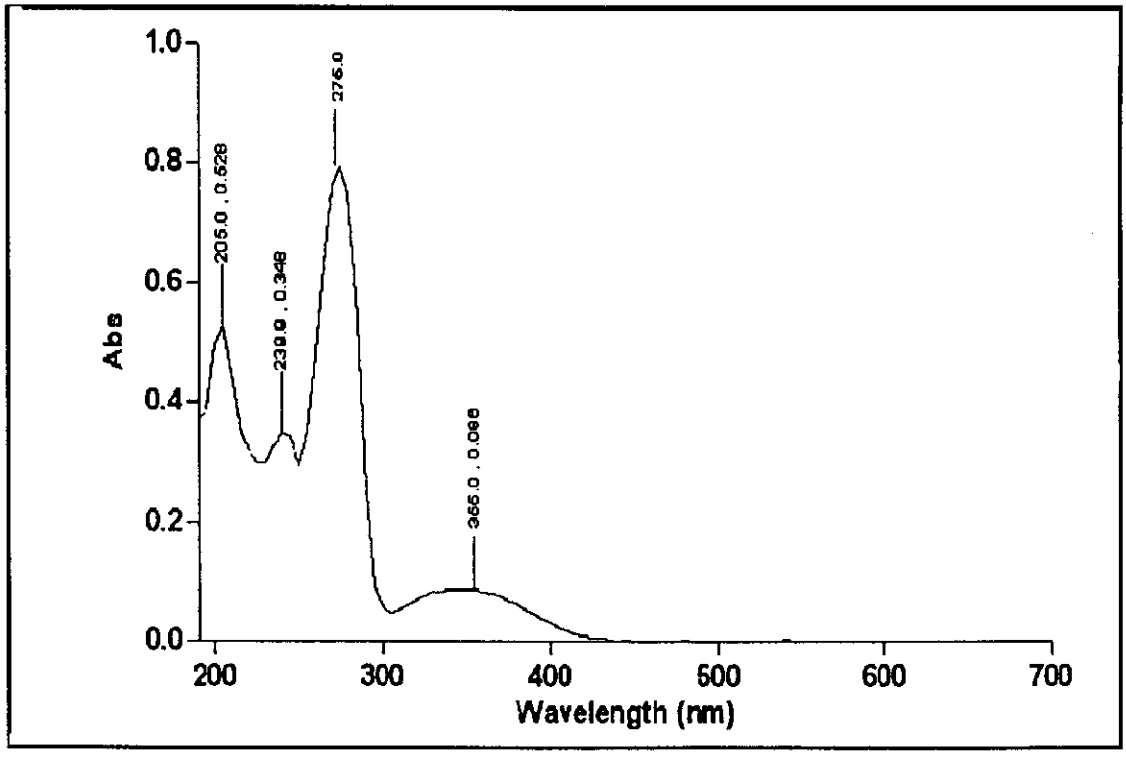

Figure 78 UV-Visible spectrum of 2 x 10^{-5} M of Damnacanthal in CH_3CN

The UV-VIS spectrum of Damnacanthal in the visible region contains $n \longrightarrow \pi^*$ band which peak of Damnacanthal appears at the wavelength is 355.0 nm and absorbance is 0.980 (Figure 78). A typical series of UV-VIS spectra at various ligand : metal ratios is presented in Figure 79. The position and the intensity of the 345.0 nm band in the Ag^+- Damnacanthal system remains practically changed.

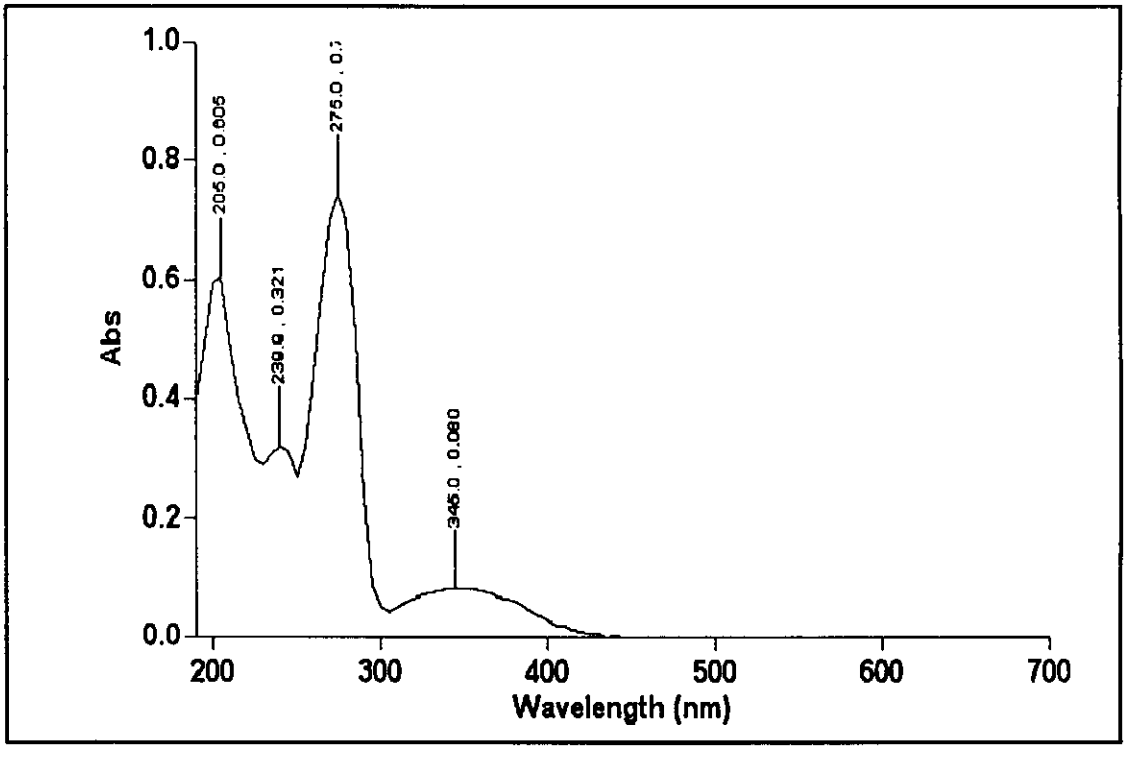

Figure 79 UV-Visible spectrum between 2 x 10^{-5} M of Damnacanthal and 1 x 10^{-4} M Silver ion in the ratio 2 to 1

Another interesting aspect is the ratio of silver ion and various ligands in the complexes. The intersection between two straight lines in the plot of absorbance of the complex and mole ratio indicates the stoichiometry in the complex (Douglas *et al.*, 1996) as shown in the case of Damancanthal (Figure 80).

Table 42 The relationship between mole ratio of Damnacanthal with silver ion and absorbance

Mole ratio of Damnacanthal and silver ion	Absorbance
0.75 to 1	0.072
1 to 1	0.075
1.25 to 1	0.077
1.5 to 1	0.078
2 to 1	0.080
2.5 to 1	0.081
3 to 1	0.082
4 to 1	0.084
4.5 to 1	0.084
5 to 1	0.084
6 to 1	0.084

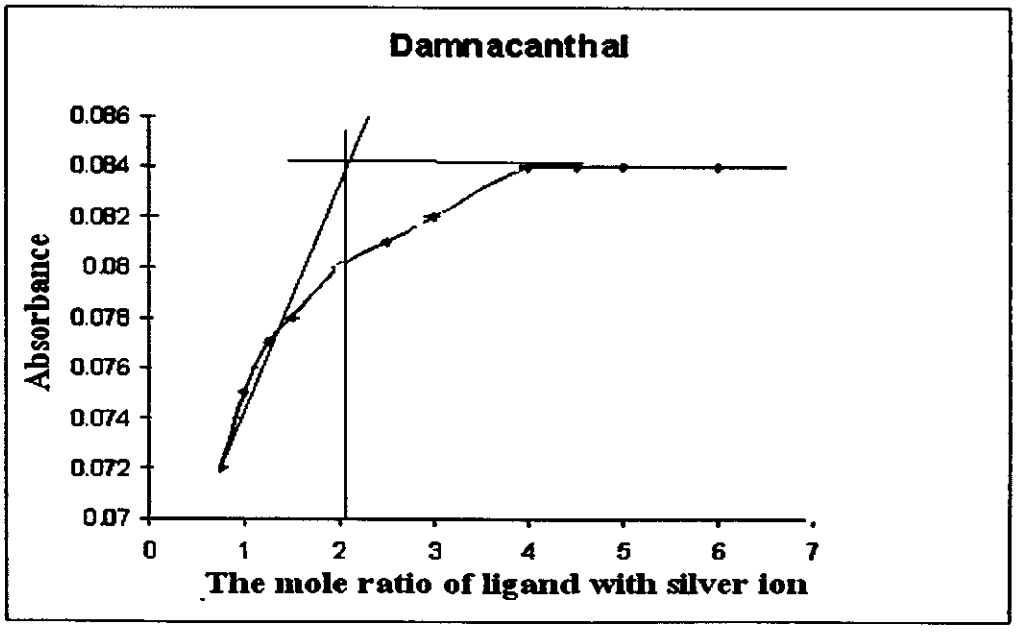

Figure 80 Mole ratio plot of complex of Damnacanthal with silver ion

Plots of absorbance *vs.* Ag^+ : Damnacanthal mole ratio indicate the formation of 1 : 2 complex. The results of the mole ratio of the test solutions are concluded in Table 43.

The results are shown in Table 34. The formation of the complex of ketone with silver ion exhibits one to one which silver ion will interact at position of carbonyl group in the structure of ketone. In contrast, the additional carbonyl group in quinone compounds make them possible to form complex with silver ion in the ration two to one which is summarized in Table 43.

Table 43 Mole ratio of complex between quinones with silver ion in CH_3CN.

Compounds	Mole ratio of complex (ligands to silver)
p-Benzoquinone	2 : 1
Tetrahydroxybenzoquinone	2 : 1
1,4-Naphthoquinone	2 : 1
Anthraquinone	2 : 1
1,2-Dihydroxyanthraquinone	2 : 1
1,4-Dihydroxyanthraquinone	2 : 1
1,8-Dihydroxyanthraquinone	2 : 1
Damnacanthal	2 : 1

There are only few reports about more complex sandwich aggregates with the 1 : 2 (Ag^+: ligand) stoichiometry. In most cases, polar side-arm groups comprise ethers, amines, amides or carbocyclic ones (Tadeusz *et al.*, 2000).

The tendency of the Ag^+ ion to form linear AgL_2^+ complexes is well known in coordination chemistry show in Figure 81.

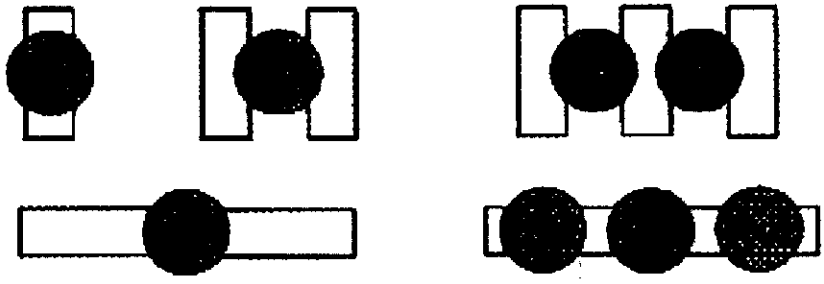

Figure 81 Possible structures of silver–quinone complexes (Cotton and Wilkinson, 1988).

3. 6 The investigation of potentiality of ketones in response to silver ion

Cyclic voltammograms (CVs) were obtained at unmodified and modified carbon paste electrode in 0.2 M nitric acid solution contain 1.0 x 10^{-3} M of silver ion.

3.6.1 The carbon paste electrode modified with Cyclohexanone

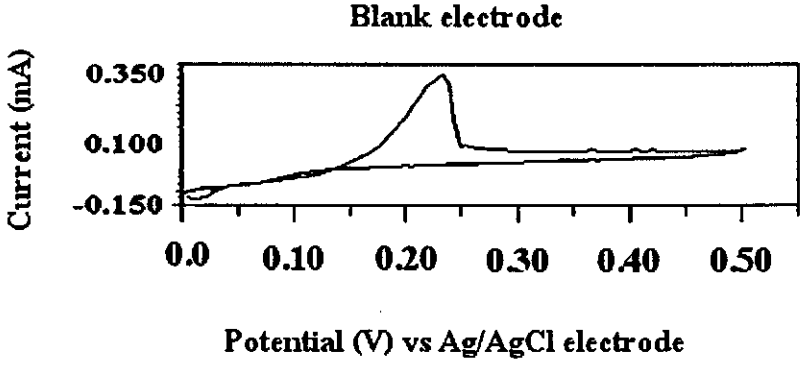

Figure 82 Cyclic voltammogram of UME of 1.0 x 10^{-3} M silver ion in 0.2 M nitric acid solution scanning within 0.000 to +0.500 V vs Ag/AgCl with the scan rate is 180 mVs^{-1}.

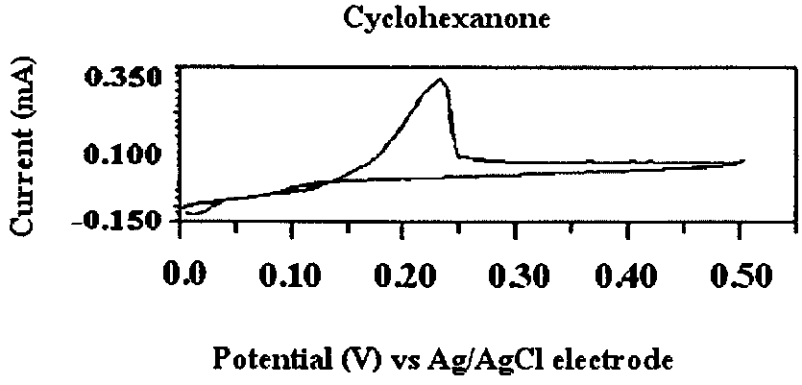

Figure 83 Cyclic voltammogram of Cyclohexanone modified carbon paste electrode of 1.0 x 10^{-3} M silver in 0.2 M nitric acid solution scanning within 0.000 to +0.500 V vs Ag/AgCl with the scan rate is 180 mVs^{-1}.

Cyclic voltammogram of modified carbon paste electrode with Cyclohexanone has not addition of current peak when compared with unmodified electrode, indicate that Cyclohexanone should be the lowest modifier to attract silver ion. The oxidation peak of silver ion occurs at 0.230 V vs Ag/AgCl.

3.6.2 The carbon paste electrode modified with Benzophenone

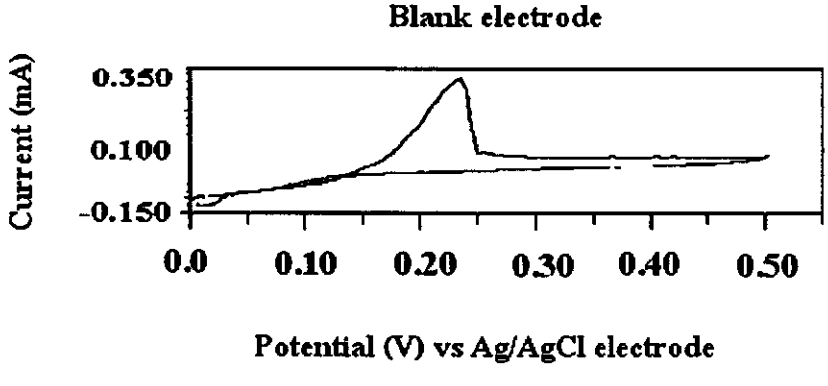

Figure 84 Cyclic voltammogram of unmodified carbon paste electrode of 1.0 x 10^{-3} M silver in 0.2 M nitric acid solution scanning within 0.000 to +0.500 V vs Ag/AgCl with the scan rate is 180 mVs^{-1}.

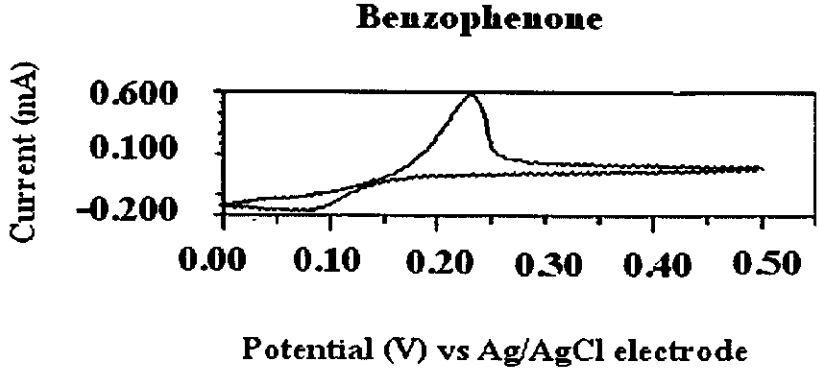

Figure 85 Cyclic voltammogram of Benzophenone modified carbon paste electrode of 1.0 x 10^{-3} M silver in 0.2 M nitric acid solution scanning within 0.000 to +0.500 V vs Ag/AgCl with the scan rate is 180 mVs^{-1}

3.6.3 The carbon paste electrode modified with α-Tetralone

3.6.3.1 Unmodified carbon paste electrode

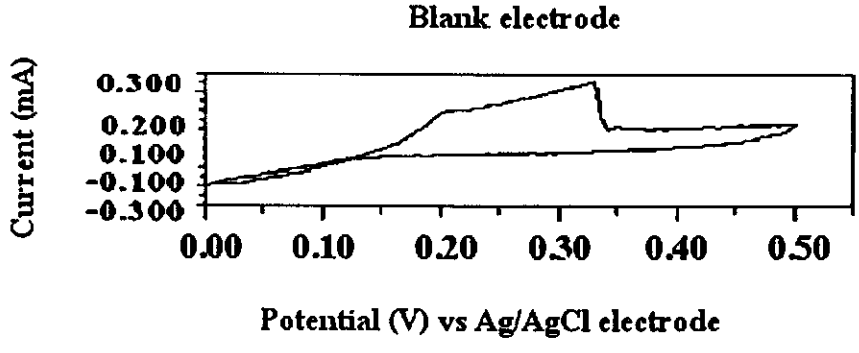

Figure 86 Cyclic voltammogram of unmodified carbon paste electrode of 1.0 x 10^{-3} M silver in 0.2 M nitric acid solution scanning within 0.000 to +0.500 V with the scan rate is 180 mVs^{-1}.

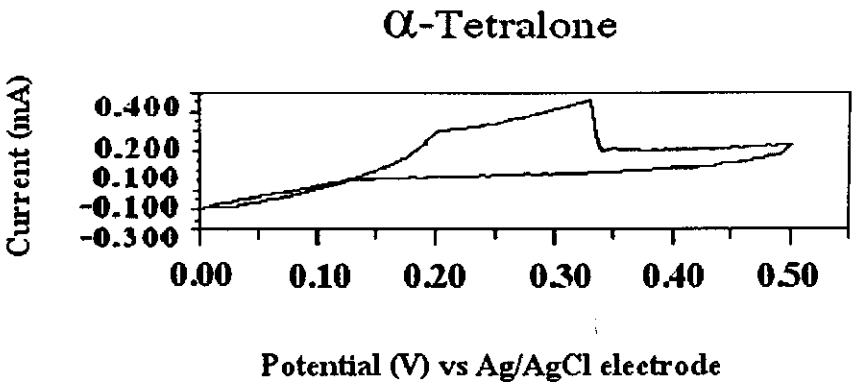

Figure 87 Cyclic voltammogram of α-Tetralone modified carbon paste electrode of 1.0 x 10^{-3} M silver in 0.2 M nitric acid solution scanning within 0.000 to +0.500 V vs Ag/AgCl with the scan rate is 180 mVs^{-1}.

3.6.4 The carbon paste electrode modified with Anthrone

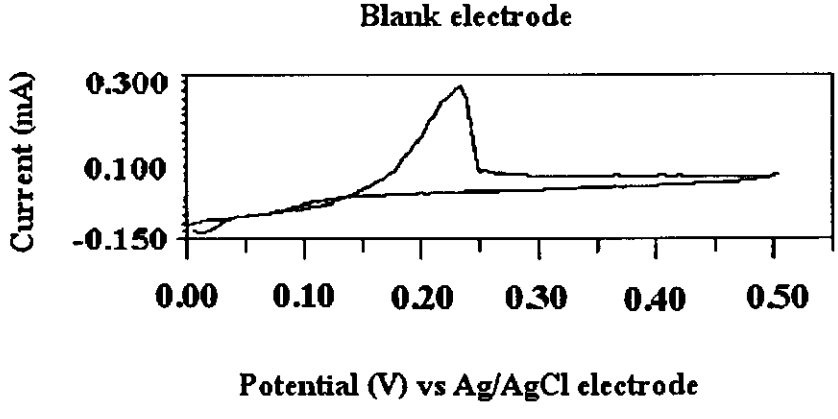

Figure 88 Cyclic voltammogram of unmodified carbon paste electrode of 1.0 x 10^{-3} M silver in 0.2 M nitric acid solution scanning within 0.000 to +0.500 V vs Ag/AgCl with the scan rate is 180 mVs^{-1}.

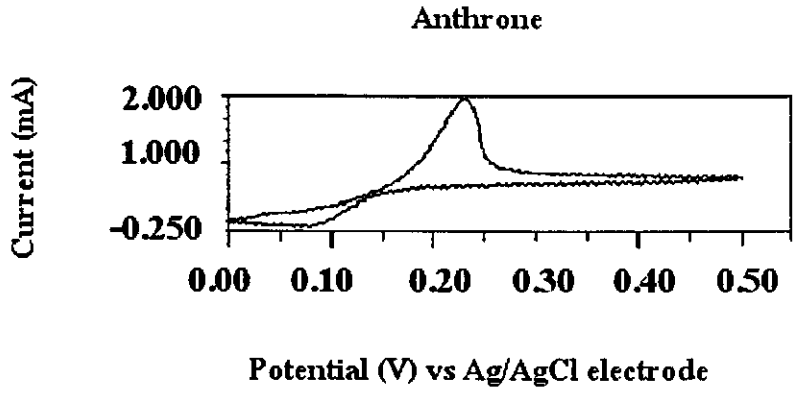

Figure 89 Cyclic voltammogram of Anthrone modified carbon paste electrode of 1.0 x 10^{-3} M silver in 0.2 M nitric acid solution scanning within 0.000 to +0.500 V vs Ag/AgCl with the scan rate is 180 mVs^{-1}.

3.6.5 The carbon paste electrode modified with Xanthone

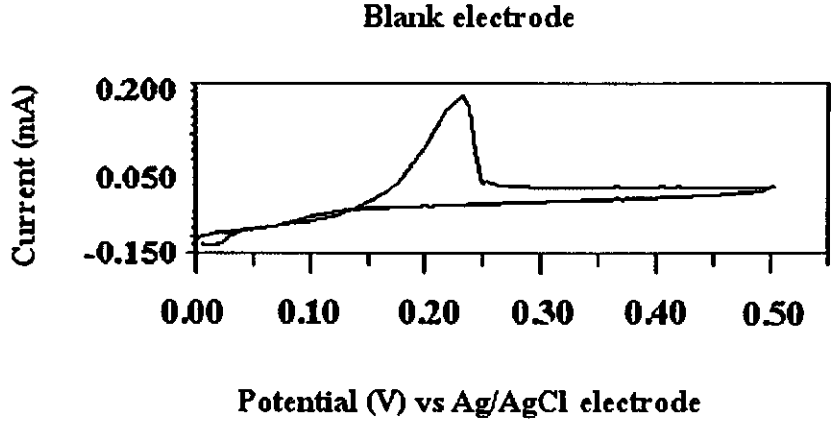

Figure 90 Cyclic voltammogram of unmodified carbon paste electrode of 1.0 x 10^{-3} M silver in 0.2 M nitric acid solution scanning within 0.000 to +0.500 V with the scan rate is 180 mVs^{-1}.

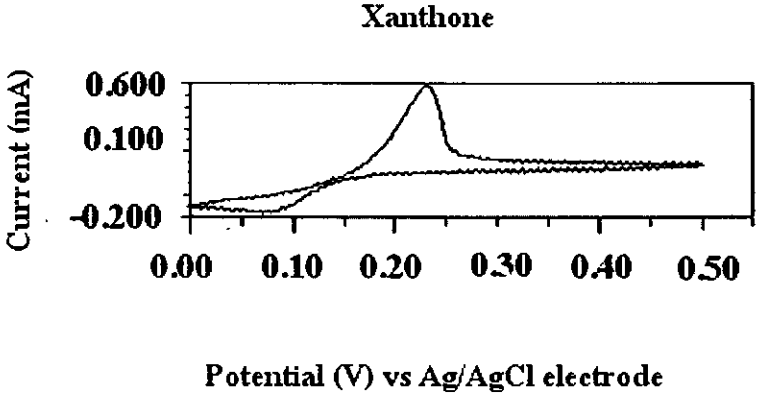

Figure 91 Cyclic voltammogram of Xanthone modified carbon paste electrode of 1.0 x 10^{-3} M silver in 0.2 M nitric acid solution scanning within 0.000 to +0.500 V vs Ag/AgCl with the scan rate is 180 mVs^{-1}.

Discussion

Affinity to silver ion of ketones

We are found that the quinones with more positive first reduction potential shows better affinity to silver ion [J. Rannurak, et.al, 2004]. Therefore, it is conceivable that it would be the same in the case of ketones, i.e., Anthrone would exhibit the best affinity to silver ion due to the fact that the order of more positive reduction potential of the first couple: Anthrone > Xanthone > Benzophenone > α–Tetralone > Cyclohexanone. And this is really the case as can be seen from the study of chemically modified carbon paste electrode (Table 44).

Table 44 The formal potential of the first couple of ketones compared with oxidation current peak of silver ion at the modified carbon paste electrode with ketones.

Compounds	$E_1^{0'}$ (V) vs NHE in CVs	Ipa (mA)
Cyclohexanone	no peak	0.000
Benzophenone	-1.560	0.218
α-Tetralone	-1.799	0.028
Anthrone	-0.640	1.548
Xanthone	-1.444	0.431

3. 7 The investigation of potentiality of quinones in response to silver ion

Cyclic voltammograms (CVs) were obtained at unmodified and modified carbon paste electrode in 0.2 M nitric acid solution contain 1.0×10^{-3} M of silver ion. The CVs of modified carbon paste electrode which the anodic peak current of silver ion at the modified electrode is larger than of unmodified electrode. Thus there is a substantial enhancement in silver oxidation peak current when modified electrode is used.

3.7.1 The carbon paste electrode modified with *p*-Benzoquinone

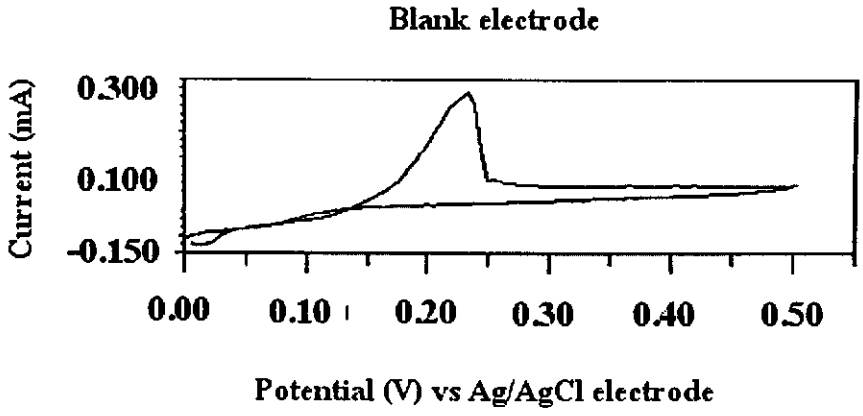

Figure 92 Cyclic voltammogram of unmodified carbon paste electrode of 1.0 x 10^{-3} M silver in 0.2 M nitric acid solution scanning within 0.000 to +0.500 V vs Ag/AgCl with the scan rate is 180 mVs^{-1}.

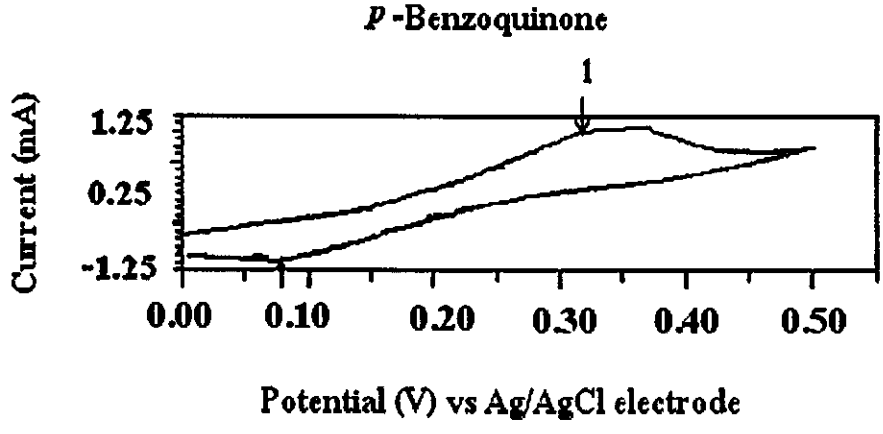

Figure 93 Cyclic voltammogram of *p*-Benzoquinone modified carbon paste electrode of 1.0 x 10^{-3} M silver in 0.2 M nitric acid solution scanning within 0.000 to +0.500 V vs Ag/AgCl with the scan rate is 180 mVs^{-1}.

3.7.2 The carbon paste electrode modified with 1,4-Naphthoquinone

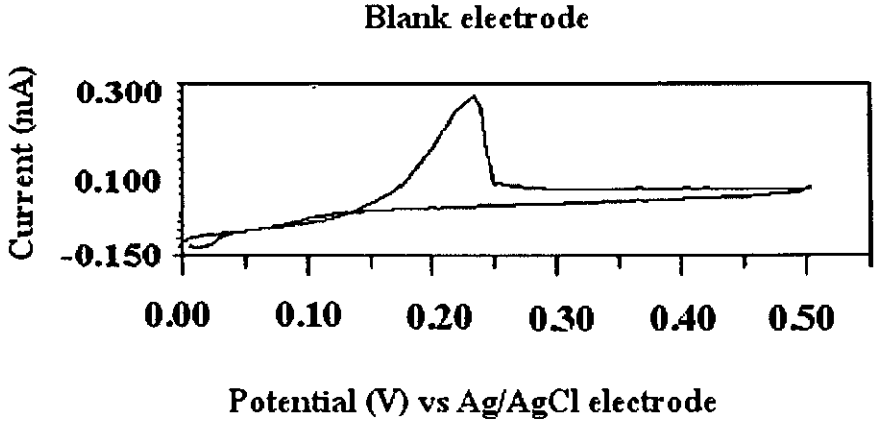

Figure 94 Cyclic voltammogram of unmodified carbon paste electrode of 1.0×10^{-3} M silver in 0.2 M nitric acid solution scanning within 0.000 to +0.500 V vs Ag/AgCl with the scan rate is 180 mVs^{-1}.

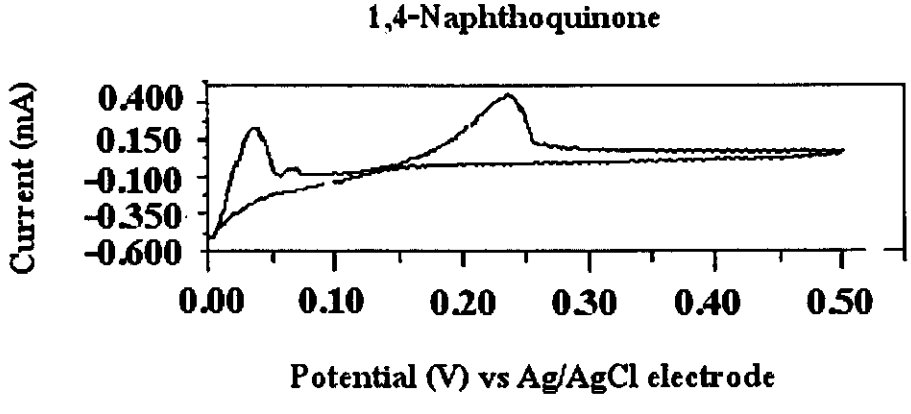

Figure 95 Cyclic voltammogram of 1,4-Naphthoquinone modified carbon paste electrode of 1.0×10^{-3} M silver in 0.2 M nitric acid solution scanning within 0.000 to +0.500 V vs Ag/AgCl with the scan rate is 180 mVs^{-1}.

3.7.3 The carbon paste electrode modified with Anthraquinone

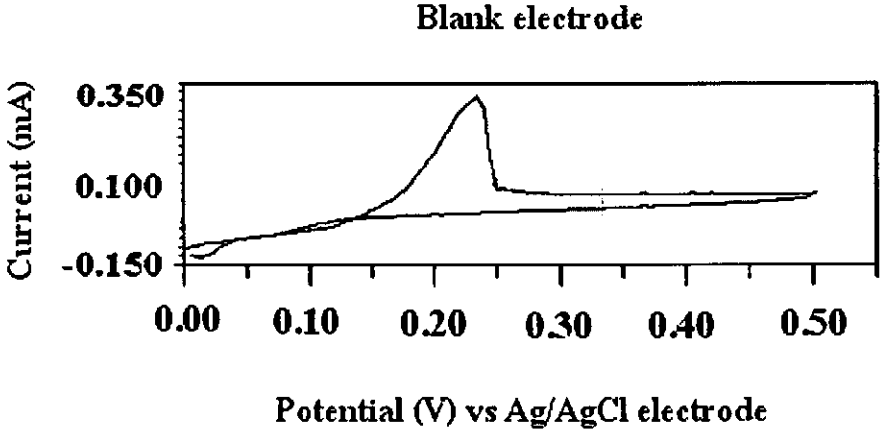

Figure 96 Cyclic voltammogram of unmodified carbon paste electrode of 1.0 x 10^{-3} M silver in 0.2 M nitric acid solution scanning within 0.000 to +0.500 V vs Ag/AgCl with the scan rate is 180 mVs^{-1}.

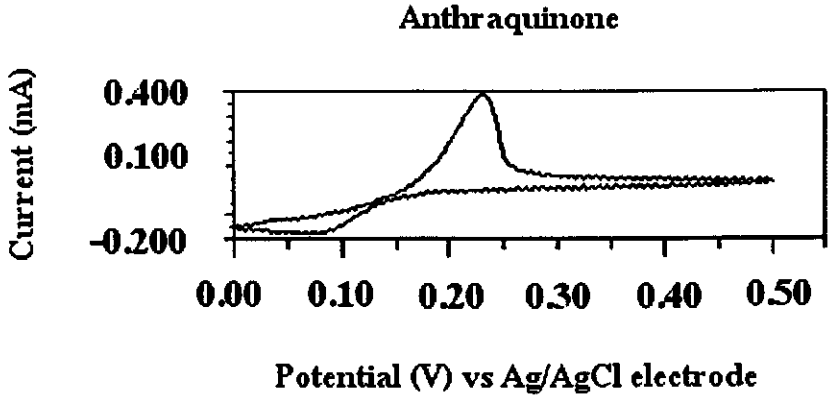

Figure 97 Cyclic voltammogram of Anthraquinone modified carbon paste electrode of 1.0 x 10^{-3} M silver in 0.2 M nitric acid solution scanning within 0.000 to +0.500 V vs Ag/AgCl with the scan rate is 180 mVs^{-1}.

3.7.4 The carbon paste electrode modified with 1,2-Dihydroxyanthraquinone

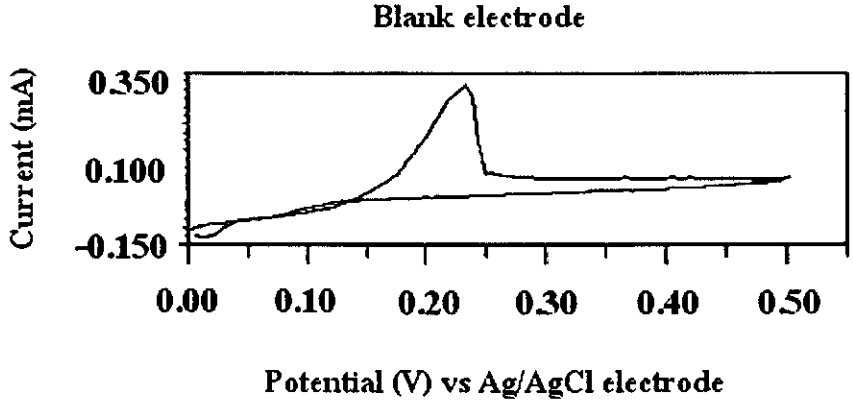

Figure 98 Cyclic voltammogram of unmodified carbon paste electrode of 1.0 x 10^{-3} M silver in 0.2 M nitric acid solution scanning within 0.000 to +0.500 V vs Ag/AgCl with the scan rate is 180 mVs^{-1}.

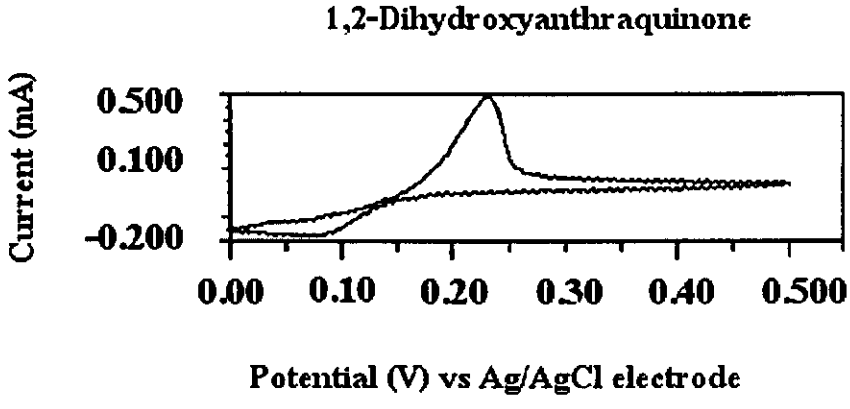

Figure 99 Cyclic voltammogram of 1,2-Dihydroxyanthraquinone modified carbon paste electrode of 1.0 x 10^{-3} M silver in 0.2 M nitric acid solution scanning within 0.000 to +0.500 V vs Ag/AgCl with the scan rate is 180 mVs^{-1}.

3.7.5 The carbon paste electrode modified with 1,4-Dihydroxyanthraquinone

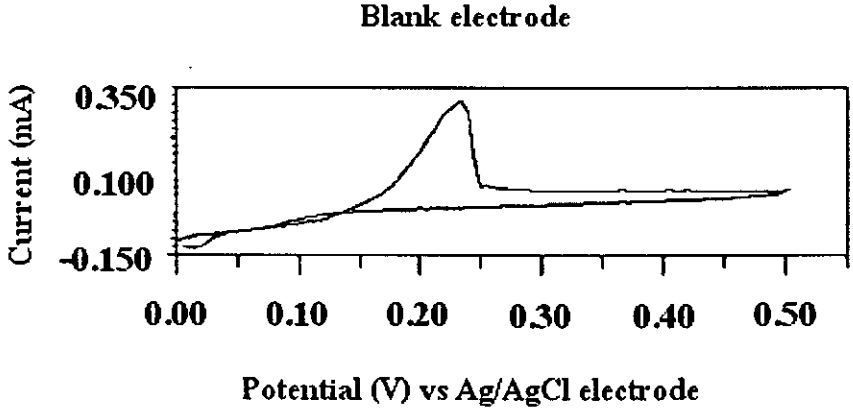

Figure 100 Cyclic voltammogram of unmodified carbon paste electrode of 1.0×10^{-3} M silver in 0.2 M nitric acid solution scanning within 0.000 to +0.500 V vs Ag/AgCl with the scan rate is 180 mVs^{-1}.

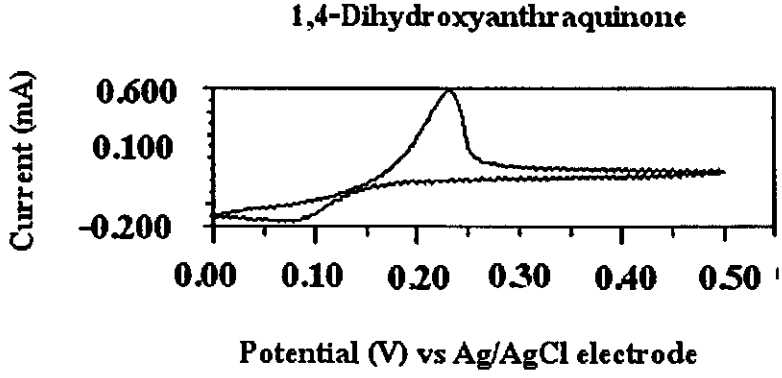

Figure 101 Cyclic voltammogram of 1,4-Dihydroxyanthraquinone modified carbon paste electrode of 1.0×10^{-3} M silver in 0.2 M nitric acid solution scanning within 0.000 to +0.500 V vs Ag/AgCl with the scan rate is 180 mVs^{-1}.

3.7.6 The carbon paste electrode modified with 1,8-Dihydroxyanthraquinone

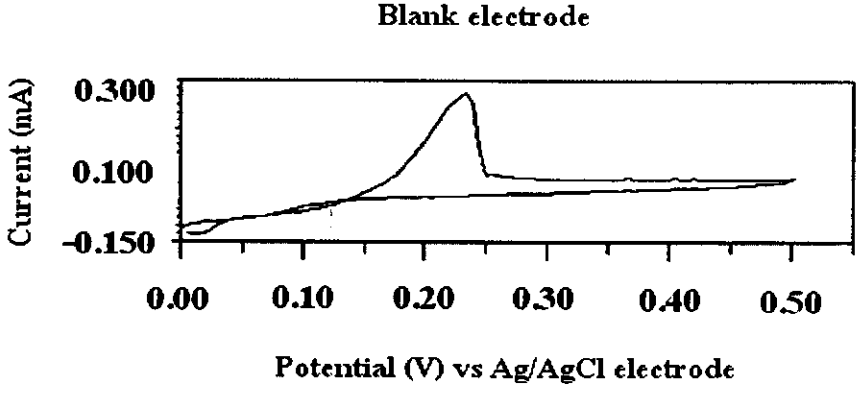

Figure 102 Cyclic voltammogram of unmodified carbon paste electrode of 1.0 x 10^{-3} M silver in 0.2 M nitric acid solution scanning within 0.000 to +0.500 V vs Ag/AgCl with the scan rate is 180 mVs^{-1}.

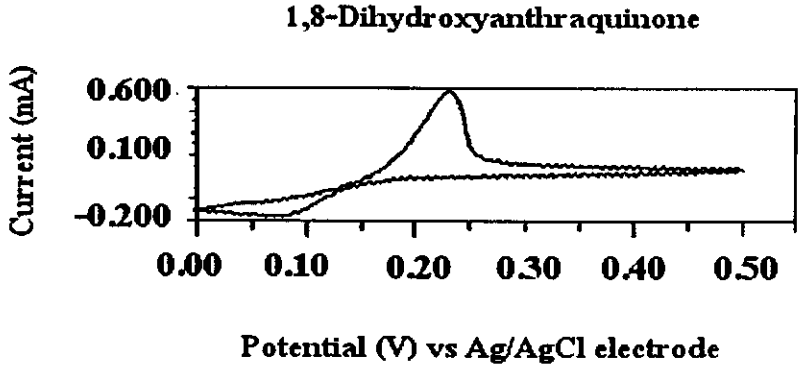

Figure 103 Cyclic voltammogram of 1,8-Dihydroxyanthraquinone modified carbon paste electrode of 1.0 x 10^{-3} M silver in 0.2 M nitric acid solution scanning within 0.000 to +0.500 V vs Ag/AgCl with the scan rate is 180 mVs^{-1}.

Discussion

Affinity to silver ion of quinones

As mentioned earlier, the quinone with higher positive reduction potential exhibit strong affinity to silver ion. Among quinones under investigation, therefore, *p*-Benzoquinone and 1,8-Dihydroxyanthraquinone should be the best modifier to attract silver ion. However Tetrahydroxybenzoquinone is solubility in nitric acid so its can not use to be modifier in the chemically modified carbon paste electrode. For Damnacanthal was limited so it was not used in this investigation. This expectation is confirmed by the chemically modifile carbon paste electrode study (Table 45). This suggests the general trend that the best modifier accept electron very well to further transfer to metal ions. This would help the selection of modifier in CME or in catalysis.

Table 45 Values of formal potential of the first couple of quinones compared with current peak at the CME with quinones (E = 0.222 V vs NHE).

Compounds	$E_1^{0'}$ (V) vs NHE	Ipa (mA)
p-Benzoquinone	-0.260	0.482
Tetrahydroxybenzoquinone	0.022	-
1,4-Naphthoquinone	-0.432	0.155
Anthraquinone	-0.656	0.077
1,2-Dihydroxyanthraquinone	-0.510	0.119
1,4-Dihydroxyanthraquinone	-0.429	0.225
1,8-Dihydroxyanthraquinone	-0.408	0.286
Damnacanthal	-0.486	-